2016-07-01

Simplified Performance-Based Analysis for Seismic Slope Displacements

Marlem Lucia Astorga Mejia
Brigham Young University

Simplified Performance-Based Analysis

for Seismic Slope Displacements

Marlem Lucia Astorga Mejia

A thesis submitted to the faculty of
Brigham Young University
in partial fulfillment of the requirements for the degree of

Master of Science

Kevin W. Franke, Chair
Paul W. Richards
W. Spencer Guthrie

Department of Civil and Environmental Engineering

Brigham Young University

July 2016

ABSTRACT

Simplified Performance-Based Analysis
for Seismic Slope Displacements

Marlem Lucia Astorga Mejia
Department of Civil and Environmental Engineering, BYU
Master of Science

Millions of lives have been lost over the years as a result of the effects of earthquakes. One of these devastating effects is slope failure, more commonly known as landslide. Over the years, seismologists and engineers have teamed up to better record data during an earthquake. As technology has advanced, the data obtained have become more refined, allowing engineers to use the data in their efforts to estimate earthquakes where they have not yet occurred. Several methods have been proposed over time to utilize the earthquake data and estimate slope displacements. A pioneer in the development of methods to estimate slope displacements, Nathan Newmark, proposed what is now called the Newmark sliding block method. This method explained in very simple ways how a mass, in this case a rigid block, would slide over an incline given that the acceleration of the block surpassed the frictional resistance created between the bottom of the block and the surface of the incline. Because many of the assumptions from this method were criticized by scientists over time, modified Newmark sliding block methods were proposed.

As the original and modified Newmark sliding block methods were introduced, the need to account for the uncertainty in the way soil would behave under earthquake loading became a big challenge. Deterministic and probabilistic methods have been used to incorporate parameters that would account for some of the uncertainty in the analysis. In an attempt to use a probabilistic approach in understanding how slopes might fail, the Pacific Earthquake Engineering Research Center proposed a performance-based earthquake engineering framework that would allow decision-makers to use probabilistically generated information to make decisions based on acceptable risk. Previous researchers applied this framework to simplified Newmark sliding block models, but the approach is difficult for engineers to implement in practice because of the numerous probability calculations that are required.

The work presented in this thesis provides a solution to the implementation of the performance-based approach by providing a simplified procedure for the performance-based determination of seismic slope displacements using the Rathje & Saygili (2009) and the Bray and Travasarou (2007) simplified Newmark sliding block models. This document also includes hazard parameter maps, which are an important part of the simplified procedure, for five states in the United States. A validation of the method is provided, as well as a comparison of the simplified method against other commonly used approaches such as deterministic and pseudo-probabilistic.

Key words: deterministic, hazard parameter maps, Newmark sliding block, PEER, performance-based earthquake engineering, probabilistic, slope failure

ACKNOWLEDGEMENTS

I express gratitude to all those who have in any way been a source of support and encouragement through my graduate school adventure. I give special thanks to Dr. Kevin Franke for his countless hours of instruction, direction, and encouragement. I appreciate the time he took to help me see my potential in this great field of geotechnical engineering.

Others who also contributed to the success of this research include fellow graduate students who spent many hours writing code, running data points, and preparing reports. Many thanks go to Braden Error, Brian Peterson, Kristen Ulmer, and Levi Ekstrom. Their examples and hard work were greatly appreciated. Others who spent many hours in the map preparation and simplified tool validation include Alex Arndt, Jasmyn Harper, Tyler Coutu, Mikayla Hatch, and Alex Corob. It was wonderful to work with all of them.

The work performed for this research would have not been possible without the help and funding provided by the Federal Highway Administration pooled fund study (Award No. TPF-5(296) with Utah, Alaska, Connecticut, Idaho, Montana, South Carolina, and Oregon Departments of Transportation). Their financial support and their valuable feedback were an important part of this work. I sincerely appreciate their time and interest in what this research entailed.

Lastly, I thank my family. The distance has not prevented them from sharing countless words of encouragement and support so that I could complete the requirements to earn a master's degree. They always believed in me, and this work is especially dedicated to them.

TABLE OF CONTENTS

LIST OF TABLES

LIST OF FIGURES

1 INTRODUCTION

Through time, earthquakes have taken the lives of many people. Although one could argue that an earthquake itself is not necessarily directly responsible for the loss of life, the effects of earthquakes result in hazards that can put many lives in danger. A report from the United States Geological Survey (USGS) provides information about earthquakes worldwide from the year 2000 to 2012 in which 800,000 deaths reported are related to the effects of earthquakes (USGS 2016). One of the hazards induced by earthquakes is slope failure.

A slope is considered a soil mass incline that can be either natural or man-made. Natural slopes are formed by natural processes, and man-made slopes are earth structures such as earth-dams and embankments. A slope failure occurs with downslope movement of soil and rock materials under the influence of gravity. Slopes can fail for many reasons, but natural ways in which these fail include heavy rains and earthquake shaking.

Earthquake-induced landslides, or seismic slope displacements, often have indirect effects as was the case in the Niigata Ken Chuetsu, Japan, earthquake in 2004. The zone of greatest landslide activity was near Yamakoshi. In the 30 km^2 area containing the greatest landslide activity, an average concentration of large landslides was 13.3 landslides/km^2, which resulted in 17% of the ground surface of this area being covered by landslides (Kieffer et al. 2006). The monetary loss that occurs after earthquakes amounts to millions of dollars, but what is arguably most alarming is the loss of life. These losses have motivated many researchers to find better ways to

estimate seismic slope displacements for better design of structures in areas where seismicity is a concern.

Seismic slope displacements have been commonly approximated deterministically and probabilistically. Deterministic approximations of seismic slope displacements involve the selection of a "controlling earthquake," and ground motions produced in such an event are used in the computation of seismic slope displacements. The challenge that this approach presents is that the likelihood of the "controlling earthquake" occurring is not accounted for. On the other hand, probabilistic approaches seek to account for the likelihood of a significant earthquake occurring.

Engineers commonly approximate probabilistic seismic slope displacements by taking probabilistic ground motions from a single return period and applying them deterministically into a slope displacement prediction model. Such an approach has been termed a "pseudo-probabilistic approach" (Rathje and Saygili 2008) and has shown to produce inaccurate and inconsistent estimates of probabilistic seismic slope displacements. Full probabilistic or performance-based methods for computing seismic slope displacements have been presented by earlier researchers (Rathje and Saygili 2008), but these methods are difficult for engineers to implement on most typical engineering projects.

The research presented in this thesis focuses on the probabilistic prediction of seismic slope displacements. More specifically, a derivation of a simplified probabilistic approach is presented that produces probabilistic seismic slope displacements that closely approximate those computed by a full probabilistic approach (Rathje and Saygili 2008). This simplified probabilistic method seeks to provide the benefits of a full performance-based seismic slope displacement analysis with the same amount of effort that traditional approaches (deterministic and pseudo-probabilistic)

require. The simplified approach is validated and then compared against other deterministic and pseudo-probabilistic approaches that are widely used in practice today.

The work presented in this thesis begins with the derivation of the simplified approach. This derivation is performed in three steps. The first step requires the estimation of a site slope displacement. The information required for the computation of the site slope displacement includes a yield acceleration (k_y), a ground acceleration (a), and an earthquake magnitude (M_w) from the site of interest. The second step requires the definition of a reference profile. For the purposes of this study, the reference profile is defined as a site with a k_y value equal to 0.1 g and a soil ground motion amplification factor f_a of 1.0. Reference displacements are computed with the full probabilistic method (Rathje and Saygili 2008) using the probabilistic liquefaction analysis spreadsheet *PBLiquefY* (Franke et al. 2014) across a grid of geographic points to develop seismic slope displacement reference parameter maps. A correction function to be used with the seismic slope displacement reference parameter maps is mathematically derived. Lastly, this correction factor is used to compute a site-specific seismic slope displacement value derived from the slope displacement reference parameter map appropriate for the area of concern and selected return period.

Following the derivation of the simplified performance-based method, a validation study is conducted to test how well the simplified approach approximates the full probabilistic approach by evaluating seismic slope displacements across 10 different locations in the United States and using a wide range of k_y values. The validation study has the intent to demonstrate that the simplified performance-based seismic slope displacement method closely approximates results produced by a full performance-based seismic slope displacement analysis. The models included

in the validation study are the Rathje & Saygili (2009) model and the Bray & Travasarou (2007) model.

Part of the scope of this research also includes the development of seismic slope displacement reference parameter maps for six states in the United States (Utah, Idaho, Montana, South Carolina, Connecticut, and portions of Alaska). The creation of these reference parameter maps required a grid spacing study to understand and quantify how spatial error can affect the accuracy and effectiveness of the reference parameter maps. This grid spacing study analyzes different grid spacing iterations varying from 2 km up to 50 km at 35 different locations across the United States. The study is performed by comparing an interpolated full performance-based slope displacement computed at an anchor point with its corresponding interpolated displacement using values computed on a grid. A maximum discrepancy between values corresponding to 5% error is established as the upper bound, and an optimum grid spacing is identified and correlated to USGS-mapped probabilistic ground motions for the different seismic hazard zones across the United States represented by the 35 locations that are analyzed. For cities not meeting the 5% error criteria, an absolute difference of 5 cm is established. Optimum grid spacings corresponding to the different seismic hazard zones in the United States are proposed. With the proper spacing, simplified performance-based seismic slope displacement reference parameter maps are created using *ArcMap*. With the availability of the reference parameter maps, engineers are able to perform site-specific simplified performance-based seismic slope displacement analyses with the benefits of a performance-based approach and the same amount of effort of traditional hazard analysis methods.

To understand the potential differences between the new simplified probabilistic approach and traditional deterministic and/or pseudo-probabilistic approaches, a comparison study is performed between seismic slope displacements computed with the various approaches at three

sites across the United States representing low, moderate, and high seismicity. Given the results from this study, engineers should use the smaller of the predicted deterministic and the simplified probabilistic seismic slope displacements for design. Furthermore, engineers are recommended to discontinue use of the pseudo-probabilistic approach due to the inconsistencies and errors that it produces.

The culmination of this research is the development of a simplified liquefaction hazard assessment tool (*SPLiq*) in which the simplified method is implemented for the use of engineering practitioners. *SPLiq* has the ability to perform simplified performance-based analysis for liquefaction triggering, lateral spread, post-liquefaction settlement, and seismic slope displacement. This thesis is limited to a discussion related to performing a simplified performance-based seismic slope displacement analysis.

2 SEISMIC-INDUCED LANDSLIDES

Landslides or slope failures occur when the stability of the slope changes from a stable to an unstable condition. A change in the stability of a slope can be caused by a number of factors, acting together or alone. Natural causes of landslides include pore water pressure acting to destabilize the slope; loss or absence of vertical vegetative structure, soil nutrients, and soil structure; weakening of a slope through saturation by snow melt or heavy rains; and earthquake loading are common causes. This chapter introduces earthquake-induced landslides, or seismic slope displacements.

Researchers have for many years sought to understand how seismic slope displacements occur, and many have focused their efforts on the development of seismic slope displacement prediction models. Newmark (1965) proposed that the seismic stability of slopes, embankments, and dams should be assessed in terms of earthquake-induced deformations. Newmark explained that it was necessary to consider all of the aspects of a strong ground motion when considering the effects of an earthquake on a structure such as an earth or rock-filled dam. He mentioned that the effects of peak ground velocity (PGV) and peak ground displacement needed to be considered in

addition to peak ground acceleration (PGA). Newmark's study was based on earthquake records from only California because earthquake data was just beginning to be collected in other parts of the world.

One of the most important conditions existing in the sites Newmark studied in California was an area of a relatively soft sediment deposit at great depths and wide extents. When a soil deposit with these characteristics is set in motion and comes in contact with underlying bedrock, the soil deposit responds as if it is in a bowl. This bowl-like response has the potential of increasing the magnitude of surface displacements and velocities, but it also causes the resultant motion to increase periodically. Newmark concluded that a structure built on soft sediments and exposed to a similar motion as the one just described would have a larger response than it would have if it were subject to the same motions in bedrock.

2.1 Earthquake effects

During the earthquake in 1964 in Anchorage, Alaska, large motions resulted in major failures of natural embankments comprised of sensitive clay strata and loose sand layers. An entire block of material about 1,000 ft long and 60 to 100 ft high moved tens of feet horizontally with a PGA between 0.15 g to 0.18 g. Under certain soil conditions, successive slides of limited displacement on the upstream and downstream faces of a dam or embankment may look like the example shown in Figure 2-1.

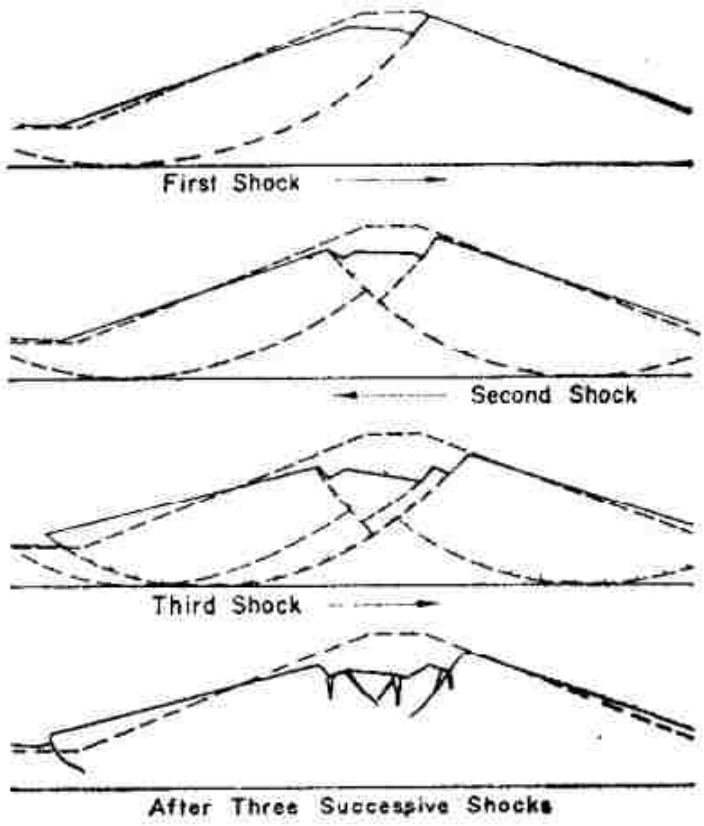

Figure 2-1: Slope deformation pattern (after Ambraseys 1958)

Motions in different types of materials are somewhat different. In general, for both cohesive (clay) and cohesionless (sand) materials where a well-defined plane of weakness can develop, the motion will most likely occur along these planes. However, in highly cohesive materials, the motion is more elastic, and a well-defined plane of weakness may not be formed. A general dynamic analysis of the slope can be performed in these cases, but the situation can become a lot more complex when many different planes of weakness develop. The multiple planes of weakness can make it very difficult to tell which plane might fail first. For this latter case, Newmark's sliding block method should be used only as an approximation, whereas it can be

applied with greater confidence in the case in which the failure plane is known or approximated with high levels of confidence.

An additional important aspect to consider is the resistance to sliding motion. The resistance to earthquake motion of a block of soil or rock that slides on a surface is a function of the shearing resistance of the soil, which is typically a function of soil friction, cohesion, and particle interlock. Although the magnitude of the resistance depends on the amount of displacement due to the constitutive properties of the soil, the displacement necessary to mobilize peak soil resistance is typically not very large. If the block of soil continues to be loaded by the earthquake motion once the peak soil resistance has been reached, then the soil block may experience significant sliding displacements in the downslope direction.

2.1.1 Dynamic Response Theory and the beginnings of Newmark's sliding block method

The dynamic response of a deformable body can be computed by the direct application of Newton's laws of motion. Some basic concepts taken from this theory have been used to provide a simple summary of the responses to earthquake motions. Blume et al. (1961) presented what he called Reserve Energy Technique, in which it was possible to estimate inelastic displacement by equating elastic energy with inelastic energy. Using Blume's methodology, Newmark presented a response spectrum in a dynamic system (Figure 2-2) for a variety of conditions as shown in the tripartite logarithmic plot shown in Figure 2-3.

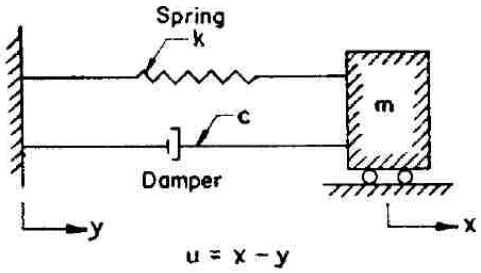

Figure 2-2: System analyzed (after Newmark 1965)

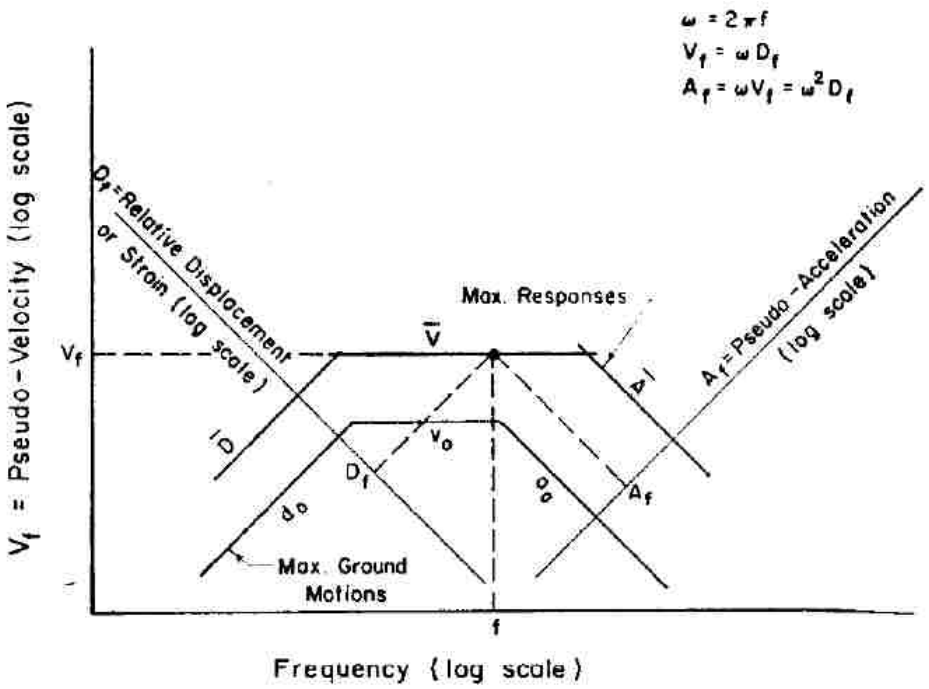

Figure 2-3: Tripartite logarithmic response spectrum (after Newmark 1965).

For a particular motion of the base, the maximum strain in the spring or relative displacement (D_f) of the mass with reference to the base is plotted along the axis sloping up to the left in Figure 2-3. The maximum energy absorbed in this system is represented in terms of pseudo-velocity (V_f) and maximum acceleration of the mass (A_f). Relationships among the pseudo-velocity, pseudo-acceleration, and relative displacement are as shown in Figure 2-3. Maximum

values for ground displacement, ground velocity, and ground acceleration are labeled as d_0, v_0, and a_0, respectively.

The spectrum described in Figure 2-3 is for an elastic system, but inelastic behavior typically better represents soil behavior. Although inelastic behavior is not explicitly labeled in Figure 2-3, the displacement for an inelastic system is bounded by at least one of the following terms shown in Figure 2-3, as defined by Newmark (1965): displacements corresponding to a force bound ($\bar{A}$), an energy bound ($\overline{V}$), or the elastic spectrum bound ($\overline{D}$).

For very large amounts of inelastic or plastic deformation as shown in Figure 2-3, Newmark (1965) showed that the acceleration upper bound ($\bar{A}$) for the inelastic spectrum is so high that the energy bound ($\overline{V}$) is the only one of importance. When large plastic deformations are observed, it is appropriate to consider conservation of energy; preservation of force can be neglected provided the displacement does not exceed the maximum elastic displacement delimited by ($\overline{D}$). At this point, the maximum elastic displacement becomes the upper bound for displacement. Understanding of the bounds of elastic behavior therefore became the key in the development of Newmark's sliding block method.

2.2 Newmark's sliding block

Newmark (1965) presented empirical methods to analyze systems in which resistance varies with displacement. However, the cases accounted for are those in which resistance is rigid-plastic, corresponding to no displacement until the yield point is reached, and the displacement may develop a non-zero value. Figure 2-4 shows applications of Newmark's sliding block model to varying sliding surfaces.

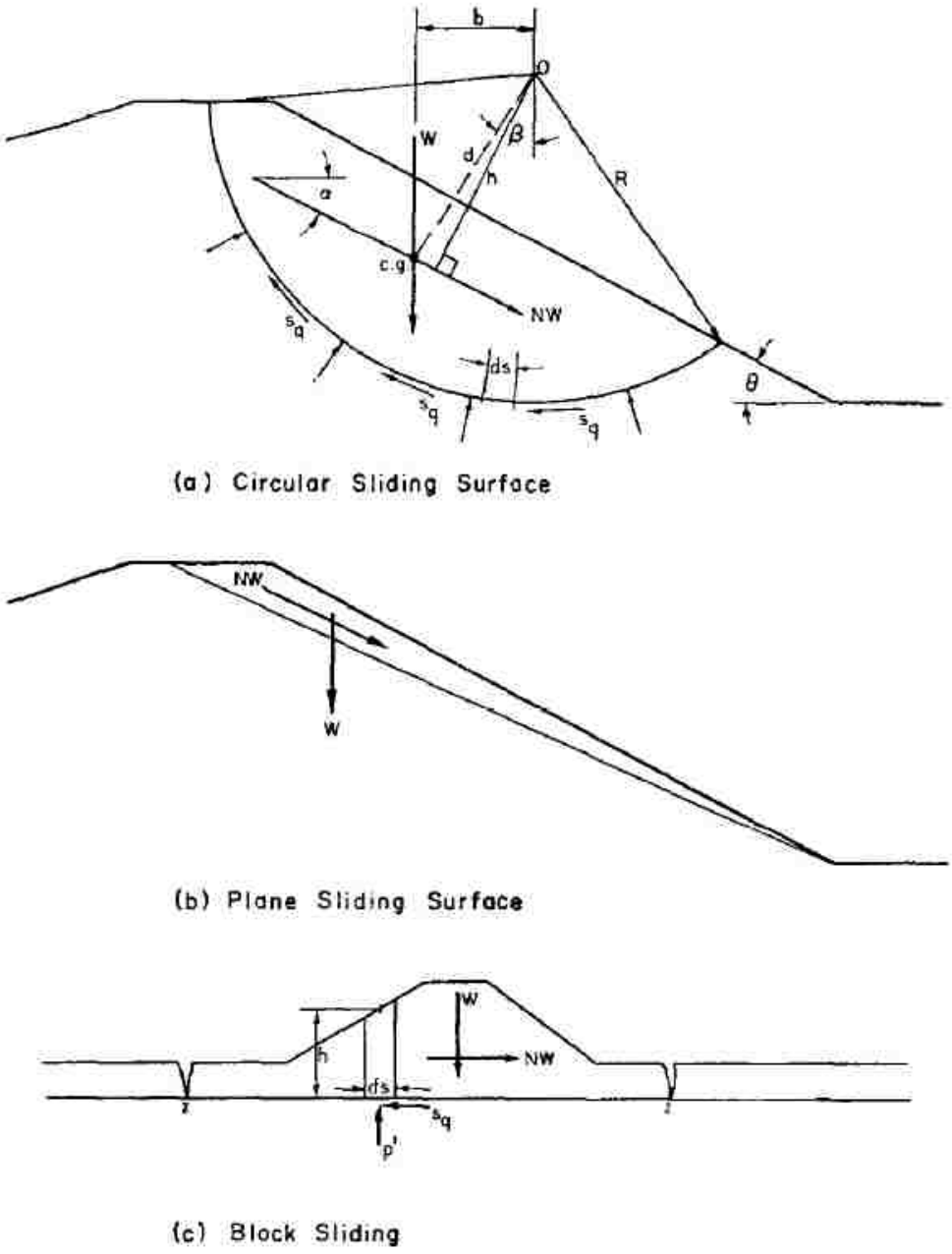

Figure 2-4: Forces acting on sliding mass (after Newmark 1965).

To simplify calculations, Newmark's model only considers the dynamic force acting in the downslope direction to be significant in initiating slope displacements. The resistance coefficient is defined as N (Figure 2-4), which is multiplied by the weight of the sliding mass. N is then

multiplied by g, the acceleration of gravity, which corresponds to a steady acceleration. When this acceleration is acting in the proper direction, it just barely overcomes the resistance to sliding, driving the sliding mass in motion. Later models identify this acceleration as k_y, which is the acceleration required to trigger sliding of a slope.

Another important simplification was that of the cases of motion. To accomplish this, Newmark chose the motion of a rigid block of weight (W, see Figure 2-4), supported on a base that moves as a function of time. The motion of concern therefore becomes the motion of the block relative to the motion of the base. The same model was applied to all the cases of sliding for a dam or embankment as shown in Figure 2-4.

When block sliding is considered, the force N required to mobilize the block is computed by summing the forces in the downslope direction. For a static condition of equilibrium, it can be assumed that the shear stress along the horizontal surface is zero and that the only disturbing force is the effect of the constant horizontal acceleration. The maximum shear strength mobilized under an earthquake therefore becomes the undrained shear strength of the slope material.

When a plane sliding surface is considered, which can be the case with cohesionless materials located on an infinite slope, the most dangerous sliding plane (i.e., the plane with the least amount of relative resistance and greatest amount of relative driving force) is located at shallow depths parallel to the ground surface. In general, the factor of safety against slope failure for this case comes from the relationship between the slope angle and the friction angle of the material.

An important conclusion made by Newmark with his proposed method was that a slope does not necessarily fail just because the dynamic stress induced by earthquake motions reaches the yield strength of the soil material. He found that the stability of a slope during an earthquake

cannot be correctly reflected by the conventional factor of safety of driving forces against resisting forces through a pseudo-static slope stability analysis because the application of the driving forces is actually temporary and not permanent. There are cases when a factor of safety drops below one during periods of the seismic loading, leading to incremental horizontal displacements of the slope. However, catastrophic failure may not occur for such cases. Rather, Newmark found that catastrophic slope failure is governed more by the magnitude of the permanent displacement caused by the earthquake when the factor of safety is below one (Lin & Whitman 1986).

Because permanent deformation is arguably the item of greatest concern in slope stability, Lin and Whitman (1986) suggested two things to consider as permanent slope deformation is evaluated:

1) Important ground motion characteristics must be properly incorporated, and
2) The physical mechanism of the permanent displacement buildup must be incorporated in the formulation.

Newmark (1965) was the first to experiment with incorporating a suite of earthquake motions to develop simplified engineering design charts in which one could estimate slope displacements. Limitations to his assumptions stemmed from the fact that only four earthquakes were included in his study. Examples of these limitations include the slope displacements provided in Newmark's design charts, which were normalized to a maximum acceleration of 0.5 g and maximum velocity of 76.2 cm/s (Newmark 1965). With computer software availability, engineers are now able to perform Newmark sliding block analyses using earthquake acceleration time histories with much more data than has been collected in the last few decades, thus improving the incorporation of ground motion characteristics in the models.

In an attempt to address the proper use of a physical mechanism for permanent displacements, several simplified Newmark-based models have been presented over the years. The first thing that researchers needed to consider was the set of simplifying assumptions that Newmark (1965) proposed, which included:

1) The soil behaves in a rigid, perfectly plastic manner,

2) Displacements occur along a single, well defined slip surface, and

3) The soil does not undergo strength loss as a result of shaking.

Awareness of Newmark's assumptions in developing his sliding block method made it apparent that there could be a better way to approximate soil behavior. In an attempt to obtain better predictions of seismic slope displacements, many researchers developed modified models of the original Newmark sliding block model.

2.2.1 Modified Newmark analysis

Many researchers later modified the seismic slope displacement method introduced by Newmark (1965). For example, Kramer and Smith (1997) considered dynamic response of soil above a potential failure zone to model a more realistic response from the sliding soil. Kramer and Smith focused their study on landfills because they are generally constructed with softer materials having many different planes of weakness that can drive critical potential failure surfaces to greater depths than those encountered in other native and/or non-native soil slopes.

The modified version of the Newmark analysis developed by Kramer and Smith (1997) became a simple and practical method of seismic slope stability analysis that would account for the dynamic response of a landfill and for the effects of permanent displacement on that seismic response. In their modified Newmark analysis, the single rigid block was replaced by two or more

blocks connected by springs and dashpots. The masses, spring constants, and dashpot coefficients were selected to approximate the dynamic characteristics of a potential failure mass.

After testing the proposed modified Newmark method, which accounted for a dynamic response, researchers observed permanent displacements to be more consistent with those predicted by nonlinear dynamic response analyses and appeared to represent a practical approach for analyzing seismic slope displacement in many different types of soil slopes. Another advantage of the modified Newmark method by Kramer and Smith (1997) was that it accounted for progressive failure by using peak shear strengths initially to define the soil resistance but then gradually switching to degraded residual strengths as shear strains increased in the soil. This was a viable solution to the third assumption of the original Newmark model that assumed that soil would not undergo any soil strength reduction during and after earthquake shaking.

2.2.2 Inclined plane studies of the Newmark's sliding block method

Although some of the assumptions made in the original Newmark method were addressed with the introduction of the modified method as presented by Kramer and Smith (1997) and others, one of the main assumptions that remained was that a mass of soil behaves like a rigid block. Wartman et al. (2003) considered the seismic-induced displacement, the dynamic response of a rigid block, and deformable columns of soil on an inclined plane. They tested both scenarios to check the validity of Newmark's rigid block assumption and compared it with a deformable column of soil, which is closer to how soil actually behaves.

The experiments were conducted in phases in which different input motions were used, including sinusoidal, frequency sweep, and recorded earthquake input motions. The first experiment required a steel block placed on an inclined plane and shaken on a single-degree-of-

freedom hydraulic shaking table. A geosynthetic interface was used to provide resistance to sliding without adhering the block to the incline. The second experiment was done in soil columns at different moisture contents. The soil used for the test was a high-plasticity clay. The soil column was surrounded by a latex membrane and two plastic disks on each end. In both experiments, the natural frequency of the sliding mass was measured and, as both experiments were performed, accelerations were recorded. The accelerations were integrated to obtain displacements produced by the shaking.

The results obtained from these tests indicated that the Newmark (1965) sliding block procedure underestimates seismic slope displacement of a deformable mass when the predominant frequency of the shaking (earthquake) motion is somewhat less than or near the natural frequency of the sliding mass. The tests also found that the sliding block procedure generally over-predicts seismic slope displacement when the predominant frequency of the input motion is significantly greater than the natural frequency of the sliding mass.

2.3 Simplified Newmark sliding block models

After testing of the original Newmark sliding block method, researchers obtained results as explained in the previous section. Many Newmark sliding block simplified models have subsequently been developed over the years. Some of the models used today are based on Newmark's sliding block method with the assumption of a rigid block. When the rigid block assumption remains, the engineer must understand that the displacements produced are just rough estimates of actual conditions in the field. Others have decided to use a non-rigid block to mimic conditions that are closer to what one might encounter in the field. Researchers have commonly used generalized soil and slope assumptions to perform thousands of Newmark sliding block

calculations using large suites of actual earthquake time histories. From these computed displacements, empirical seismic slope displacement models have been developed. These models have been developed for both the rigid soil block assumption and the flexible soil block assumption. This research incorporates only rigid soil block models for simplification. As mentioned previously, with the rigid block assumption, engineers must be fully aware that the displacements computed with this approach are likely inaccurate but are still recognized by most engineers today as a useful relative indicator of seismic slope displacement hazard (Saygili and Rathje 2008). This research uses two different seismic slope displacement empirical models. The models included in this study were developed by Rathje & Saygili (2009) and Bray & Travasarou (2007).

2.4 Rathje and Saygili (2009) model

The Rathje and Saygili (2009) model is an update and improvement of the Saygili and Rathje (2008) model. The revised model includes a *Mw* term that reduces scatter in the model and also includes an improved estimate of the standard deviation. This method utilizes a probabilistic framework for computing the annual rate of exceedance of different levels of displacement in the form of a hazard curve for sliding displacement. The model focuses on the computation of displacements on natural slopes, in which case the Newmark's rigid sliding procedure arrives at reasonable estimates.

The analysis incorporates uncertainties in the prediction of earthquake ground shaking, in the prediction of sliding displacement, and in the assessment of soil properties. The two main parameters required to compute the earthquake-induced sliding displacement of a slope are k_y for the slope and a as previously defined.

K_y represents the horizontal acceleration that results in a factor of safety of 1.0 and initiates sliding in the slope. K_y can be derived from an infinite slope approximation of a shallow failure surface, along with the geometry and shear strength parameters of the slope with the following equations based on Rathje and Saygili 2009.

$$k_y = \frac{(FS-1)\cdot g}{(\cos\alpha \cdot \tan\phi + 1/\tan\alpha)} \tag{2-1}$$

$$FS = \frac{c'}{\gamma \cdot t \cdot \sin\alpha} + \frac{\tan\phi'}{\tan\alpha} - \frac{\gamma_w \cdot m \cdot \tan\phi'}{\gamma \tan\alpha} \tag{2-2}$$

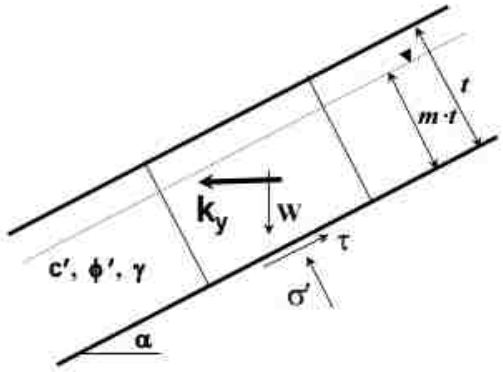

Figure 2-5: Infinite slope conditions to calculate k_y (after Rathje & Saygili 2009)

The Rathje and Saygili (2009) model incorporates both a scalar and a vector model. The scalar model predicts sliding displacement in terms of a single ground motion parameter *PGA* or maximum ground acceleration *(a_{max})* and the M_w. The vector model includes two ground motion parameters, *PGA* and *PGV*. For the purposes of simplification of this study, the scalar model is the only one that is used.

The empirical displacement model is based on rigid sliding block displacements computed from recorded horizontal acceleration-time histories. Over 2,000 motions are used in the development of the model, and each is scaled by factors of 1.0, 2.0, and 3.0. Displacements are calculated for k_y values of 0.05, 0.1, 0.2, and 0.3. The proposed model is given as follows:

$$\ln D = 4.89 - 4.85\left(\frac{k_y}{a_{\max}}\right) - 19.64\left(\frac{k_y}{a_{\max}}\right)^2 + 42.49\left(\frac{k_y}{a_{\max}}\right)^3 - 29.06\left(\frac{k_y}{a_{\max}}\right)^4 + 0.72\ln\left(a_{\max}\right) + 0.89\left(M - 6\right) \quad (2\text{-}3)$$

where D is the seismic slope displacement in units of cm, k_y is in units of gravity (g), $a_{\max}$ is also in units of g, and M is unitless. The standard deviation is calculated as follows:

$$\sigma_{\ln} = 0.732 + 0.789\left(\frac{k_y}{a_{\max}}\right) - 0.539\left(\frac{k_y}{a_{\max}}\right)^2 \quad (2\text{-}4)$$

2.5 Bray and Travasarou (2007) model

Bray and Travasarou (2007) propose a simplified semi-empirical predictive relationship for estimating permanent displacements due to earthquake-induced deviatoric deformations. The basis of this method is the use of a nonlinear, fully coupled, stick-slip sliding block to capture the dynamic performance of an earth structure such as an earth dam, natural slope, compacted earth fill, or municipal solid-waste landfill. This model also seeks to account for uncertainty in assessing the likely performance of the earth system under earthquake motions.

The model is created by implementing 688 recorded ground motions to compute seismic slope displacements. A single model is developed to capture the primary influence of the system's k_y its initial fundamental period (T_s), and the ground motion's spectral acceleration at a period of

$1.5T_S$. Like the Rathje and Saygili (2009) model, this is a fully probabilistic model in which the probability of "zero" displacement (≤1 cm) occurring from the distribution of "nonzero" displacement is not included in the calculation of total probability, so that very low values of calculated displacement do not bias the results. The model is proposed to be implemented in both a fully probabilistic framework as well as used deterministically to evaluate seismic slope displacement potential.

One of the main aspects for the prediction of seismic slope displacement deals with the determination of an intensity measure that accounts for the intensity of the shaking affecting the slope being analyzed. Rathje and Saygili (2009) propose the use of a second intensity measure, but Bray and Travasarou (2007) use only one intensity measure, which is spectral acceleration.

Although the Bray and Travasarou (2007) methodology has the ability to model the sliding of a non-rigid block, for the purposes of this research the Newmark rigid sliding block case (T_s=0) is used. The natural logarithm of the seismic displacement can be computed as follows:

$$\ln(D) = -0.22 - 2.83\ln(k_y) - 0.333\left(\ln(k_y)\right)^2 + 0.566\ln(k_y)\ln(a_{\max}) + 3.04\ln(a_{\max}) \\ -0.244\left(\ln(a_{\max})\right)^2 + 0.278(M-7) \tag{2-5}$$

where the standard deviation for this model is $\sigma_{\ln(D)} = 0.67$.

Over the years, the Bray and Travasarou (2007) model has been used in different ways. For example, in 2013 the California Department of Transportation (Caltrans) proposed guidelines on foundation loading and deformation close to bridge abutments. The guidelines were based on specific recommendations for the calculation of loads and deformation demands on bridge foundations and abutments resulting from liquefaction-induced ground spreading. The design they proposed includes a characterization of the seismic hazard using *PGA* and M_w, determination of

areas in which soil could liquefy (experience a reduction of strength and stiffness under earthquake shaking), and finding a model that would fit the behavior of the soil under specific conditions.

The displacement of the ground surface resulting from liquefaction can be highly variable and depends upon local topography, soil stratigraphy, material properties, and ground motion. Because of the complexity of obtaining all information required about these parameters, Caltrans proposed the use of several simplified Newmark sliding methods, including the Bray and Travasarou (2007) model. Caltrans identified two sources of failure: strain and shear. The Bray and Travasarou (2007) model was recommended for estimation of shear-induced failures as shown in Figure 2-6. However, one should remember that simplified Newmark sliding block models like the Bray and Travasarou (2007) and Rathje and Saygili (2009) models were never intended to be used with liquefiable soils.

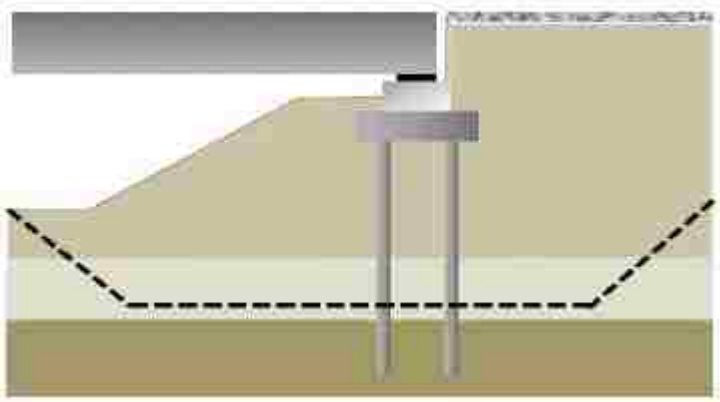

Figure 2-6: Shear failure surface near bridge abutment (after Caltrans 2013)

2.6 Summary

This chapter provided background information about earthquake effects and methods developed through time to estimate earthquake-induced slope displacements. The Newmark

sliding block method was introduced together with assumptions, tests performed to prove its validity, and recommended applications. Some of the assumptions made in the original Newmark sliding block method were challenged by some researchers, resulting in the creation of modified Newmark sliding block methods. Two of the methods available for estimating seismic slope displacements were selected for this study, including the Rathje & Saygili (2009) and Bray & Travasarou (2007) models. The following chapter discusses how these two methods fit within the performance-based earthquake engineering framework.

3 PROBABILISTIC ANALYSIS AND PERFORMANCE-BASED EARTHQUAKE ENGINEERING

In developing appropriate models to predict seismic slope displacements, proper characterization of the seismic loading is one of the largest challenges. In practice, it is typical for engineers to compute seismic slope displacements by performing a deterministic analysis, in which a suite of earthquake ground motions appropriate for a design event is selected. The sliding displacement for the selected ground motion is computed using k_y of the slope. The displacements corresponding to the median ground motion parameters and also to the median plus a standard deviation are typically computed.

Ground motion parameters computed from probabilistic seismic hazard analysis (PSHA) are also used for computation of seismic slope displacements. However, because these ground motions are an aggregated representation of the hazard from multiple seismic sources, engineers often struggle to select the "most appropriate" set of seismic loading parameters (i.e., M_w, a_{max}) for computation of seismic slope displacements. Most engineers select seismic loading parameters using the deaggregation of the probabilistic ground motion, which typically specifies both mean and modal estimates of M_w and source-to-site distance (R). The use of probabilistic ground motions in a deterministic response analysis is called a *pseudo-probabilistic approach* (Rathje and Saygili 2008). Several researchers have presented results where the pseudo-probabilistic method showed biased and inconsistent estimates of various geotechnical response parameters (Franke and Kramer 2014, Franke et al. 2014b, Franke et al. 2014c, Kramer and Mayfield 2007, Mayfield et al. 2010,

Rathje and Saygili 2008). Unfortunately, most engineering practitioners in the United States continue to adopt the pseudo-probabilistic approach in their designs due to requirements from current seismic design provisions and/or current standards of engineering practice.

As probability has become important in the attempt to account for variability in hazard analysis, The Pacific Earthquake Engineering Research (PEER) Center developed a more robust methodology. The main objective of this methodology was to break down the performance assessment and design process of earthquake hazard analysis into logical elements so that decision-makers could use important probabilistic information to make informed decisions. This proposed methodology is called performance-based earthquake engineering (PBEE).

A performance-based approach to seismic slope displacement computation uses a probabilistic soil/ground response model and considers contributions from all possible M_w and R combinations at all ground motion hazard levels (Kramer 2008). This approach has proven to produce more reasonable results in areas of low to medium seismicity where the selection of appropriate seismic loading parameters is less clear to engineers. The challenge with this approach has been its implementation in routine projects because the computation of full performance-based seismic slope displacements can be lengthy and complicated. Chapter 4 presents a solution to this problem with the derivation of a simplified performance-based seismic slope displacement model. The remainder of this chapter reviews concepts related to the full performance-based framework.

3.1 Seismic hazard analysis

Seismic hazard analyses involve the quantitative estimation of ground-shaking hazards at a particular site. Seismic hazards can be analyzed deterministically, as when a particular earthquake scenario is assumed, or probabilistically, in which uncertainties in earthquake size,

location, and time of occurrence are explicitly considered. Although a seismic hazard analysis is a critical part of the development of design ground motions, other parts including the consideration of potential effects of local site effects can highly influence the design of ground motions used in an analysis.

3.1.1 Identification and evaluation of earthquake sources

When evaluating seismic hazards for a particular site or region, all possible sources of seismic activity must be identified, and their potential for generating strong ground motions must be evaluated. The availability of modern seismographs and seismographic networks has simplified the observation and interpretation of current earthquakes. The occurrence of a large earthquake is now recorded by hundreds of seismographs around the world. Within hours, seismologists can estimate its M_w, locate its rupture surface, and even evaluate source parameters.

The current ability to identify and locate all earthquake sources is a relatively recent development, particularly when compared with the time scales in which large earthquakes usually occur. The fact that no strong motions have been instrumentally recorded in a particular area does not guarantee that they have not occurred in the past or that they will not occur in the future. This is why identification of seismic sources requires geologic evidence, tectonic evidence, and historical seismicity besides instrumental seismicity (Kramer 1996).

3.1.2 Deterministic seismic hazard analysis

A deterministic seismic hazard analysis (DSHA) involves the development of a particular seismic scenario upon which a ground motion hazard evaluation is based. The scenario consists of the postulated occurrence of an earthquake of a specified size occurring at a specified location. Typically, a DSHA is performed in four steps (Reiter 1990):

1) Identification and characterization of all earthquake sources capable of producing significant ground motion at the site. The source characterization will include a definition of geometry and earthquake potential at each source.

2) Selection of a source-to-site distance parameter for each source zone (i.e., R). In most cases, the shortest distance between the source zone and the site of interest is selected. The distance can be expressed as an epicentral or hypocentral distance, depending on the measure of the distance of the predictive relationship used in step 3.

3) Selection of the "controlling earthquake," usually expressed in terms of some ground motion parameter at the site. The selection is made by comparing the levels of shaking produced by earthquakes assumed to occur at the distances specified in step 2. The controlling earthquake is described in terms of M_w and R.

4) The hazard at the site is formally defined, usually in terms of the ground motions produced at the site by the controlling earthquake. Its characteristics are usually described by one or more ground motion parameters obtained from predictive relationships. Some of these include peak acceleration, peak velocity, and response spectrum ordinates, which are used to characterize the seismic hazard.

Figure 3-1 shows a schematic of the DSHA procedure previously described.

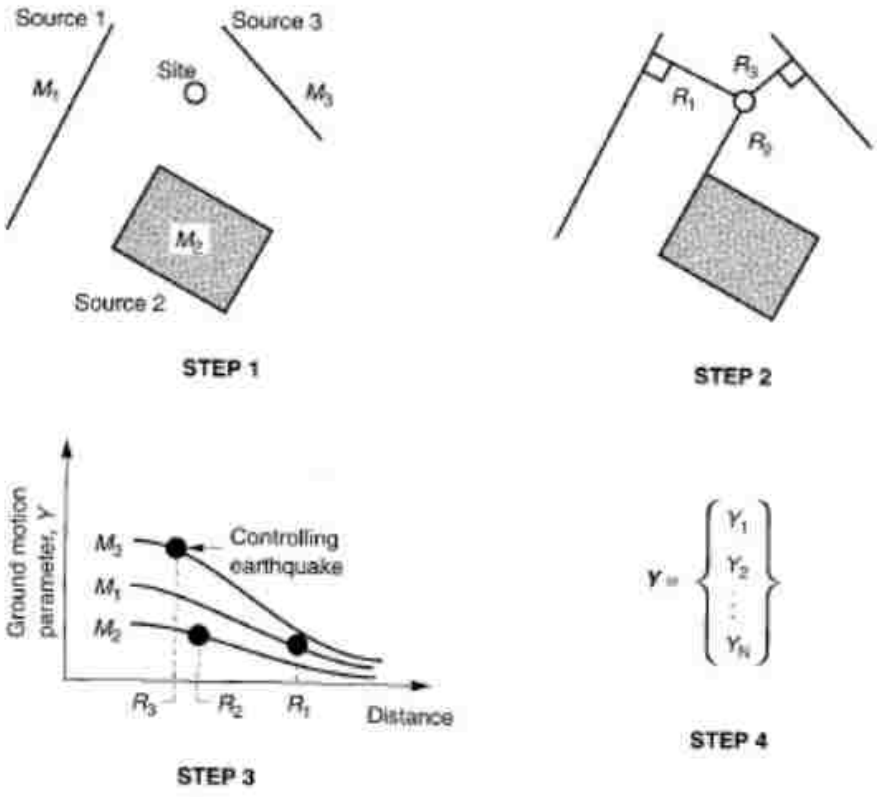

Figure 3-1: Four steps of a deterministic seismic hazard analysis (after Kramer 1996).

A DSHA provides a straightforward framework for the evaluation of worst-case ground motions. A limitation of this method is that it does not provide information on the likelihood of it occurring where it is assumed to occur, the level of shaking that might be expected during a specific finite period, or the effects of uncertainties in the various steps required to compute the resulting ground motion characteristics. Ultimately, one of the main aspects of a DSHA is that it will involve subjective decisions, particularly regarding earthquake potential, that can require the expertise in the field of earthquake engineering.

3.1.3 Probabilistic seismic hazard analysis

Probabilistic concepts have revolutionized seismic hazard analyses in that uncertainties in the size, location, rate of recurrence, and variation of ground motions of earthquakes can be accounted for. A PSHA provides a framework in which these uncertainties can be identified, quantified, and combined in a rational manner to provide a more complete picture of the seismic hazard.

As was the case of a DSHA, the PSHA methodology can be described in four steps (Reiter 1990):

1) Identification and characterization of earthquake sources, which is the same first step of a DSHA with the exception that the probability distribution of potential rupture locations within the source must also be characterized. Usually, uniform probability distributions are assigned to each seismic source zone, implying that earthquakes are equally likely to occur at any point within the source zone. The seismic source zone's distributions are combined with the source geometry to obtain what is called a probability distribution source-to-site distance. A DSHA, on the other hand, will assume that the probability of occurrence is one at the points in each source zone closest to the site and zero everywhere else.

2) Characterization of the seismicity or temporal distribution of earthquake recurrence. This is done by using a recurrence relationship, which specifies the average rate at which an earthquake of some size will be exceeded.

3) The ground motion produced at the site by earthquakes of any possible size occurring at any possible point in each source zone must be determined using predictive

relationships. The uncertainty of these predictive relationships is also accounted for in a PSHA.

4) The uncertainties in earthquake location, earthquake size, and ground motion parameter prediction are combined to obtain the probability of a particular time period.

The following figure presents a graphical representation of the four steps of a PSHA.

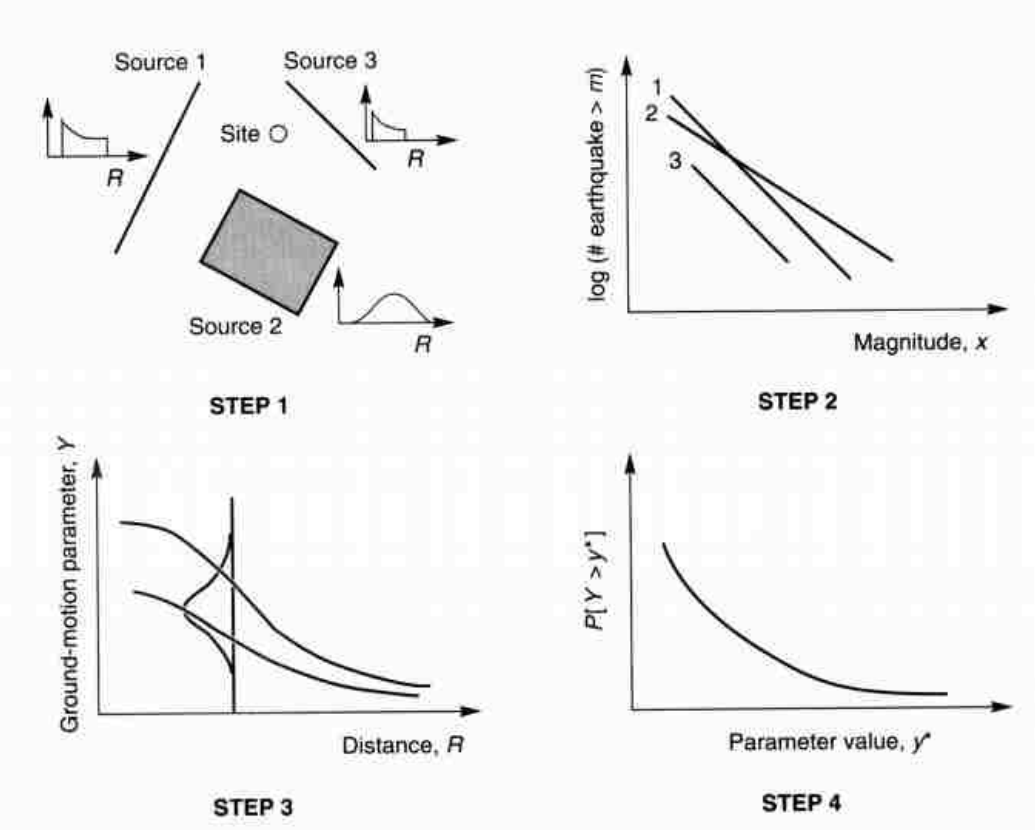

Figure 3-2: Four steps of a probabilistic seismic hazard analysis (after Kramer 1996).

One of the most important parts of a PSHA is that of the earthquake source characterization. After the earthquake sources are properly characterized, the engineer must consider the uncertainty of the spatial characteristics of the source and of the distribution of earthquakes within that source, the distribution of earthquake size for each source, and the distribution of earthquakes with time.

Spatial Uncertainty

The geometry of earthquake sources depends on the tectonic processes involved in their formulation. Point sources are those in which earthquakes originate from zones that are small with very distinct characteristics, such as zones near volcanoes. Areal sources are those in which fault planes are clearly defined and where earthquakes can occur at many different locations (Kramer 1996). Volumetric sources are areas in which earthquake mechanisms are poorly defined, or where faulting is so extensive that individual fault effects cannot be clearly identified. In seismic hazard analyses, the source zones are defined depending on the relative geometry of the source and site of interest and on the quality of the information available about the sources. Another important assumption that is made is that earthquakes are generally uniformly distributed within a source zone. This happens in most cases since uniform source-to-site distance distributions are used when defining spatial uncertainty in predictive relationships within a PSHA. The uncertainty in source-to-site distance is usually described by a probability density function.

Size Uncertainty and Recurrence Laws

After identifying the earthquake sources, the size of the earthquake that can be expected in the source zone must be evaluated. In general, the source zone will produce earthquakes of different sizes up to the maximum earthquake, with smaller earthquakes occurring more frequently than larger ones. The distribution of earthquake sizes in a given period of time is described as a recurrence law. A basic assumption of a PSHA is that the recurrence law obtained from past seismicity is appropriate for the prediction of future seismicity. In general, recurrence laws involve taking the number of exceedances of each M_w and dividing it by the length of the time period of interest, which value is defined as the mean annual rate of exceedance (λ_m). For example, the λ_m

of a small earthquake is greater than that of a very large earthquake. Another important term that is used to describe recurrence is the return period, which is the inverse of the annual rate of exceedance.

Predictive Relationships

In most cases, predictive relationships are obtained empirically by least-squares regression on a particular set of strong motion parameter data in which scatter will be a concern reflecting the different areas of uncertainty. The probability that a particular ground motion parameter Y exceeds a certain value (y*), for an earthquake of a given magnitude (m), occurring at a given distance (r), is illustrated by equation 3-1.

$$P\left[Y > y^* \middle| m, r\right] = 1 - F_Y(y^*) \tag{3-1}$$

where $F_Y(y)$ is the value of the cumulative density function of Y at magnitude m and distance r.

Temporal Uncertainty

When computing the probabilities of various hazards occurring in a given time period, the distribution of earthquake occurrence with respect to time must be considered. The Poisson model is one of the tools used to describe temporal occurrence of an earthquake. Poisson processes have the following properties:

1) The number of occurrences in one-time interval is independent of the number that occurs in any other time interval.
2) The probability of occurrence during a very short time interval is proportional to the length of the time interval.

3) The probability of more than one occurrence during a very short time interval is negligible.

The Poisson model is used to account for the probability of a random variable (N). The number of occurrences of a particular event during a given time interval is given in equation 3-2.

$$P\left[N = n\right] = \frac{(\lambda t)^n e^{-\lambda t}}{n!} \tag{3-2}$$

When the event of interest is the exceedance of a particular M_w, which is usually the case in a PSHA, the Poisson model can be combined with a suitable recurrence law to predict the probability of at least one λ in a period of t years as shown in equation 3-3.

$$P\left[N \geq 1\right] = 1 - e^{-\lambda_m t} \tag{3-3}$$

Seismic Hazard Curves

The results of a PSHA can be expressed in many different ways. All involve some level of probabilistic computations to combine the uncertainties in earthquake size, location, frequency, and effects to estimate seismic hazard. A common approach involves the development of hazard curves, which indicate λ of different values of a selected ground motion parameter. The seismic hazard curves can then be used to compute the probability of exceeding the selected ground motion parameter in a specified period of time. Seismic hazard curves can be obtained for individual source zones and combined to express the aggregate hazard at a particular site. Calculations required to build a hazard are fairly simple as described in the following paragraphs.

For a given earthquake occurrence, the probability that a ground motion parameter (Y) will exceed a particular value (y*) can be computed using the total probability theorem,

$$P\left[Y > y^*\right] = P\left[Y > y^* \middle| X\right] P\left[X\right] = \int P\left[Y > y^* \middle| X\right] f_x(X) dx \tag{3-4}$$

where X is a vector of random variables that influence Y. In most cases the quantities of X are limited to m and r. Under the assumption that m and r are independent, the probability of exceedance can be written as

$$P\left[Y > y^*\right] = \iint P\left[Y > y^* \middle| m, r\right] f_M(m) f_R(\mathrm{r}) dm dr \tag{3-5}$$

where the probability of Y exceeding y* is obtained from the predictive relationship of $f_M(m)$ and $f_R(r)$, which are the probability density functions for magnitude and distance, respectively.

Deaggregation

A PSHA is a technique for estimating the annual rate of exceedance of a specified ground motion at a site while taking into account both known and suspected earthquake sources and their corresponding uncertainties. The relative contributions of the various sources to the total seismic hazard are determined as a function of their occurrence rates and their ground motion potential. The separation of the exceedance contributions into bins whose base dimensions are M_w and R is called deaggregation (Harmsen et al. 1999). As the contributions of a total seismic hazard are identified, these can be incorporated in the computation of λ as functions of both m and r as shown in equation 3-6.

$$\lambda_{y^*}(m_j, r_k) \approx P\left[M = m_j\right] P\left[R = r_k\right] \sum_{i=1}^{N_s} v_i P\left[Y > y^* \middle| m_j, r_k\right] \tag{3-6}$$

If the site of interest is a region of (N_s) potential earthquake sources, each of which has an average rate of threshold magnitude exceedance (v_i), the total average exceedance rate for the region is given by the summation, which is multiplied by the probability of exceedance of both magnitude (m_j) and source-to-site distance (r_k). An example of a hazard curve for *PGA* is presented in Figure 3-3.

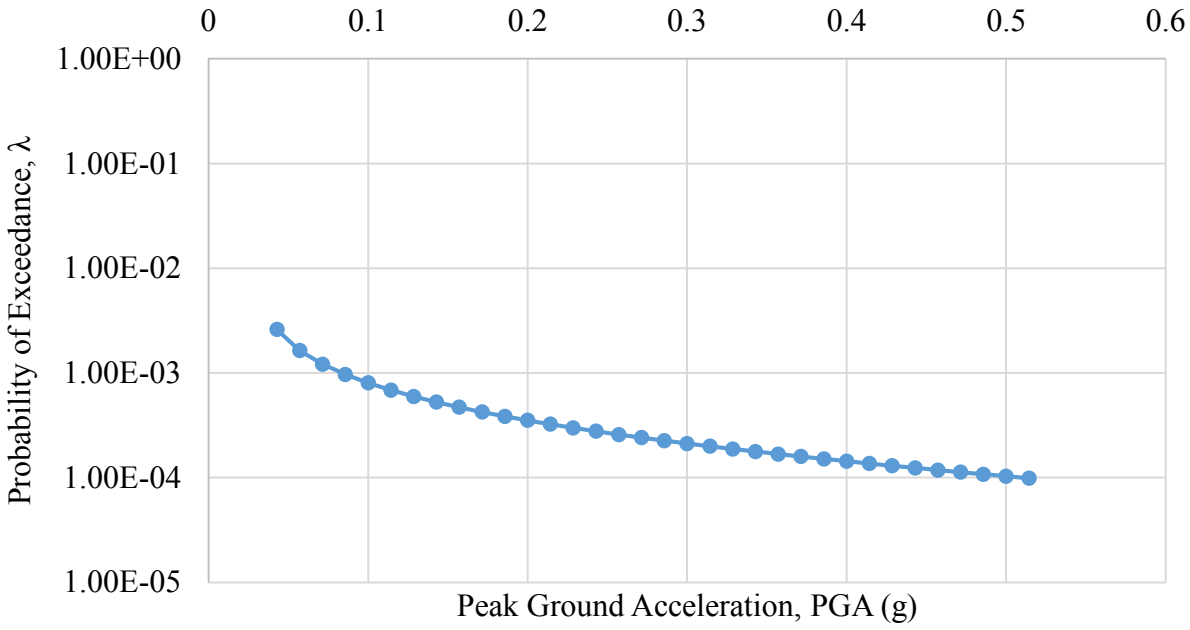

Figure 3-3: Example hazard curve

Figure 3-3 is an example hazard curve corresponding to the probability of exceeding given PGA values at certain return periods of interest. An important aspect that was accounted for in this hazard curve was the variability in the ground motion prediction at a specific site. Once a ground motion hazard curve is created, a dominant ground motion from the location can be selected. The selected ground motion could at that point be used in a probabilistic equation for the generation of a seismic slope displacement hazard curve for example. With the information provided in a hazard

curve, the engineer can use the data to make more informed decisions as to the hazard that could be expected in a particular area.

3.2 Performance-based earthquake engineering framework

The PEER Center developed a new methodology for hazard assessment (Porter 2003). The PBEE methodology differs from other designs such as load-and-resistance-factor design in that the latter seeks to assure performance primarily in terms of failure probability of individual structural components, whereas the PBEE seeks to address performance primarily at the system level in terms of risk of collapse, fatalities, repair costs, and post-earthquake loss of function. In design, when considering global performance level, it must be detailed in terms of performance of individual elements. A design is believed to satisfy its global objectives if it achieves the acceptable performance criteria as established by some consensus standard such as the Vision 2000 report (SEAOC 1995). The performance criteria of the Vision 2000 report are shown graphically in Figure 3-4.

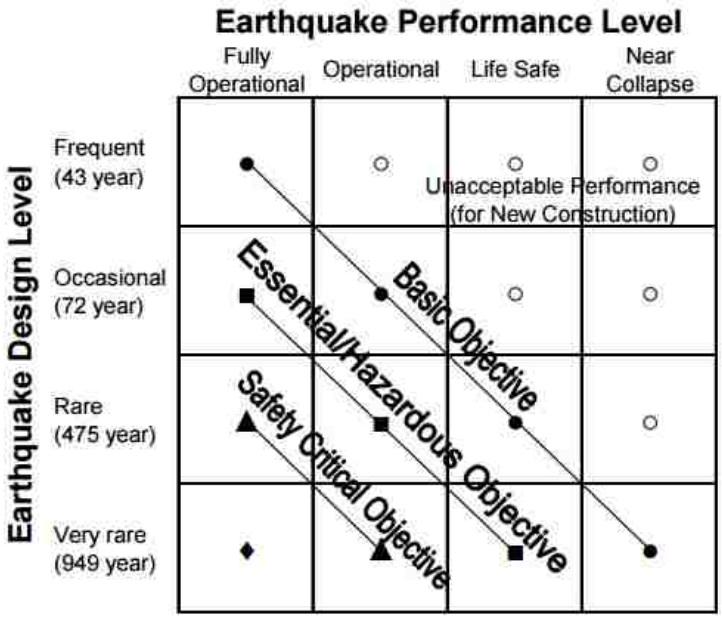

Figure 3-4: Basic approach of Vision 2000 (after SEAOC 1995).

The PBEE framework came in full force following the release of the Vision 2000 report. The PBEE framework is characterized by reporting its principal outputs as system-level performance measures in terms of probabilistic estimates of repair costs, casualties, and loss-of-use duration. The main objective of the methodology is to estimate the frequency with which a particular performance metric will exceed several levels for a design given at a specific location, which can be used to create probability distributions of performance measures during any planning period of interest (in a way of a hazard curve). From the frequency and the probability distributions, a point performance metric meaningful for stakeholders can be extracted and used as an upper-bound economic loss during the planning period (Porter 2003).

The PBEE methodology involves four stages: hazard analysis, structural analysis, damage analysis, and loss analysis. The methodology is graphically described in Figure 3-5.

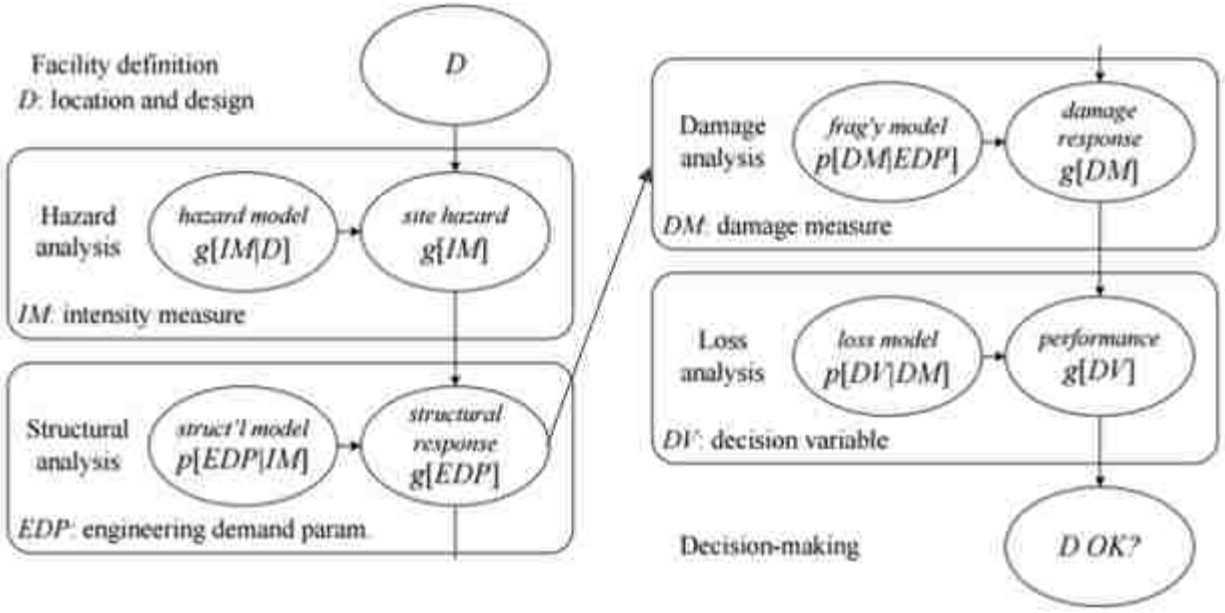

Figure 3-5: PEER analysis methodology (after Porter 2003)

As Figure 3-5 shows, seismic hazard analyses are just the beginning of the ultimate goal of PBEE in the decision-making process, but it is an important step in the continuation of the process towards making well-educated decisions when the lives of people and the services that infrastructure can provide are on the line.

With the goal in mind of improving the way earthquake analysis can be used in making decisions related to design and measuring the amount of risk and damage that an organization might be willing to take, this research focuses on developing a simplified approach for computing probabilistic performance-based analyses for seismic slope displacements. A simplified approach is valuable because many engineers might not be completely comfortable running a full performance-based analysis, and they subsequently fail to benefit from the application of this analysis as it has been explained.

3.3 Summary

This chapter introduced the different analyses used in estimating earthquake hazards, including deterministic, probabilistic, and pseudo-probabilistic approaches. The concept of a hazard curve was introduced, as well as its use in a probabilistic assessment. The performance-based earthquake engineering framework proposed by the PEER Center was outlined in preparation for the introduction of the simplified performance-based seismic slope displacement procedure in the following chapter.

4 SIMPLIFIED PROBABILISTIC PERFORMANCE-BASED SEISMIC SLOPE DISPLACEMENT PROCEDURE

Probabilistic assessment of seismic slope displacements is often based on permanent sliding displacement due to earthquake shaking as mentioned in previous chapters. Empirical probabilistic seismic slope displacement models presented in Chapter 2, Rathje & Saygili (2009) and Bray & Travasarou (2007), are used in this research to create a numerical tool to compute full performance-based seismic slope displacements. The capability to evaluate these models in a probabilistic manner was added to the specialized software, *PBLiquefY* (Franke et al. 2014) as part of this research. The use of specialized software is important in the process of developing a simplified procedure because a full performance-based seismic slope displacement analysis is required for the generation of seismic slope displacement reference parameter maps, which are introduced in this chapter.

4.1 Performance-based implementation of seismic slope displacement models

The performance-based application of a seismic slope displacement model involves the incorporation of a probabilistic hazard framework such as that presented by Rathje and Saygili (2008) and Rathje and Saygili (2009). Rathje and Saygili explain that variability in ground motion can be more explicitly considered in a slope displacement analysis through a probabilistic assessment of the ground motion. A fully probabilistic seismic slope displacement analysis incorporates a seismic hazard curve for the ground motion parameter of interest. This curve

therefore defines λ_{GM} of different levels of ground motion. This hazard curve accounts for all potential earthquake/ground motion scenarios (i.e. *M*, *R*), the probability of occurrence of each scenario, and the probability that a ground motion level exceeds various specified values.

To account for the variability in the sliding block displacement, a fully probabilistic analysis examines all possible displacements generated by the probabilistic ground motions. The fully probabilistic seismic slope displacement analysis convolves the full ground motion hazard curve with the empirical seismic slope displacement model and its corresponding uncertainty, resulting in a seismic slope displacement hazard curve. This curve provides the mean annual rate of exceedance for the different levels of sliding displacement (λ_d). Equation 4-1 presents the equation for probabilistic seismic slope displacement framework introduced by Rathje and Saygili (2008), and Rathje and Saygili (2009); which gives the corresponding λ_d exceeding some slope displacement (d^*) as

$$\lambda_{d^*} = \sum P\left[D > d^* \mid \mathrm{GM}_i, k_y \right] \cdot \Delta\lambda_{GM} \tag{4-1}$$

where $\sum P\left[D > d^* \mid \mathrm{GM}_i, k_y \right]$ is the conditional probability of exceeding displacement d^* given ground motion level (GM_i),k_y, and the incremental mean annual rate of exceedance ($\Delta\lambda_{GM}$) comes from the ground motion hazard curve. The sum in the equation represents the integration over all possible ground motion levels. Because only a single ground motion parameter is used to predict the displacement (*D)*, this approach is considered a scalar probabilistic assessment.

4.1.1 Application of the fully probabilistic methodology of sliding displacements to a site in northern California (Rathje and Saygili 2009)

To demonstrate the probabilistic procedure for sliding displacements, Rathje and Saygili (2009) present a hypothetical landslide site in northern California. Potential slides are considered with k_y values of 0.1 g and 0.2 g.

The ground motion hazard is computed using the fault system representation provided by personal communication from Rathje and Saygili and Dr. Norm Abrahamson in 2007. Figure 4-1 shows the site location with the 12 faults that are used in computing the ground motion hazard for the hypothetical scenario. The ground motion hazard for *PGA* is computed using the scalar PSHA code presented by Abrahamson (2007), and Boore and Atkinson (2008). The hazard curve generated from this analysis can be seen in Figure 4-2.

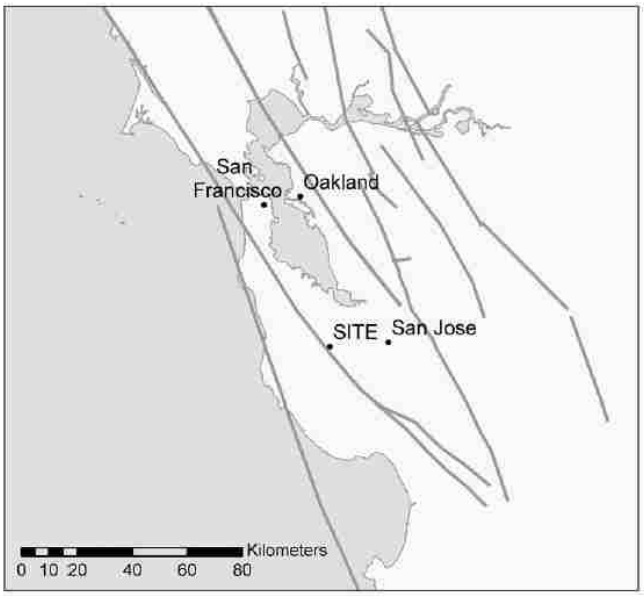

Figure 4-1: Site location and faults included in computation of ground motions for the application of the fully probabilistic seismic slope displacement method (from Rathje and Saygili 2009)

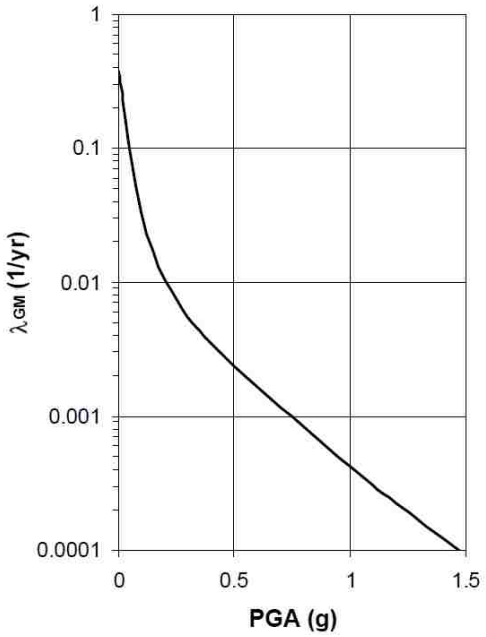

Figure 4-2: Scalar *PGA* hazard curve.

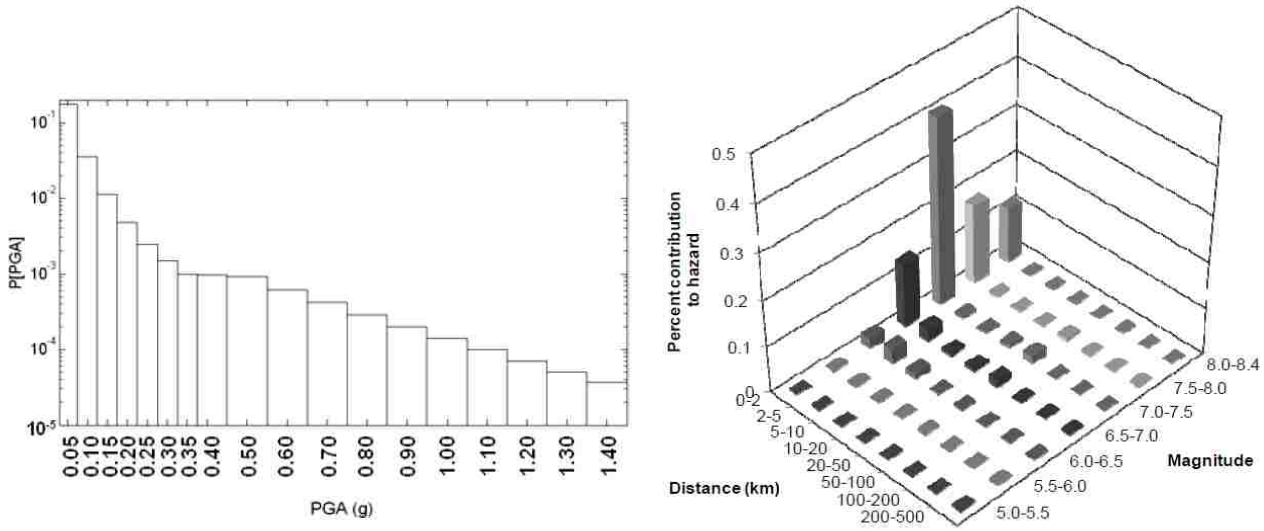

a) **b)**

Figure 4-3: a) Annual probability of occurrence for each *PGA* level from Fig.4-1 and b) deaggregation of *PGA* hazard at λ_{GM}=0.0021 (about 475 year return period).

From Figure 4-2, the hazard curve shows that the seismic hazard at this site is significant, with a PGA of 0.57 g at a return period of 475 years (i.e., 10% probability of exceedance in 50 years) and PGA of 1.02 g at a return period of 2475 years (i.e., 2% probability of exceedance in 50 years). The ground motion hazard curve presented in Figure 4-2 is used in the development of a seismic slope displacement hazard curve using the scalar approach from equation 4-1 and λ is approximated using the mid-point rule for integration as shown in Figure 4-3(a). The hazard curve in Figure 4-2 is used to derive λ using *PGA* bins ranging from 0.05 g to 0.1 g. Lastly, the M_w deaggregation shown in Figure 4-3(b) shows the probability of occurrence for each M_w bin, which was computed by adding the values for all distances within a magnitude bin. As observed in the plot, the seismic hazard is dominated by M_w greater than 6.5.

The seismic hazard curve is used in the computation of the seismic slope displacement hazard curve using equation 4-1. The resulting seismic slope displacement hazard curve is shown in Figure 4-4 for both the Rathje and Saygili (2008) model (i.e., *PGA* model) and the Rathje and Saygili (2009) model (i.e., *PGA*, *M* model).

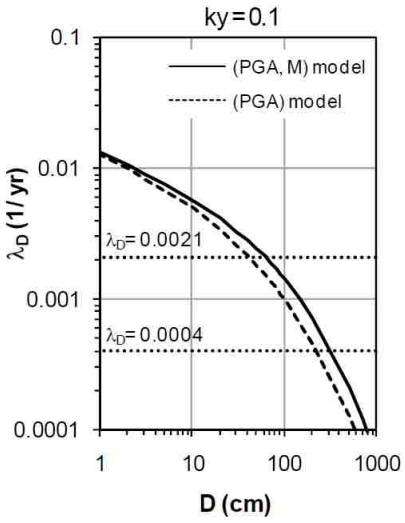

Figure 4-4: Displacement hazard curves for k =0.1 g using the (*PGA*) and (*PGA, M*) displacement models.

For this example, the (*PGA*, *M*) model for displacement predicts larger displacements than those computed with the *PGA* model. The *PGA* model predicts less hazard because M_w between 7.0 and 8.0 dominate the hazard as seen in Figure 4-3 (b). These displacement hazard curves could be used to evaluate displacement levels for different return periods or hazard levels.

The Rathje and Saygili (2009) example summarized in this previous section shows the importance of accounting for the uncertainty in both the ground motion prediction and seismic slope displacement computation. However, it is not easy for engineers working on routine projects to perform a fully probabilistic seismic slope displacement assessment because of the numerous probability calculations that must be performed and integrated. Hence, this thesis proposes a simplified performance-based procedure as a solution to this challenge.

4.2 Simplified procedure to approximate a performance-based Newmark seismic slope displacement procedure

The simplified performance-based seismic slope displacement procedure seeks to approximate displacements calculated by the fully probabilistic seismic slope displacement procedure presented by Rathje and Saygili (2008) and Rathje and Saygili (2009). The models described in sections 2.4 and 2.5 were incorporated in the simplified procedure at the targeted return periods of 475, 1,033, and 2,475 years.

The first step in the derivation of a simplified seismic slope displacement method is the development of a governing relationship, which can be expressed as

$$\ln D^{site} = \ln D^{ref} + \Delta \ln D \tag{4-2}$$

where D^{site} is the actual performance-based seismic slope displacement at the desired return period, D^{ref} is a reference performance-based seismic slope displacement that is computed or

approximated with a constant set of reference parameter inputs, and $\Delta \ln D$ is a displacement correction function.

The simplified performance-based seismic slope displacement method approximates displacements computed by the full performance-based seismic slope displacement procedure by first computing D^{ref}. This term is computed using a reference set of site conditions k_y^{ref} as indicated in equation 2-1. Depending on the empirical model used, D^{ref} was approximated using equations 2-3 and 2-5.

The reference displacement $\ln D^{ref}$ is computed by performing a full probabilistic seismic slope displacement analysis (Rathje and Saygili 2008, Rathje and Saygili 2009) using *PBLiquefY*. If these values are computed over a geographic grid of points for k_y^{ref}, then the resulting seismic slope displacement hazard curves can be used to obtain uniform hazard estimates of seismic slope displacements for all of the analyzed grid points. If these uniform hazard displacement values are mapped using an interpolation function such as kriging, then the resulting contour map provides reference seismic slope displacement values at the hazard level or return period of interest. These maps are called seismic slope displacement reference parameter maps. Such maps are very useful because, regardless of the site of interest, the reference displacement values do not change for the areas depicted in the maps.

The essence of the simplified approach is therefore the development and use of the seismic slope displacement reference parameter maps. They remove the requirement for the user to perform probabilistic calculations because the necessary probabilistic calculations are already incorporated into the mapped D^{ref} values. Thus, researchers perform the difficult probabilistic calculations beforehand so that engineers using the maps at a later date do not need to perform

probabilistic calculations. With a seismic slope displacement reference parameter map in hand, an engineer simply needs to compute the correction term ΔlnD and then use equation 4-2 to compute the site-specific probabilistic seismic slope displacement at the return period of interest. However, to perform this calculation, the engineer must know how to compute ΔlnD. This derivation is explained as follows.

To compute the value of ΔlnD for a particular hazard level or return period, an engineer can use estimates or approximations of $\ln D^{site}$ and $\ln D^{ref}$ to back-calculate ΔlnD. The value of $\ln D^{site}$ can be approximated with the Rathje and Saygili (2009) model as

$$\ln D^{site} \approx 4.89 - 4.85\left(\frac{k_y^{site}}{a_{\max}}\right) - 19.64\left(\frac{k_y^{site}}{a_{\max}}\right)^2 + 42.49\left(\frac{k_y^{site}}{a_{\max}}\right)^3 - 29.06\left(\frac{k_y^{site}}{a_{\max}}\right)^4 + 0.72\ln\left(a_{\max}\right) + 0.89\left(M - 6\right) \quad (4\text{-}3)$$

where $a_{\max}$ is obtained from the seismic hazard curve at the return period of interest; k_y^{site} is usually estimated using a two-dimensional pseudo-static slope stability analysis; and M_w comes from the ground motion deaggregation at the return period of interest.

Using the Bray and Travasarou (2007) model, the same approach is applied to approximate $\ln D^{site}$ as

$$\ln D^{site} \approx -0.22 - 2.83\ln\left(k_y^{site}\right) - 0.333\left(\ln\left(k_y^{site}\right)\right)^2 + 0.566\ln\left(k_y^{site}\right)\ln\left(a_{\max}\right) + 3.04\ln\left(a_{\max}\right) - 0.244\left(\ln\left(a_{\max}\right)\right)^2 + 0.278\left(M - 7\right) \quad (4\text{-}4)$$

The reference seismic slope displacement is approximated using the Rathje and Saygili (2009) model as

$$\ln D^{ref} \approx 4.89 - 4.85\left(\frac{k_y^{ref}}{a_{\max}^{ref}}\right) - 19.64\left(\frac{k_y^{ref}}{a_{\max}^{ref}}\right)^2 + 42.49\left(\frac{k_y^{ref}}{a_{\max}^{ref}}\right)^3 - 29.06\left(\frac{k_y^{ref}}{a_{\max}^{ref}}\right)^4 + 0.72\ln\left(a_{\max}^{ref}\right) + 0.89\left(M-6\right) \quad (4\text{-}5)$$

where the maximum reference ground acceleration($a_{\max}^{ref}$) is obtained from the seismic hazard curve at the return period of interest corresponding to bedrock conditions (i.e., average shear wave velocity in the upper 30m ((Vs_{30}) equal to 760m/s).

Similarly, the reference seismic slope displacement is approximated using the Bray and Travasarou (2007) model as

$$\ln D^{ref} \approx -0.22 - 2.83\ln\left(k_y^{ref}\right) - 0.333\left(\ln\left(k_y^{ref}\right)\right)^2 + 0.566\ln\left(k_y^{ref}\right)\ln\left(a_{\max}^{ref}\right) + 3.04\ln\left(a_{\max}^{ref}\right) - 0.244\left(\ln\left(a_{\max}^{ref}\right)\right)^2 + 0.278\left(M-7\right) \quad (4\text{-}6)$$

With approximated values of $\ln D^{ref}$ and $\ln D^{site}$, ΔlnD can now be computed as

$$\Delta\ln D = \ln D^{site} - \ln D^{ref} \quad (4\text{-}7)$$

Substituting equations 4-3 and 4-5 into equation 4-7, ΔlnD for the Rathje and Saygili (2009) model can be expressed as

$$\left(\Delta\ln D\right)_{rathje} \approx \frac{4.85}{PGA}\left(\frac{k_y^{ref}}{f_a^{ref}} - \frac{k_y^{site}}{f_a^{site}}\right) + \frac{19.64}{(PGA)^2}\left[\left(\frac{k_y^{ref}}{f_a^{ref}}\right)^2 - \left(\frac{k_y^{site}}{f_a^{site}}\right)^2\right] + \frac{42.49}{(PGA)^3}\left[\left(\frac{k_y^{site}}{f_a^{site}}\right)^3 - \left(\frac{k_y^{ref}}{f_a^{ref}}\right)^3\right] + \frac{29.06}{(PGA)^4}\left[\left(\frac{k_y^{ref}}{f_a^{ref}}\right)^4 - \left(\frac{k_y^{site}}{f_a^{site}}\right)^4\right] + 0.79\ln\left(\frac{f_a^{site}}{f_a^{ref}}\right) \quad (4\text{-}8)$$

where (f_a^{ref}) and (f_a^{site}) are the reference and site-specific soil amplification factors corresponding to *PGA*. The *PGA* value selected for the site is used to determine f_a^{site} from Table 4-1 using the site class corresponding to the soil found in the area of interest (AASHTO 2012).

Table 4-1: Values of site factor, f_a, at zero-period on acceleration spectrum (from AASHTO 2012 Table 3.10.3.2-1)

Site Class	Peak Ground Acceleration Coefficient (*PGA*)[1]				
	PGA ≤ 0.10	*PGA* = 0.20	*PGA* = 0.30	*PGA* = 0.40	*PGA* ≥ 0.50
A	0.8	0.8	0.8	0.8	0.8
B	1.0	1.0	1.0	1.0	1.0
C	1.2	1.2	1.1	1.0	1.0
D	1.6	1.4	1.2	1.1	1.0
E	2.5	1.7	1.2	0.9	0.9
F[2]	*	*	*	*	*

Notes:

[1]Use straight-line interpolation for intermediate values of *PGA*.

[2]Site-specific geotechnical investigation and dynamic site response analysis should be performed for all sites in Site Class F.

Similarly, ΔlnD is expressed for the Bray and Travasarou (2007) model as

$$\left(\Delta \ln D\right)_{bray} = 2.83\left[\ln\left(\frac{k_y^{ref}}{f_a^{ref}}\right) - \ln\left(\frac{k_y^{site}}{f_a^{site}}\right)\right] + 0.333\left[\ln\left(\frac{k_y^{ref}}{f_a^{ref}}\right)^2 - \ln\left(\frac{k_y^{site}}{f_a^{site}}\right)^2\right] + 0.566\ln(PGA)\left[\ln\left(\frac{k_y^{site}}{f_a^{site}}\right) - \ln\left(\frac{k_y^{ref}}{f_a^{ref}}\right)\right] \quad (4\text{-}9)$$

With this simplified performance-based approach for estimating seismic slope displacements, an engineer can compute uniform hazard estimates of seismic slope displacements at a targeted hazard level in a relatively simple manner. Certain assumptions are needed as inputs such as k_y for the specific slope. It is also required to obtain the probabilistic estimate of PGA from the USGS website for rock (i.e., $V_{s,30} = 760$ m/s) at the targeted return period corresponding to a hazard level. It is also needed to obtain f_a for the ground motion from either the AASHTO seismic design provisions (based on soil site classification) or from a site-specific site response analysis.

Once ΔlnD is computed for one or both simplified Newmark sliding block procedures, site-specific, hazard-targeted estimates of seismic slope displacement can be computed as

$$D^{site} = \exp\left[\ln D^{ref} + \Delta \ln D\right] = (D^{ref}) \exp\left[\Delta \ln D\right] \tag{4-10}$$

where D^{ref} is obtained from the appropriate seismic slope displacement reference parameter map.

As part of the culmination of this research, seismic slope displacement reference parameter maps were created, and with the use of *SPLiq*, an engineer is be able to compute site-specific simplified performance-based seismic slope displacements with the same amount of effort that current deterministic and pseudo-probabilistic methods require.

4.3 Summary

This chapter introduces the simplified probabilistic seismic slope displacement procedure. The chapter begins by discussing applications of probability in seismic slope displacement analyses such as those described in Rathje and Saygili (2009). Some of the results obtained from an application of the fully probabilistic methodology of sliding displacements to a site in northern

California is also presented. Lastly, the main equation for the development of the simplified method is introduced and applied to the two models used in the study presented in this thesis: Rathje and Saygili (2009), and Bray and Travasarou (2007). Chapter 5 presents a validation study of the simplified models described in this chapter.

5 VALIDATION OF THE SIMPLIFIED PROBABILISTIC PERFORMANCE-BASED SEISMIC SLOPE DISPLACEMENT MODEL

The effectiveness of the simplified probabilistic performance-based seismic slope displacement model depends on how closely it approximates the results of a fully probabilistic site-specific performance-based seismic slope displacement analysis. To validate the procedure and to quantify the accuracy of the introduced simplified procedure, a comparison between the simplified and full performance-based methods is performed for 10 sites throughout the United States. These sites are evaluated at return periods of 475, 1,033, and 2,475 years.

5.1 Sites used in the analysis

The selected sites for the analysis are used in previous published performance-based liquefaction studies (e.g., Kramer and Mayfield 2007). The sites represent 10 different cities across the United States and are listed in Table 5-1. Two of the locations (Charleston and Memphis) are in areas of low recent seismicity with very large historical earthquakes. Four of the sites (Santa Monica, San Jose, San Francisco, and Eureka) are located in very active seismic environments. Three of the sites (Seattle, Portland, and Eureka) are in areas subject to large-magnitude subduction earthquakes. Two sites (San Francisco and San Jose) are in relatively close proximity (~60 km) to each other. Finally, two of the sites (Salt Lake City and Butte) are located in extensional seismic regimes governed largely by normal faults.

Table 5-1: Locations used for the validation of the simplified models

Site	Latitude	Longitude
Butte, MT	46.003	-112.533
Charleston, SC	32.726	-79.931
Eureka, CA	40.802	-124.162
Memphis, TN	35.149	-90.048
Portland, OR	45.523	-122.675
Salt Lake City, UT	40.755	-111.898
San Francisco, CA	37.775	-122.418
San Jose, CA	37.339	-121.893
Santa Monica, CA	34.015	-118.492
Seattle, WA	47.53	-122.3

5.2 Simplified probabilistic seismic slope displacement model validation

To evaluate the accuracy of the simplified probabilistic performance-based procedure for seismic slope displacements, reference parameters of $k_y^{ref} = 0.1$ g and $f_a^{ref} = 1.0$ are selected. Values chosen to represent actual site conditions are k_y^{site} values ranging between 0.1 g to 0.5 g. Site Class D conditions are assumed to exist for all sites, which is a common assumption in engineering practice. Values of *PGA* and mean M_w are obtained for the 10 selected cities in the United States from the 2008 USGS deaggregation at return periods of 475, 1,033, and 2,475 years. Values of f_a^{site} are obtained from current AASHTO seismic design provisions using tabulated values of *fa* as a function of *PGA* as shown in Table 4-1. Subsequent values of mean M_w, *PGA*, and f_a for the three return periods are summarized in Table 5-2 for the 10 cities evaluated in this study.

Table 5-2: Summary of M_w, PGA and f_a site used for each city used in the validation

Site	Tr = 475 year			Tr = 1,033 year			Tr = 2,475 year		
	Mean M_w	PGA (g)	f_a	Mean M_w	PGA (g)	f_a	Mean M_w	PGA (g)	f_a
Butte	6.03	0.0834	1.600	6.03	0.1206	1.559	6.05	0.1785	1.443
Charleston	6.61	0.1513	1.497	6.87	0.3680	1.132	7.00	0.7287	1.000
Eureka	7.33	0.6154	1.000	7.40	0.9662	1.000	7.45	1.4004	1.000
Memphis	6.98	0.1604	1.479	7.19	0.3346	1.165	7.24	0.5711	1.000
Portland	7.24	0.1990	1.402	7.29	0.2980	1.204	7.31	0.4366	1.063
Salt Lake City	6.75	0.2126	1.375	6.84	0.4030	1.097	6.90	0.6717	1.000
San Francisco	7.31	0.4394	1.061	7.38	0.5685	1.000	7.44	0.7254	1.000
San Jose	6.66	0.4560	1.044	6.67	0.5627	1.000	6.66	0.6911	1.000
Santa Monica	6.74	0.3852	1.115	6.79	0.5372	1.000	6.84	0.7415	1.000
Seattle	6.75	0.3110	1.189	6.82	0.4444	1.056	6.88	0.6432	1.000

The full performance-based seismic slope displacement equations for both Rathje and Saygili (2009) and Bray and Travasarou (2007) presented in chapter 2 are implemented in *PBLiquefY* to develop values of $\ln D^{ref}$ for each site. The reference values $k_y^{ref} = 0.1$ g and $f_a^{ref} = 1.0$ are used in the full probabilistic analysis to compute D^{ref} for the 10 cities in the United States at the three return periods of interest. Additionally, *PBLiquefY* is also used to compute site-specific, full performance-based seismic slope displacements, D^{site}, using the selected values of k_y^{site} at each of the 10 cities for all three return periods. These fully probabilistic values of D^{site} are used to validate the simplified performance-based approach.

Figure 5-1 and Figure 5-2 show the comparison of the full and simplified performance-based seismic slope displacement predictions for both the Rathje and Saygili (2009) and Bray and Travasarou (2007) models, respectively.

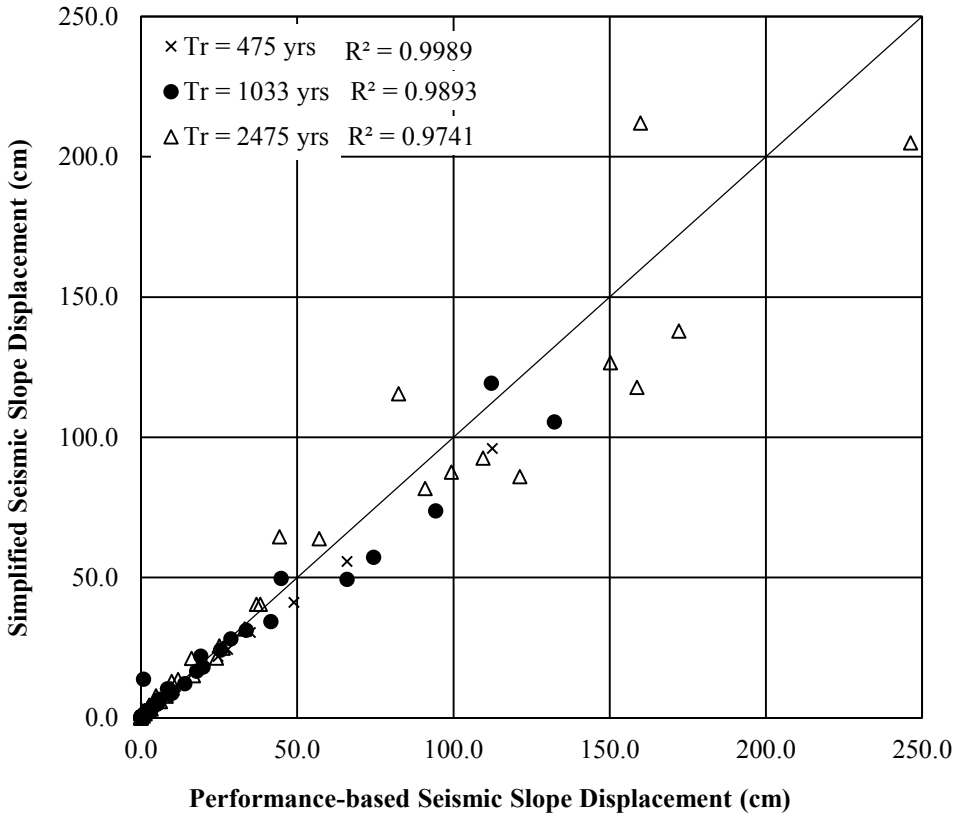

Figure 5-1: Comparison of seismic slope displacements for the simplified and full performance-based models based on Rathje and Saygili (2009).

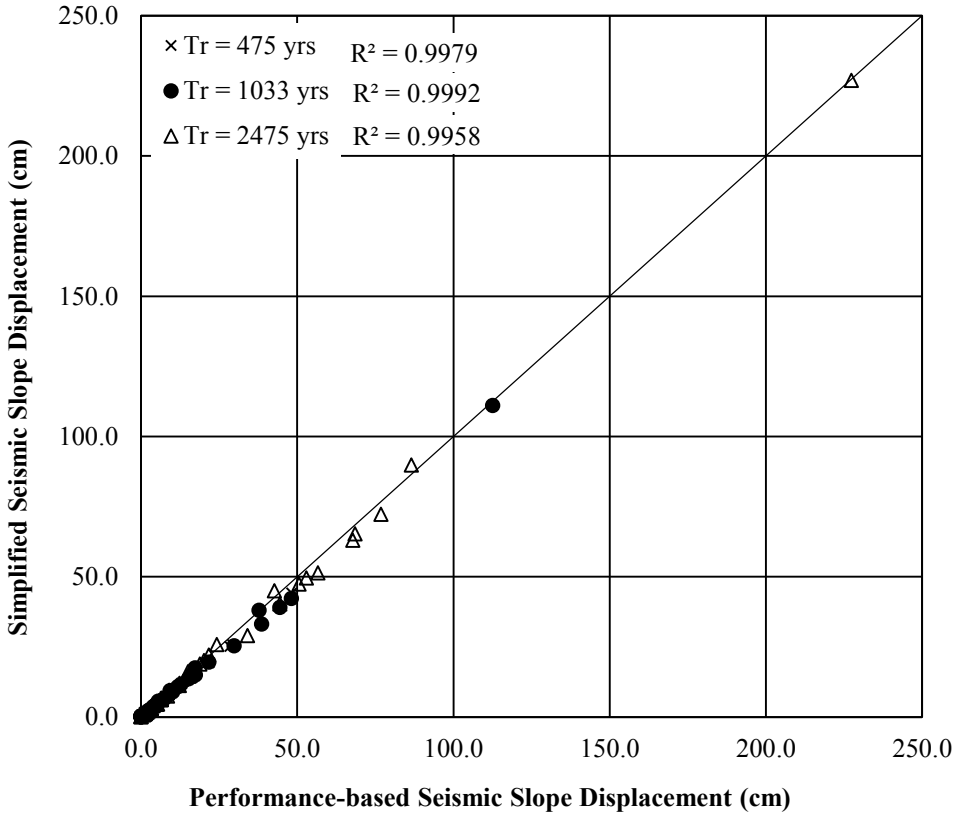

Figure 5-2: Comparison of seismic slope displacements for the simplified and full performance-based models based on Bray and Travasarou (2007).

As shown in Figure 5-1 and Figure 5-2, there is generally a good correlation between the results from the full performance-based procedure and the simplified performance-based procedure with both models, although the simplified procedure using the Bray and Travasarou (2007) model shows less scatter than the procedure using the Rathje and Saygili (2009) model. The Rathje and Saygili (2009) model incorporates a 4th-order polynomial function of (k_y/PGA), which can lead to greater discrepancies between the simplified performance-based slope displacements and the full performance-based slope displacements at higher predicted displacements. Nevertheless, relatively high R^2 values indicate that the correlation accounts for

nearly all of the variability in the computed response data. The average error across all return periods and yield accelerations included in this study for the simplified procedure using the Rathje and Saygili (2009) model is 4.9 cm. The average error for the simplified procedure using the Bray and Travasarou (2007) model is 0.8 cm. However, note that the simplified procedure incorporating the Rathje and Saygili (2009) model accurately and precisely approximates the results of the full performance-based procedure up to predicted displacements of about 50 cm, which is a much greater displacement than what is typically considered acceptable for most bridge foundations. In other words, predicted displacements greater than about 30 cm, regardless of their M_w, are typically considered unacceptable and result in the recommendation of slope remediation or ground improvement (Caltrans 2013). For predicted displacements greater than about 50 cm, the engineer should interpret the results with caution, understanding that the simplified Rathje and Saygili (2009) results may be imprecise. From these results, it is concluded that the simplified procedure adequately approximates the results of a full performance-based procedure for most practical design applications, particularly if an allowable limit state of 30 cm (i.e., 12 in) is specified for foundation design (Caltrans 2013).

5.3 Summary

Ten sites throughout the United States are analyzed using both the full and simplified performance-based post-liquefaction settlement and seismic slope displacement procedures for the 475, 1,033, and 2,475 year return periods. The simplified seismic slope displacement procedure demonstrates accurate and precise approximations of its respective full performance-based procedure at predicted slope displacements of 30 cm or less. At greater predicted displacements, the simplified procedure with the Rathje and Saygili (2009) model shows more scatter in its ability to approximate the full performance-based procedure. Caution is advised is such cases.

6 SIMPLIFIED PERFORMANCE-BASED SEISMIC SLOPE DISPLACEMENT REFERENCE PARAMETER MAPS

An important aspect of the simplified performance-based seismic slope displacement procedure is the use of reference parameter maps. These maps are developed using a k_y^{ref} value and require an analysis of a grid of points covering the desired area. The results of the analysis are then interpolated to create a contour map providing the reference value. This chapter provides the methodology and process in developing these maps.

6.1 Grid spacing evaluation

Because biases due to spacing of grid points in gridded seismic hazard analyses are known to exist, the grid spacing study presented in this chapter evaluates the potential for bias to occur due to grid spacing effects in a gridded probabilistic seismic slope displacement hazard assessment. Because the states involved in this study comprise areas of varying seismicity levels, evaluations are performed in each state to assess the optimum grid spacing for development of seismic slope displacement parameter maps as shown in Appendix B.

The grid spacing assessment is performed by comparing interpolated results from a simple 4-point grid placed in various parts of the country with site-specific results. The difference between the interpolated and site-specific results is quantified. By minimizing these computed differences, the optimum grid spacing for the seismic slope displacement reference parameter maps in each state is obtained.

Note that this grid spacing study does not provide estimates of accuracy between the simplified performance-based method and the full performance-based method. The accuracy between the two methods is explained and quantified in Chapter 5. The measurements of error calculated in this grid spacing study reflect only the error involved in interpolating a reference displacement from a seismic slope displacement reference parameter map.

6.2 Performance-based seismic slope displacement grid spacing evaluation

This section describes the methods used to derive the optimum grid spacing to ensure an acceptable level of interpolation error when using seismic slope displacement reference parameter maps. First, it is necessary to define an acceptable level of error. In many fields of science and engineering, an error of 5% or less is generally considered acceptable. However, for some sites, the criterion of 5% error does not work due to complex seismic regimes and/or very small predicted displacements. For such sites, an absolute error of 5 cm is defined as "acceptable" for this study rather than using the 5% error criterion.

6.2.1 Methodology for grid spacing study

From a preliminary study performed by Ulmer et al. (2015), the relationship between percent error and grid spacing is observed to be reasonably correlated with the *PGA* of the site of interest. To estimate the effect of *PGA* on optimum grid spacing, a similar study is conducted here focusing on 35 cities throughout the United States with a wide range of associated *PGA* values (i.e., seismicity levels). The *PGA* values for the 35 sites is plotted in Figure 6-1.

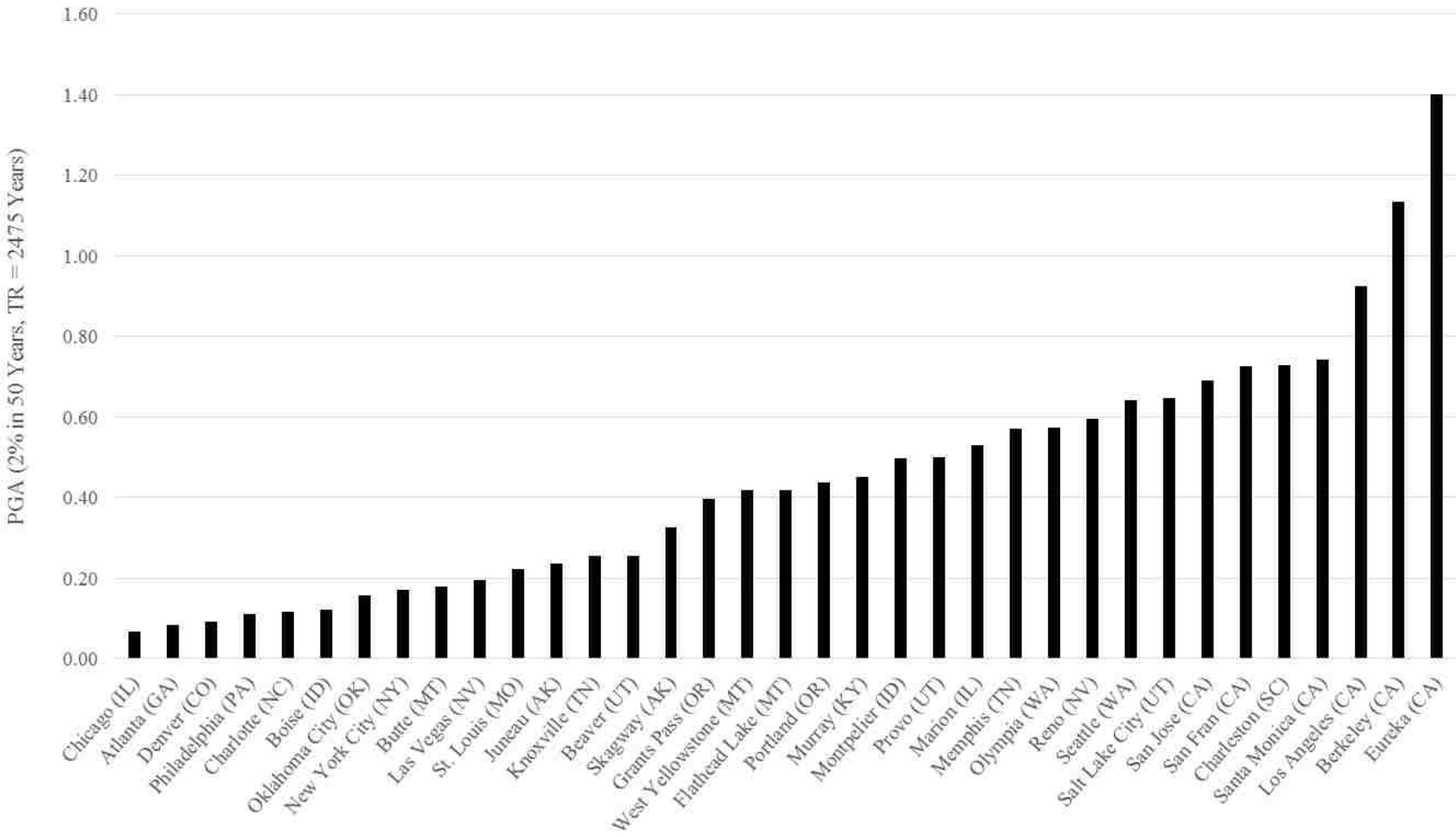

Figure 6-1: Cities used in grid spacing study and their respective expected PGA for the 2475 year return period.

Based on the premise that *PGA* is correlated to the seismic slope displacement values that are computed on a grid, the USGS 2008 Deaggregation website is used to obtain the *PGA* at each site for the 2,475 year return period. The hazard level at each site as well as the hazard range for each state is found based on the USGS 2008 *PGA* hazard map for the 2,475 year return period shown in Figure 6-2.

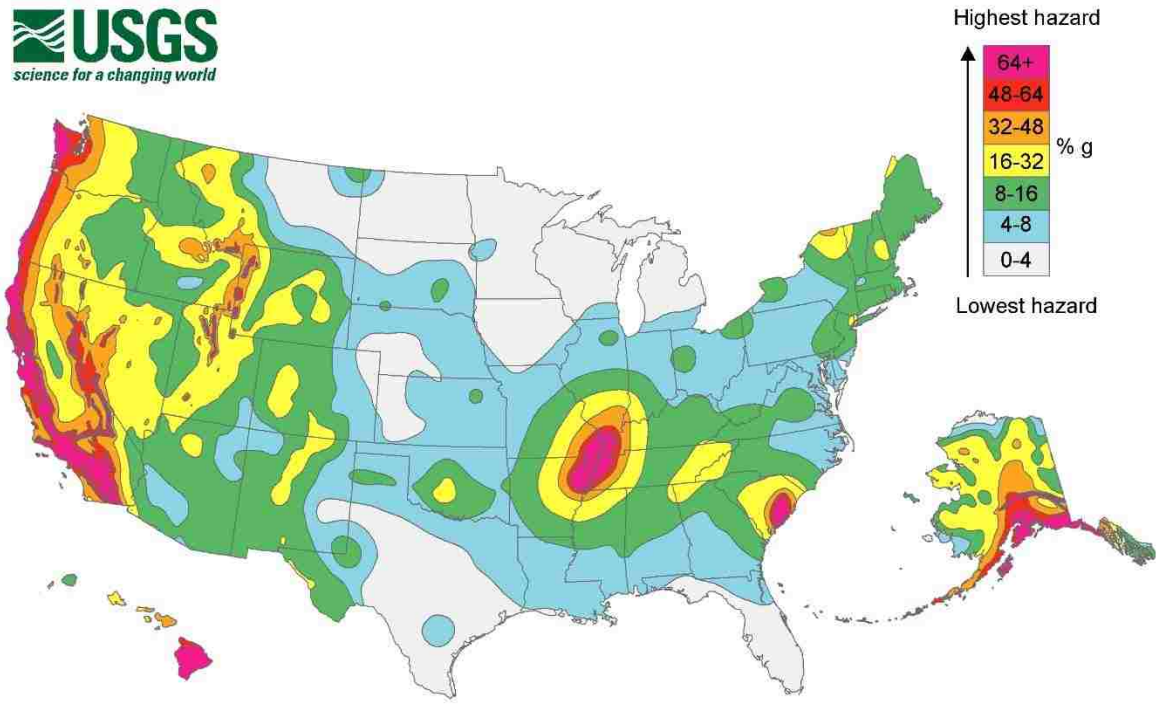

Figure 6-2: USGS 2008 PGA hazard map (*Tr* = 2,475 years).

The grid spacing for the corresponding hazard zone is determined by calculating seismic slope displacements on a grid as seen in Figure 6-3. This process is repeated at 2 km, 4 km, 8 km, 16 km, 25 km, 35 km, and 50 km grid spacings.

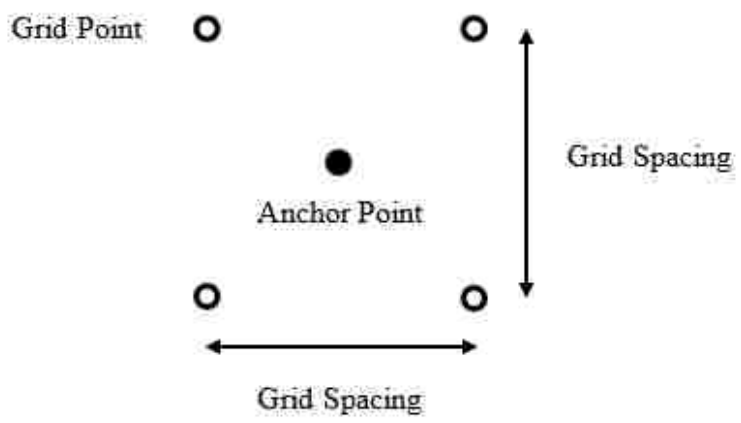

Figure 6-3: Layout of grid points centered on each city's anchor point.

An estimate of the seismic slope displacement at the center point (i.e., interpolated D^{ref}) is computed from each of the four corner points of the grid. The interpolated value at the center point is then compared with D^{site} computed with the full probabilistic approach using *PBLiquefY*. The percent error due to interpolation is computed as

$$PercentError = \frac{|InterpolatedValue - ActualValue|}{ActualValue} \times 100\% \quad (6\text{-}1)$$

A plot of each city using the simplified performance-based seismic slope displacement method is generated. The optimum grid spacing corresponding to 5 % error is found using a best fit line. Example plots of this process are shown in Figure 6-4, 6-5, and 6-6.

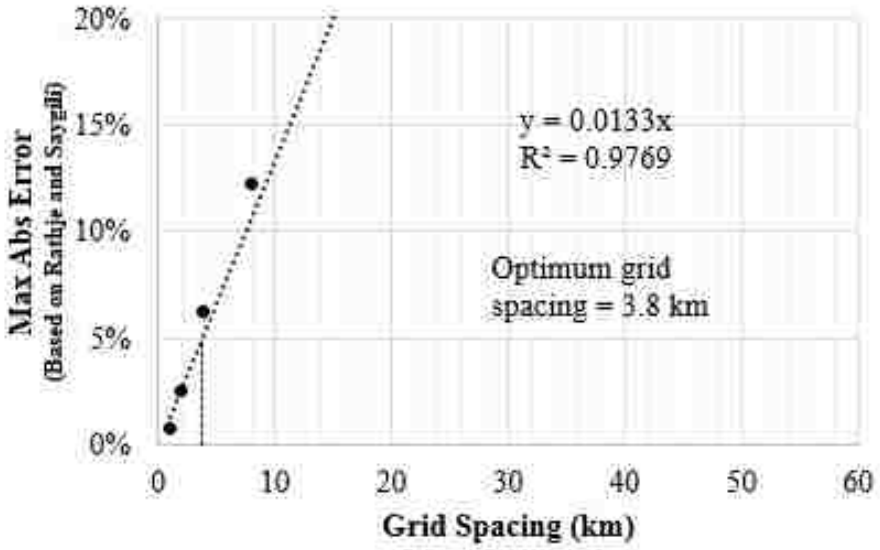

Figure 6-4: Variation of maximum percent error (based on Rathje & Saygili 2009) with increasing distance between grid points for Eureka, CA (Pink zone, PGA = 1.4004).

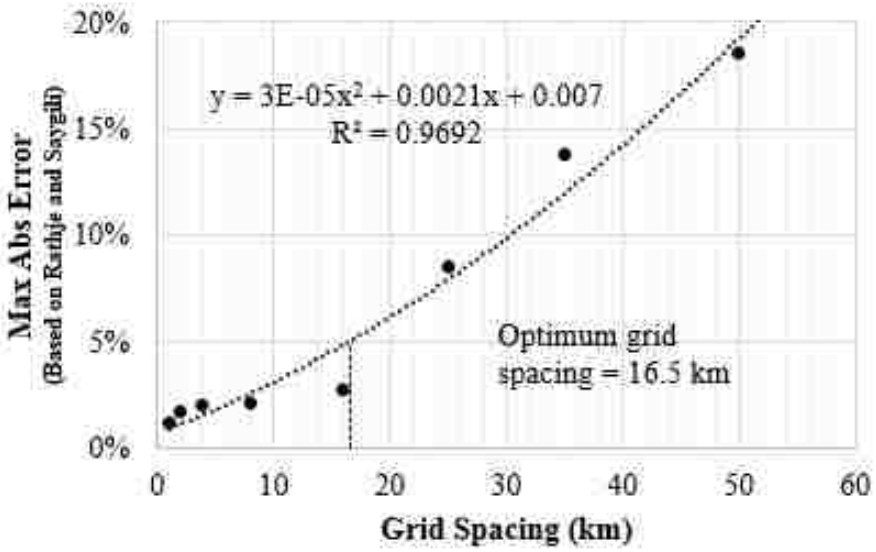

Figure 6-5: Variation of maximum percent error (based on Rathje & Saygili 2009) with increasing distance between grid points for Portland, OR (Orange zone, PGA = 0.4366).

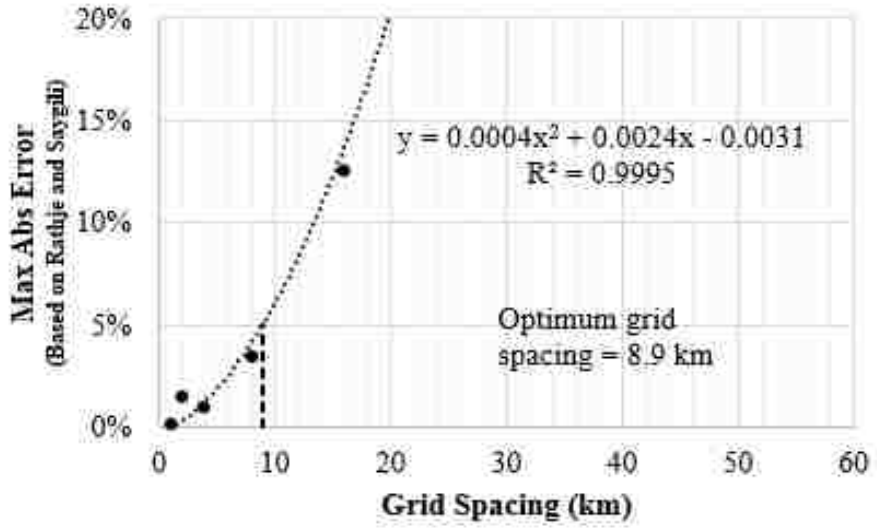

Figure 6-6: Variation of maximum percent error (based on Rathje & Saygili 2009) with increasing distance between grid points for Butte, MT (Yellow zone, PGA = 0.1785).

The grid spacing study is repeated for each city listed in Figure 6-1. Grid spacings corresponding to 5% error or less are plotted against *PGA* to show how the grid spacing differed from site to site. This plot is presented in Figure 6-7.

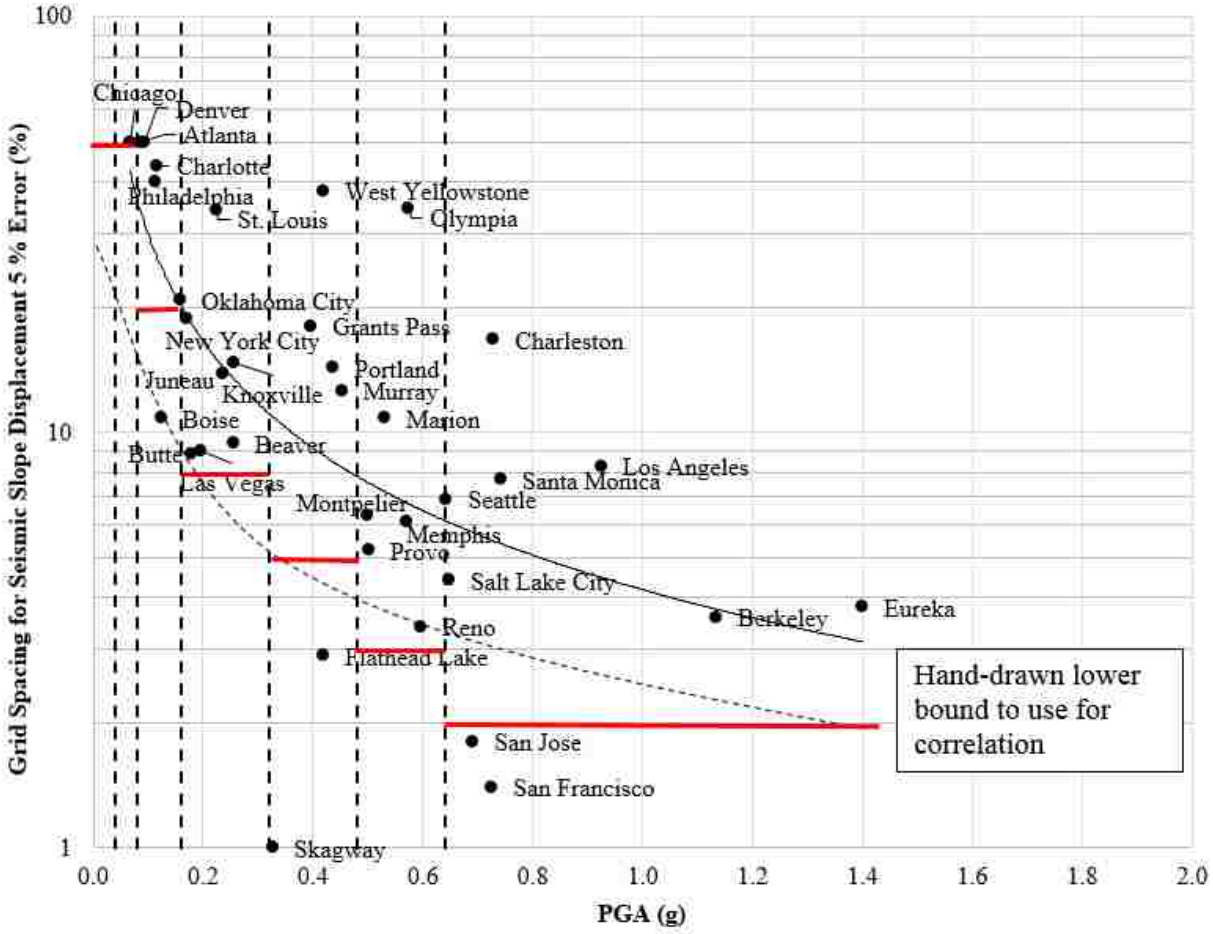

Figure 6-7: Grid spacing based on 5% error plotted against PGA for all sites.

Figure 6-7 shows significant scatter in the correlation between acceptable grid spacing and *PGA*, but a downward trend is evident. A best fit line was applied to the data and is shown as a thin solid line. The thin dashed line is manually drawn following the slope of the best-fit line to establish a lower bound corresponding to the recommended grid spacing for the cities analyzed.

Finally, a lower bound series of lines (thick red lines) is used to assign the recommended grid spacing based on USGS-mapped PGA zones (vertical dashed lines).

Five out of the 35 cities used in the study do not meet the acceptable criterion of 5% error. These cities are Skagway, Alaska; Flathead, Montana; Salt Lake City, Utah; San Jose, California; and San Francisco, California. The allowable absolute difference criterion of 5 cm is applied to these cities. The absolute difference is computed as

$$AbsoluteDifference_{CITY,x} = \left| InterpolatedValue_{CITY,x} - AnchorValue_{CITY} \right| \quad (6\text{-}2)$$

where CITY indicates the city of interest and x is the grid spacing in question. Table 6-1 presents a summary of the grid spacing required by all five cities using the absolute difference criterion.

Table 6-1: Summary of spacing results necessary to achieve an absolute difference of 5 cm.

City	*PGA* (g)	Spacing (km)
Skagway	0.3264	1
Flathead Lake	0.4195	29.2
Salt Lake City	0.6478	4.4
San Jose	0.6911	3.8
San Francisco	0.7254	1.3

Although this grid spacing is suggested for the outlier cities, the proposed final spacing included in Table 6-2 corresponds to results obtained from all other 30 cities analyzed. The proposed grid spacing is based on the general trend of the data shown in Figure 6-7 using not just the curve generated from the average but also the dotted curve created to envelope the cities. A

few outliers are still visible, but assigning even more conservative spacings for the different PGA areas seems unnecessary for the limited number of cities analyzed in the study. To reiterate, the grid spacing study does not deal with the accuracy of the model (see Chapter 5), but with the accuracy of the interpolation of computed values on a seismic slope displacement reference parameter map.

Table 6-2: Proposed grid spacing for seismic slope displacement analysis.

PGA (g)	Hazard zone color	Spacing (km)	Spacing (mi)
0 - 0.04	Gray	50	31.1
0.04 - 0.08	Blue	50	31.1
0.08 - 0.16	Green	20	12.4
0.16 - 0.32	Yellow	8	5.0
0.32 - 0.48	Orange	5	3.1
0.48 - 0.64	Red	3	1.9
0.64+	Pink	2	1.2

6.3 Map development

With the optimum grid spacing computed and presented in Table 6-2, the grid points used in the analysis for the selected states need to be determined with the full probabilistic approach (embedded in *PBLiquefY*) using $k_y^{ref} = 0.1$ g. Upon completion of the gridded analysis, the slope displacement hazard curves associated with their corresponding grid points are used to create the hazard-targeted seismic slope displacement reference parameter maps. The physical creation of a reference parameter map requires the use of several specialized software programs. To create the grid spacing and the maps, the Geographic Information System (GIS) software *ArcMap*, developed

by ESRI, Inc., is used extensively. The full performance-based seismic slope displacement values are obtained using PBLiquefY as explained previously.

6.4 Creation and analysis of the grid points

The process of developing reference parameter maps is started by dividing each state into sections based on the USGS 2008 *PGA* hazard map. This is done by creating GIS shapefiles developed from downloaded data from the USGS website representing the 2008 *PGA* hazard map. Each *PGA* hazard zone is then assigned the appropriate grid spacing as recommended in Table 6-2**.** Then, using *ArcMap*, the grid of points with their respective set of latitude and longitude coordinates is generated for each *PGA* hazard zone at the specified grid spacing. After computing displacements in all the different *PGA* hazard zones, all zones are combined into one general grid for an entire state. An example of the overall grid of points for Utah can be seen in Figure 6-8.

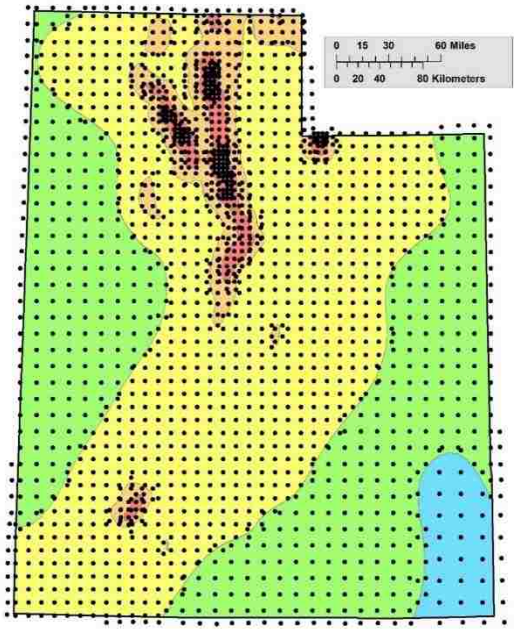

Figure 6-8: Grid points for Utah combined with USGS 2008 PGA hazard map.

Once the grid points are developed for all the states, the location of each point is evaluated with the fully probabilistic seismic slope displacement method in *PBLiquefY* using k_y^{ref}, as discussed previously. Following completion of the probabilistic analysis, the reference seismic slope displacements corresponding to return periods of 475, 1,033, and 2,475 years are retrieved from the reference slope displacement hazard curves associated with the points. These reference seismic slope displacements are then imported back into *ArcMap* to begin the process of contouring the seismic slope displacement reference parameter maps.

The first step in contouring the seismic slope displacement reference parameter maps is the conversion of the individual points (seismic slope displacements) into a surface raster using the *ArcMap* kriging tool. This tool interpolates values between each grid point and creates a surface raster. From the surface raster, contour lines are created. To ensure that the contours of each state extend to the state borders, the state shape is buffered slightly.

To make the contour from the raster, the contour interval is first determined. The contour interval varies depending on the range of displacements computed for the specific state as shown in the maps provided in Appendix B. An example of a surface raster and contour for the state of Utah can be seen in Figure 6-9. Once the proper contour spacing is determined for each map, the contour is labeled and clipped to fit the state shapefile. A basemap and reference features are then added to provide more detail about the topography to the seismic slope displacement reference parameter map. An example of a completed seismic slope displacement reference parameter map for the Bray and Travasarou (2007) model is shown in Figures 6-10.

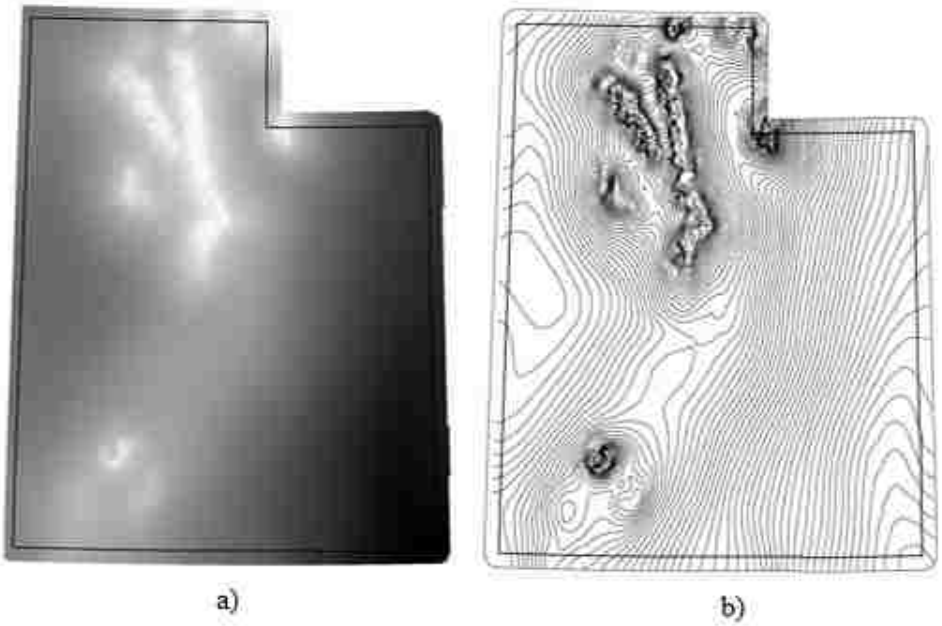

Figure 6-9: a) Surface raster and b) contours for Utah (T_R = 2475 yrs).

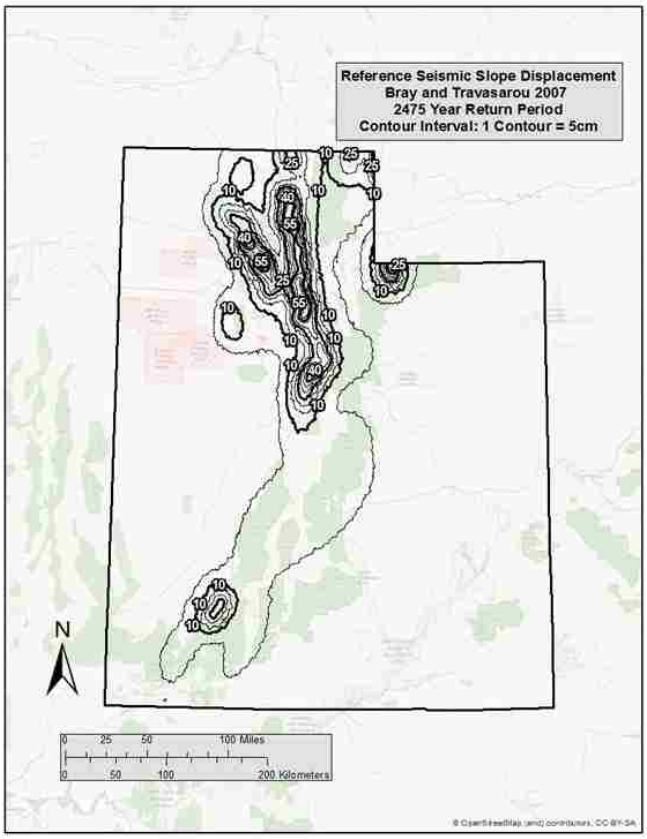

Figure 6-10: D^{ref} for Utah (T_R = 2475 years).

Each seismic slope displacement model has D^{ref} values represented by the contours on the map. For the Rathje and Saygili (2009) model $D^{ref}_{Rathje\&Saygili}$ is in units of cm. For the Bray and Travasarou (2007) model, $D^{ref}_{Bray\&Travasarou}$ is also in units of cm. Careful attention needs to be given to the labeling of each map to ensure that the map references the correct model and that D^{ref} used in the later steps of the simplified method are accurately read from the contours. To help prevent errors in reading the map, as part of the development of *SPLiq*, all grid points computed (i.e., D^{ref}) are included in a database within the spreadsheet from which the user can automatically interpolate D^{ref}. The option to read D^{ref} directly from the map is also included in *SPLiq*.

Maps generated as part of this study correspond to the states of Connecticut, Idaho, Montana, South Carolina, and Utah at return periods of 475,1,033, and 2,475 years. These maps are found in Appendix B.

6.5 Summary

In developing a simplified performance-based procedure for the estimation of seismic slope displacements, reference parameter maps are developed. This chapter describes a grid spacing evaluation in which values computed from an interpolation of four known points are compared to values computed at the location of interest. The grid spacing selected is influenced by the PGA of the region. The final grid spacing selected for the creation of maps for the five states involved in the study is determined by computing percent error of the interpolated values against the computed values of the site of interest. The tolerance was a 5% error, or a maximum of 5 cm of absolute difference in cases where the percent error fell outside the established bound. Completed seismic slope displacement reference parameter maps for the states of Connecticut, Idaho, Montana, South Carolina, and Utah at return periods of 475,1,033, and 2,475 years are found in Appendix B.

7 COMPARISON OF PROBABILISTIC, PSEUDO-PROBABILISTIC, AND DETERMINISTIC ANALYSES

In seismic hazard analysis, different approaches to dealing with seismic sources and their corresponding uncertainties are recommended to ensure that the resulting ground motions meet requirements established by the seismic design provisions, but also remain within a reasonable range of ground motion levels that could be expected to occur from an actual earthquake. Predicted ground motions that are too conservative could potentially result in unnecessary expenses. Thus, probabilistic ground motions may govern in some circumstances, while deterministic ground motions may govern in others. Similar behavior might exist in the computed results from probabilistic, pseudo-probabilistic, and deterministic seismic slope displacement analysis. This chapter compares the results from simplified performance-based seismic slope displacement analyses to deterministic and pseudo-probabilistic analyses to investigate under what conditions (i.e., seismicity levels) one will govern over the other. All three of these analyses use a series of different assumptions as they were introduced in Chapter 3 and all should be considered in engineering design as demonstrated in the following sections.

7.1 Methodology

This study begins with the selection of three cities based on varying seismicity levels: San Francisco (high seismicity), Salt Lake City (moderate seismicity), and Butte (low seismicity). For each city, three seismic slope displacement analyses are performed: probabilistic (simplified

performance-based procedure developed as part of this research), pseudo-probabilistic (as currently prescribed by AASHTO 2014), and deterministic. For simplification, k_y^{site} = 0.1 g is assumed for all locations in this comparison study.

7.1.1 Simplified performance-based seismic slope displacement analysis

The simplified performance-based procedure involves computing the seismic slope displacement at a centralized location within each of the three cities at the targeted return periods using the full probabilistic approach (Rathje and Saygili 2008, Rathje and Saygili 2009). *PBLiquefY* is used to compute the values with k_y^{ref} = 0.1 g. Thus, the computed displacements correspond to D^{ref}, such as those included the seismic slope displacement reference parameter maps found in Appendix B. These D^{ref} values are used to compute D^{site} values at the three locations included in this comparison study.

7.1.2 Deterministic procedure

Ground motions in the deterministic procedure are obtained by performing a DSHA. As discussed previously, a DSHA involves deterministically assessing the seismic sources in the nearby region of the site of interest and identifying the source, which produces the highest hazard in the area. The software *EZ-FRISK* is used to identify the five most significant seismic sources within 200 km of the centralized site locations in San Francisco and Salt Lake City. The 2008 USGS probabilistic seismic source model implemented within *EZ-FRISK* does not include some smaller faults in low seismic regions, such as Butte. Thus, the governing fault for Butte, which is the Rocker Fault, is identified using the USGS quaternary fault database (USGS et al. 2006).

In the case of Salt Lake City and San Francisco, *EZ-FRISK* provides values of M_w, *PGA*, and *R* for both the 50th percentile (i.e. median) and the 84th percentile (i.e. median plus one standard deviation) based on the Next Generation Attenuation (NGA) models for the Western United States (Boore and Atkinson 2008, Campbell and Bozorgnia 2008, and Chiou and Youngs 2008) and weighting schemes shown in Table 7-1. For Butte, the 50th and 84th percentile M_w values are estimated using the correlation with surface rupture length by Wells and Coppersmith (1994), and *PGA* is manually calculated using the same three NGA models (Table 7-1) with the input parameters associated with the Rocker Fault. Summaries of the seismic sources considered in this DSHA and details of the Rocker Fault deterministic seismic hazard calculations are provided in Table C-1 and Table C-2 respectively, in the Appendix C. Once the ground motions are computed with the DSHA, they are deterministically used with the Rathje and Saygili (2009) and Bray and Travasarou (2007) simplified Newmark sliding block models to compute median estimates of seismic slope displacement.

Table 7-1: NGA models used in deterministic procedure.

Attenuation Model	Weight
Boore & Atkinson (2008)	0.333
Campbell & Bozorgnia (2008)	0.333
Chiou & Youngs (2008)	0.333

Table 7-2: Variables for deterministic models (a_{max} calculated using F_a from AASHTO code).

Location	Latitude	Longitude	Distance (km)	Mean M_w	Median (50%)		Median + σ (84%)	
					PGA(g)	$a_{max}(g)$	*PGA(g)*	$a_{max}(g)$
Butte	46.003	-112.533	4.92	6.97	0.5390	0.5390	0.9202	0.9202
Salt Lake City	40.755	-111.898	1.02	7.00	0.5911	0.5911	1.005	1.005
San Francisco	37.775	-122.418	12.4	8.05	0.3175	0.3754	0.5426	0.5426

7.1.3 Pseudo-probabilistic seismic hazard analysis

The variables used in the pseudo-probabilistic analysis are obtained from the USGS 2008 interactive deaggregation website (USGS 2008). This process involves entering the latitude and longitude of the target sites, then specifying the return period for the analysis. Using this tool, M_w, *PGA* for rock, and *R* are obtained for the three return periods of interest at each of the three cities in this comparison study. Because the USGS 2008 interactive deaggregation website does not have the ability to compute exact values for a 1,033 year return period, the values corresponding to the 1,039 year return period are used as the closest approximation. The resulting values are summarized in Table 7-3.

Table 7-3: Input values found using USGS 2008 Deaggregations (T_R = 1,039 years).

Location	Latitude	Longitude	Distance (km)	Mean M_w	*PGA* (g)	f_a
Butte	46.003	-112.533	24.9	6.03	0.1206	1.559
Salt Lake City	40.755	-111.898	4.20	6.84	0.4030	1.097
San Francisco	37.775	-122.418	12.0	7.38	0.5685	1.000

7.2 Results

Plots comparing side-by-side displacement results computed from the three approaches presented in the previous sections are shown in Figures 7-1 through 7-6. These plots are organized by predictive model (i.e., Rathje and Saygili 2009, Bray and Travasarou 2007) and city.

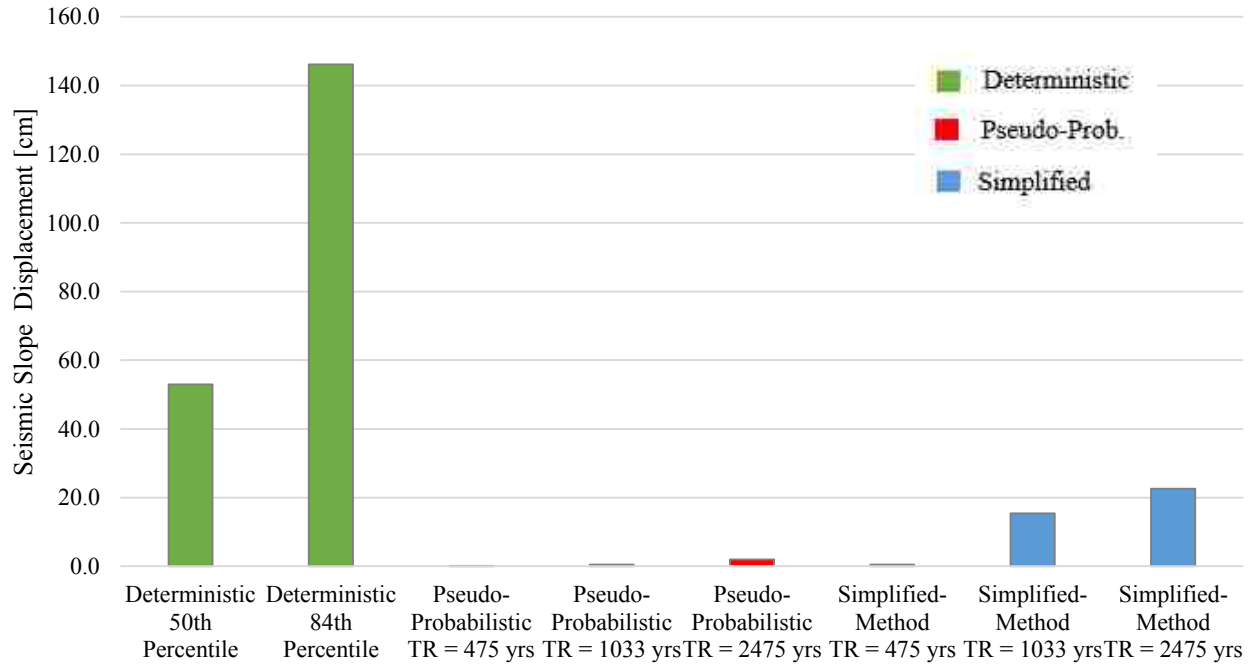

Figure 7-1: Comparison of deterministic, pseudo-probabilistic, and simplified probabilistic methods using Rathje and Saygili (2009) for Butte, MT (latitude 46.033, longitude -112.533).

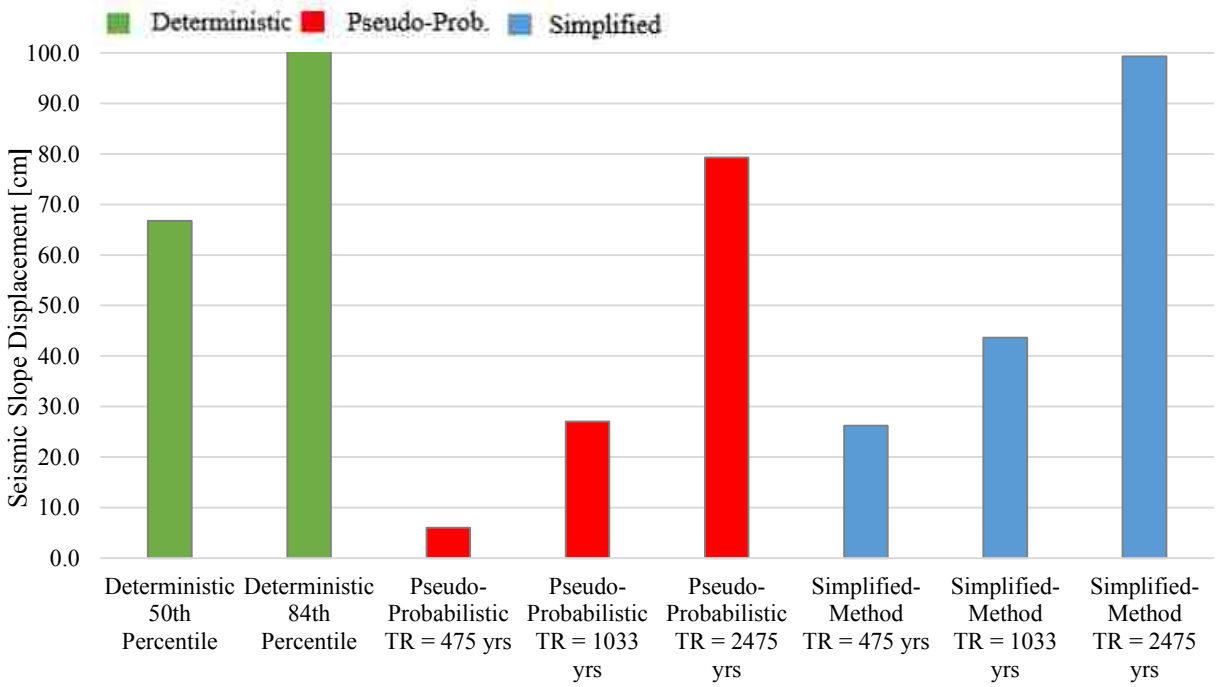

Figure 7-2: Comparison of deterministic, pseudo-probabilistic, and simplified probabilistic using Rathje and Saygili (2009) for Salt Lake City, UT (latitude 40.755, longitude -111.898).

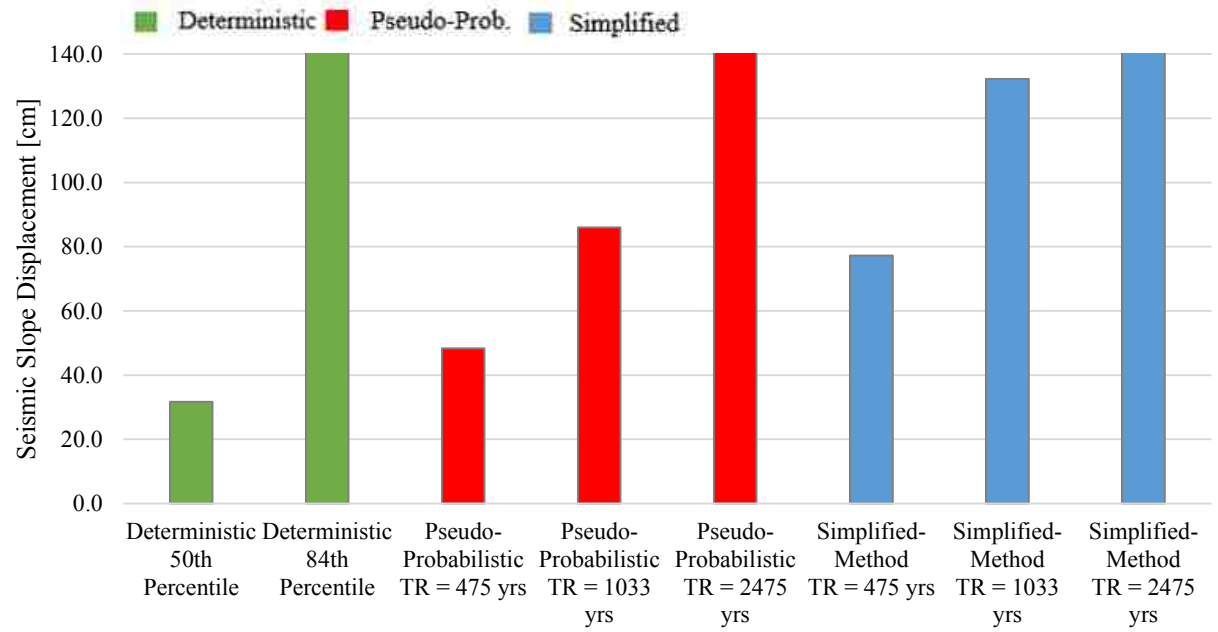

Figure 7-3: Comparison of deterministic, pseudo-probabilistic, and simplified probabilistic methods using Rathje and Saygili (2009) for San Francisco, CA (latitude 37.775, longitude -122.418).

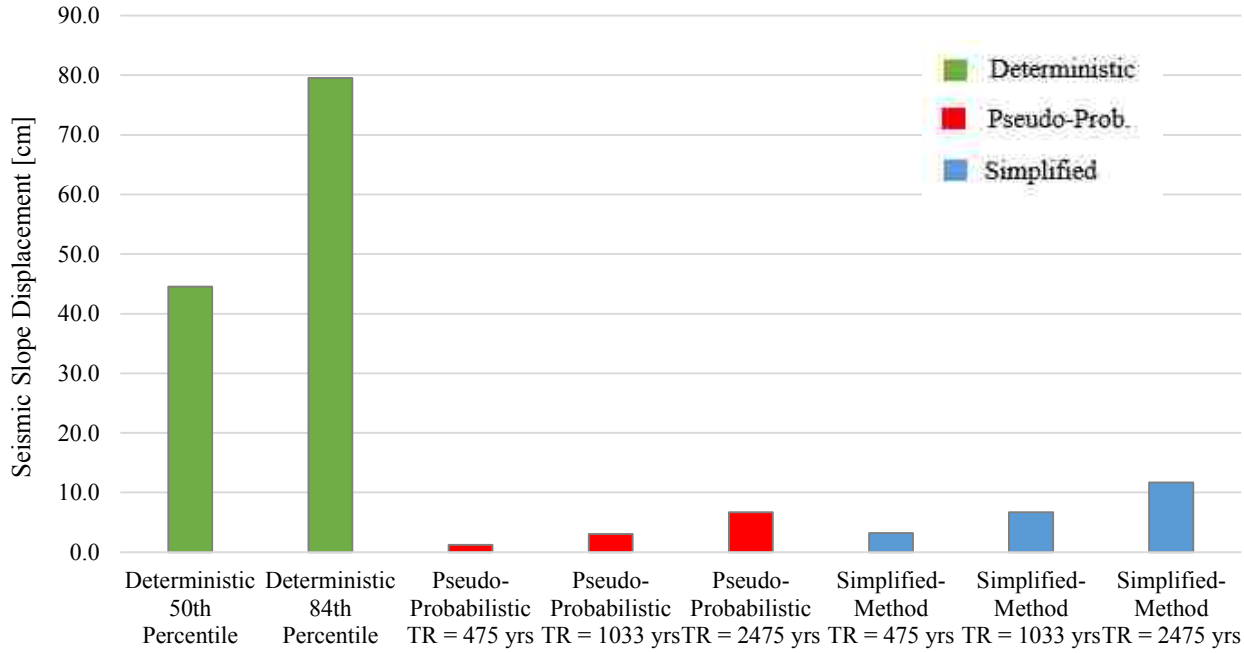

Figure 7-4: Comparison of deterministic, pseudo-probabilistic, and simplified probabilistic methods using Bray and Travasarou (2007) for Butte, MT (latitude 46.033, longitude -112.533).

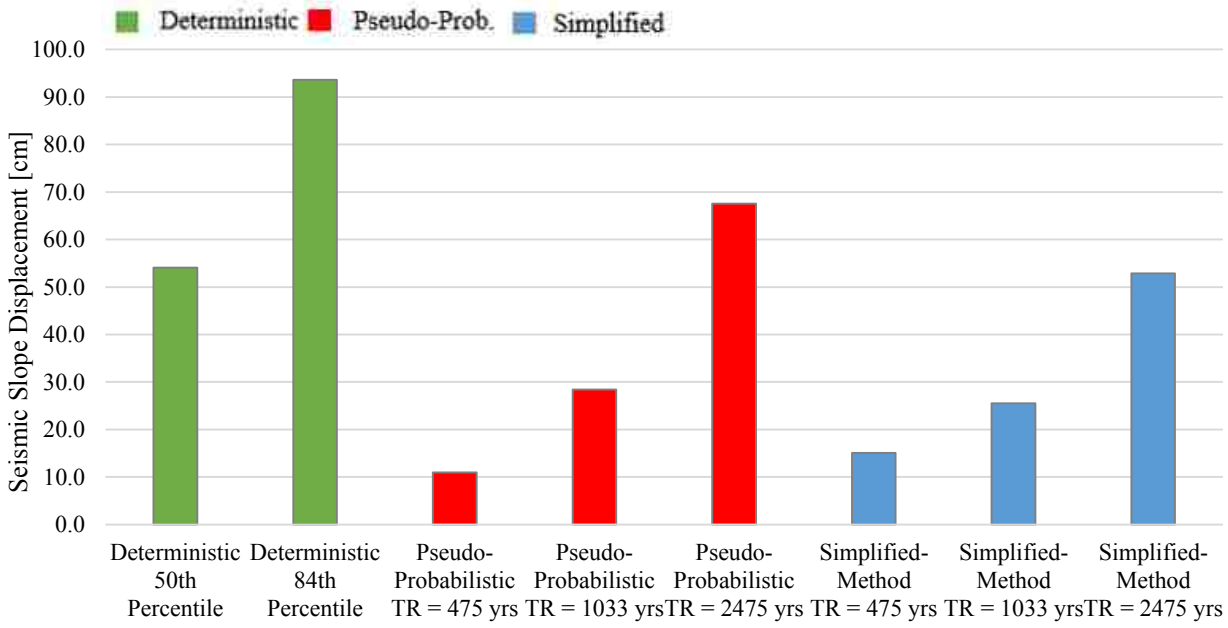

Figure 7-5: Comparison of deterministic, pseudo-probabilistic, and simplified probabilistic methods using Bray and Travasarou (2007) for Salt Lake City, UT (latitude 40.755, longitude -111.898).

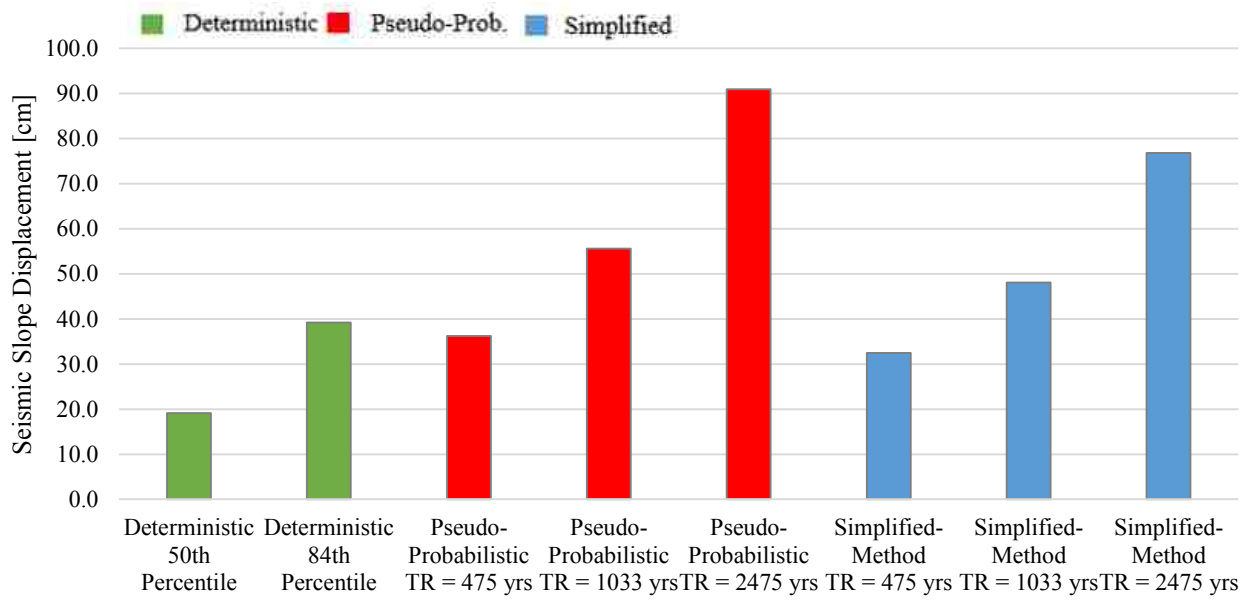

Figure 7-6: Comparison of deterministic, pseudo-probabilistic, and simplified probabilistic methods using Bray and Travasarou (2007) for San Francisco, CA (latitude 37.775, longitude -122.418).

The different seismicity areas represented by the plots shown in Figures 7-1 through 7-6 reveal some interesting findings. Figures 7-1 and 7-4 show that the deterministic approach predicts significantly larger seismic slope displacements than both the simplified probabilistic and pseudo-probabilistic methods in areas of low seismicity such as Butte with both the Rathje and Saygili (2009) model and the Bray and Travasarou (2007) model. These results can be attributed to the deterministic procedure not accounting for the likelihood of the Rocker fault rupturing, predicting a displacement with an extremely low probability of occurring.

The moderate seismicity city, Salt Lake City, presented in Figure 7-2 for the Rathje and Saygili (2009) model, shows that the deterministic approach predicts displacements higher than the simplified probabilistic and pseudo-probabilistic approaches at return periods of 475 and 1,033 years, but not at the return period of 2,475 years. The Bray and Travasarou (2007) results in Figure 7-5 show that the 84th percentile deterministic results are larger than the results from both the

simplified probabilistic and pseudo-probabilistic approaches at all three return periods. It is also important to note that the pseudo-probabilistic approach predicts slightly larger displacements than the simplified probabilistic approach. These results suggest that selecting the "most appropriate" ground motion can be particularly challenging in areas of medium seismicity.

Lastly, the results for San Francisco in Figures 7-3 and 7-6 show that the simplified probabilistic approach generally produces predicted displacements comparable to or larger than the deterministic approach with both sliding block models. Computed pseudo-probabilistic results are larger than the simplified probabilistic results when using the Bray and Travasarou (2007) model but are smaller than the simplified probabilistic results when using the Rathje and Saygili (2009) model.

7.3 Summary

The results of this study suggest that deterministic methods can predict significantly more seismic slope displacement hazard than probabilistic methods in areas of low seismicity where potential seismic sources are located near the site of interest. In areas of moderate seismicity, the application of deterministic methods can result in predicted displacements that are comparable to or slightly larger than predicted displacements from probabilistic methods. In high seismicity areas, deterministic methods can often predict smaller seismic slope displacement hazard than probabilistic methods, particularly at higher return periods. These results suggest that the deterministic results could be used as an upper-bound displacement estimate in a seismic slope displacement analysis. Engineers performing such analysis in areas of medium to high seismicity would therefore choose the lower of the deterministic and the probabilistic results to use in design. This approach is consistent with that prescribed for the development of design ground motions

according to most current seismic design provisions. Furthermore, engineers should avoid use of the pseudo-probabilistic approach when estimating seismic slope displacements because the ground motions used in this approach may not accurately represent the ground motions that would be produced from any actual earthquake, nor does the approach consider probabilistic ground motions in a complete and appropriate manner.

8 DEVELOPMENT OF THE SIMPLIFIED PROBABILISTIC LIQUEFACTION ASSESMENT TOOL (SPLIQ)

This section explains the components of *SPLiq* necessary to perform a simplified seismic slope displacement analysis and provides some guidance for how the tool should be used. This section also addresses the addition of the mapped reference parameter database to *SPLiq* and how an interpolated D^{ref} value is obtained from this database.

SPLiq has the capability of computing simplified liquefaction triggering, lateral spread, post-liquefaction settlement and, seismic slope displacement with data entered for a given location. This chapter outlines the steps the user would follow to complete a seismic slope displacement analysis, although some general information pertaining to other types of analysis are briefly mentioned and/or referred to.

8.1 Description of the spreadsheet (SPLiq) worksheets

Inputs

This section of the spreadsheet is the starting place of the analysis. Here, the user may select what analyses and options he/she would prefer (Figure 8-1). The user also enters the soil

profile information based on standard penetration testing (SPT, see Figure 8-2), mapped or interpolated reference parameter values, and other necessary parameters for the simplified performance-based analysis (Figure 8-3). At the bottom of the sheet, there is a section for deterministic inputs if the user would like to also perform a deterministic analysis.

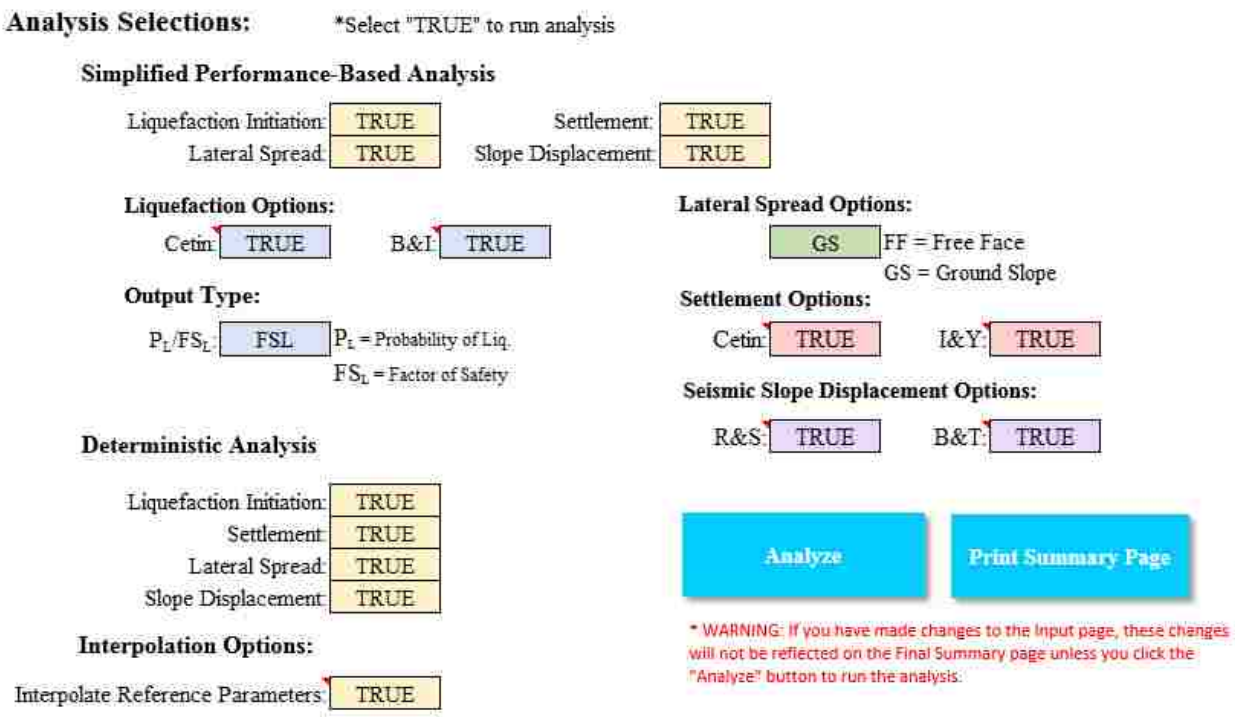

Figure 8-1: Analysis selections section on the inputs tab.

Depth to Water Table = 0 m

Depth (m)	SPT N	γ (kN/m^3)	Fines (%)	Thickness (m)	K_{DR}	Soil Type	Susceptible?
0.50	15	19.6	10.0	1.00		[SM]_Silty_san	Yes
1.50	12	19.6	10.0	1.00		[SM]_Silty_san	Yes
2.50	11	19.6	10.0	1.00		[SM]_Silty_san	Yes
3.50	8	19.6	10.0	1.00		[SM]_Silty_san	Yes
4.50	10	19.6	10.0	1.00		[SM]_Silty_san	Yes
5.50	11	19.6	10.0	1.00		[SM]_Silty_san	Yes
6.50	18	19.6	10.0	1.00		[SM]_Silty_san	Yes
7.50	19	19.6	10.0	1.00		[SM]_Silty_san	Yes
8.50	22	19.6	10.0	1.00		[SM]_Silty_san	Yes
9.50	27	19.6	10.0	1.00		[SM]_Silty_san	Yes
10.50	30	19.6	10.0	1.00		[SM]_Silty_san	Yes
11.50	25	19.6	10.0	1.00		[SM]_Silty_san	Yes
12.50	26	19.6	10.0	1.00		[SM]_Silty_san	Yes
13.50	28	19.6	10.0	1.00		[SM]_Silty_san	Yes
14.50	27	19.6	10.0	1.00		[SM]_Silty_san	Yes
15.50	29	19.6	10.0	1.00		[SM]_Silty_san	Yes
16.50	24	19.6	10.0	1.00		[SM]_Silty_san	Yes
17.50	30	19.6	10.0	1.00		[SM]_Silty_san	Yes

Hammer Efficiency (%): 60

Borehole Diameter: 120 mm

Rod Stickup Length: 1.2 m

Sampler Type: L

NL = Room for liners, but no liners
L = Standard Split Spoon

Figure 8-2: Soil profile input section (only needed for liquefaction triggering and settlement analyses).

Site Liquefaction/Slope Disp. Parameters:

PGA =	0.6000	
F_{PGA} =	1.000	
M_w =	6.9	
Vs12 =	190.0	m/s
Site Class =	D	

1 = Calculate F_{PGA} automatically
2 = User-defined F_{PGA} value entered in box above

Site Lateral Spread Parameters:

S =	1	%
W =	0	%
T_{15} =	16.75	m
F_{15} =	21.8	%
$D50_{15}$ =	1.01	mm

Site Slope Disp. Parameters:

k_y = 0.17

Mapped/Interpolated Reference Values:

Liq. Initiation/Settlement:

$CSR(\%)^{ref}$ =	11.78
N_{req}^{ref} =	11.20
$\varepsilon_{v,Cetin}(\%)^{ref}$ =	0.00
$\varepsilon_{v,J\&T}(\%)^{ref}$ =	0.00

Lateral Spread Disp:

$Log\ D_h^{ref}$ = 0.04

Seismic Slope Disp:

$D_{R\&S}^{ref}$ =	0.50
$D_{B\&T}^{ref}$ =	1.03

Figure 8-3: Ground motion and reference input parameters.

Map help

This worksheet shows an example of a D^{ref} map and shows how to retrieve a value from a particular reference parameter map of interest using *ArcMap*.

Simplified performance-based seismic slope displacement calculations

This worksheet computes the simplified and deterministic seismic slope displacements based on the Rathje and Saygili (2009) and the Bray and Travasarou (2007) models. The derivation of the simplified performance-based model is explained in Chapter 4. This worksheet provides the user with information regarding the computation of seismic slope displacement. The user does not enter any information in this worksheet. When the user clicks the "analyze" button on the *inputs* worksheet, all calculations on this worksheet are updated automatically.

Final summary

This worksheet presents the final output of the seismic slope displacement analysis as specified by the user on the *Inputs* worksheet. The format of this section is already set up for easy printing. The headers of each page are associated with the project information entered on the *inputs* worksheet. The first page of output summarizes the user-specified input from the *inputs* worksheet to facilitate review and quality assurance. The next two pages of output present the results of the various analyses selected by the user. To print only the pages with the user-specified analyses, the user must return to the *inputs* tab and click the "print final summary" button. The print preview window will appear and show only the user-specified portions of the analysis.

References

This worksheet provides references for the models used in *SPLiq* and further guidance for using this tool. The worksheet also provides information on how a reference hazard value is calculated through interpolation.

Interpolation

The included interpolation tool computes a hazard reference value of a selected location using an inverse distance weighted interpolation scheme. Once a location is entered as a latitude and longitude, the tool finds the four nearest surrounding data points and interpolates a reference hazard value from the four points. ***Figure 8-4*** displays a schematic of the interpolation performed by the *SPLiq*.

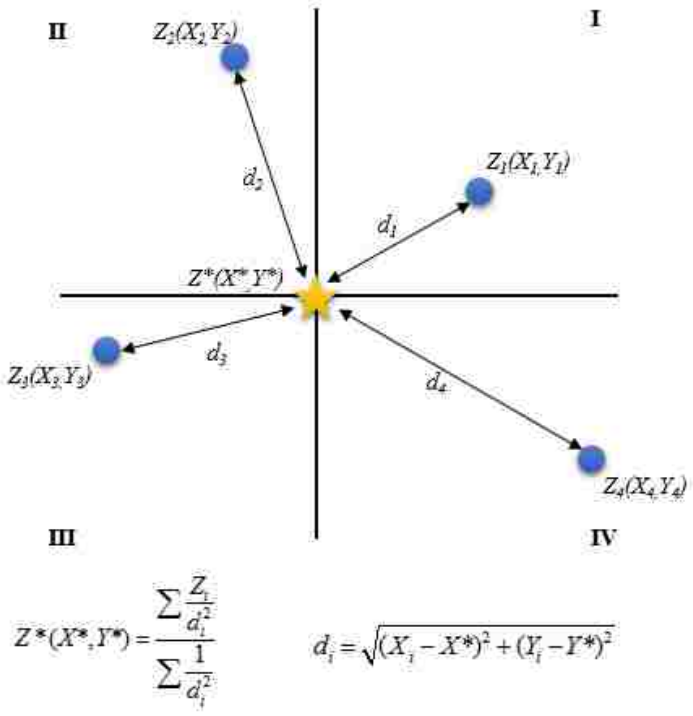

Figure 8-4: Inverse distance weighted interpolation scheme as performed in the *SPLiq*.

The user may enter a location, return period, and choose to automatically interpolate reference parameters on the *inputs* tab (Figure 8-5). If the user chooses to deactivate the automatic interpolation function, then reference parameter values must be entered manually by the user after obtaining the values from the appropriate reference parameter map(s).

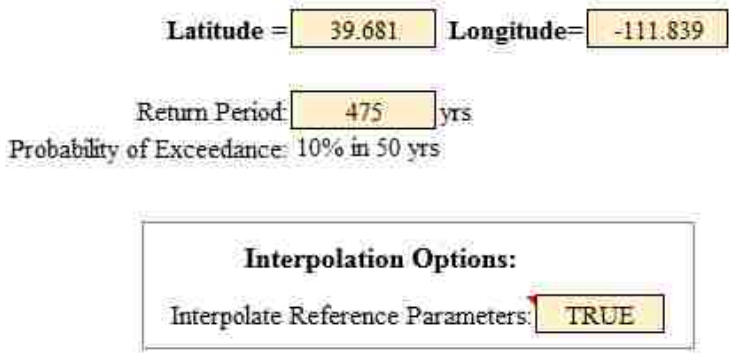

Figure 8-5: Inputs required for the included interpolation tool.

8.2 Suggested simplified probabilistic procedure for seismic slope displacement analysis

This section presents a recommended step-by-step procedure for successfully performing a simplified performance-based seismic slope displacement analysis using the Rathje and Saygili (2009) and/or the Bray and Travasarou (2007) models.

1) Select an appropriate return period for the project (this may depend on the intended use of the building, code requirements, etc.).
2) Open *SPLiq* and under "analysis selections" specify the analyses to perform.

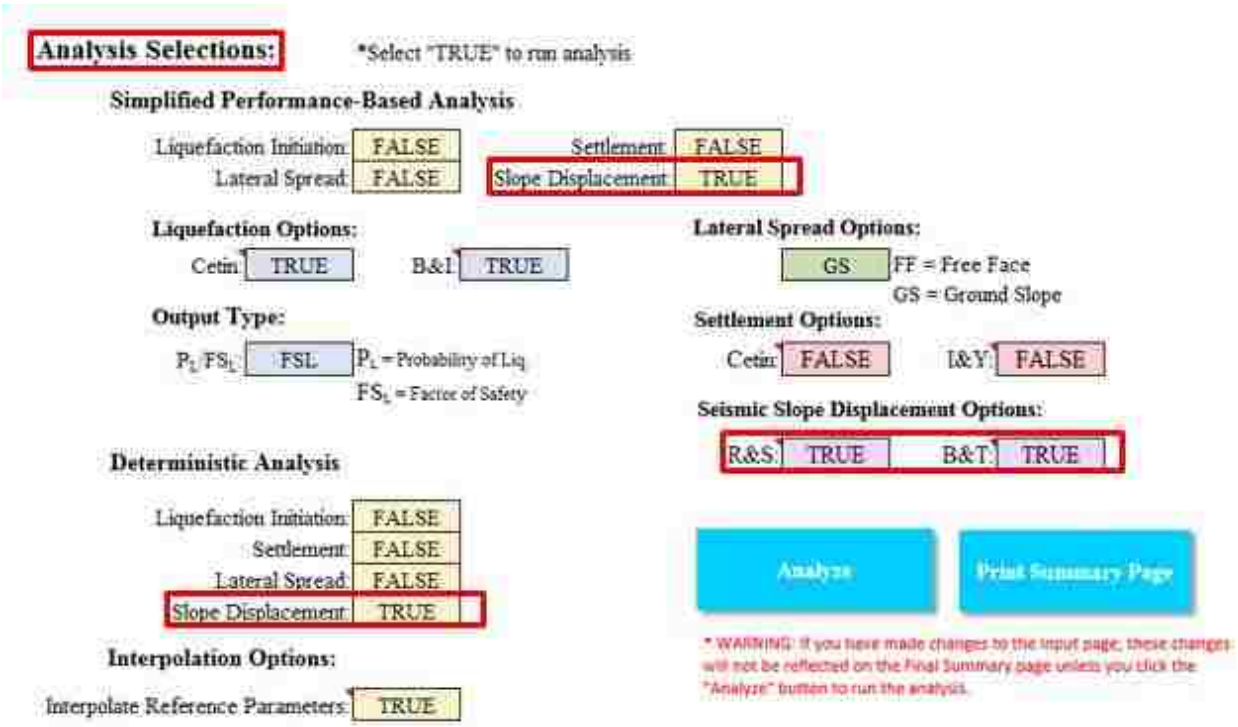

Figure 8-6: Analysis selections section for seismic slope displacement analysis.

3) Enter the required site slope displacement parameters on the *inputs* tab. Some of the parameters will be the same as those entered for a site-specific liquefaction analysis in which case the values need to be filled just once.

    a. *PGA*: This term should be retrieved from the 2008 USGS Interactive Deaggregation website (http://geohazards.usgs.gov/deaggint/2008/) at the return period specified in Step 1. Note that the website uses exceedance probabilities instead of return periods. Use Table 8-1 to convert return periods to exceedance probabilities.

Table 8-1: Conversions between return period and exceedance probability

	Exceedance Probability	
Return Period	**Percent**	**Years**
475	10 (15)	50 (75)
1,039 (1,033)	2 (7)	21 (75)
2,475	2 (3)	50 (75)

After entering the latitude and longitude of the site, exceedance probability, spectral period of 0.0 s, and $V_{s,30}$ of 760 m/s into the interactive deaggregation website, retrieve the *PGA* from the output report. This value is necessary for estimating f_a. An example of where this number is located in the output report is provided in the *references* worksheet in *SPLiq*.

b. f_a: If the user checks the "Calculate f_a automatically" checkbox, *SPLiq* will calculate f_a according to the AASHTO 2012. However, this cannot be done if the site class is specified as F (see site class in part e). For the case of a site class F, the user must manually specify a f_a value based on a site-specific site response analysis.

c. M_w: This is found in the same output report created to find the *PGA* value from the deaggregation. An example of where this number is located in the output report is provided in the *references* tab of *SPLiq*.

d. $V_{s,12}$: The shear wave velocity in the upper 12 m (40 ft) is only required for liquefaction initiation calculations. If the user is simply performing a

seismic slope displacement analysis, then he/she does not need to specify a value for $V_{s,12}$.

e. Site class: This is necessary for calculating f_a. Site class is determined based on soil type and soil properties. The *references* tab in *SPLiq* provides reference documentation and further guidance on assigning the site class.

f. k_y: This value is necessary for the computation of seismic slope displacements for both Rathje and Saygili (2009), and Bray and Travasarou (2007) models. It can be computed using slope stability analysis software available to practicing engineers.

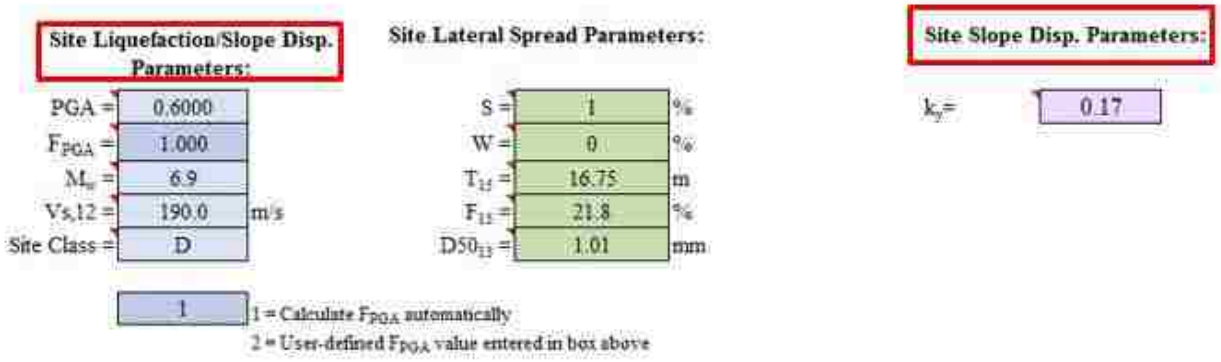

Figure 8-7: Site slope displacement parameter inputs.

4) Retrieve the logged D^{ref} for both the Rathje and Saygili (2009) and Bray and Travasarou (2007) models from the appropriate reference parameter map(s). Alternatively, these values can be automatically interpolated by activating the option in the *inputs* worksheet of *SPLiq*.

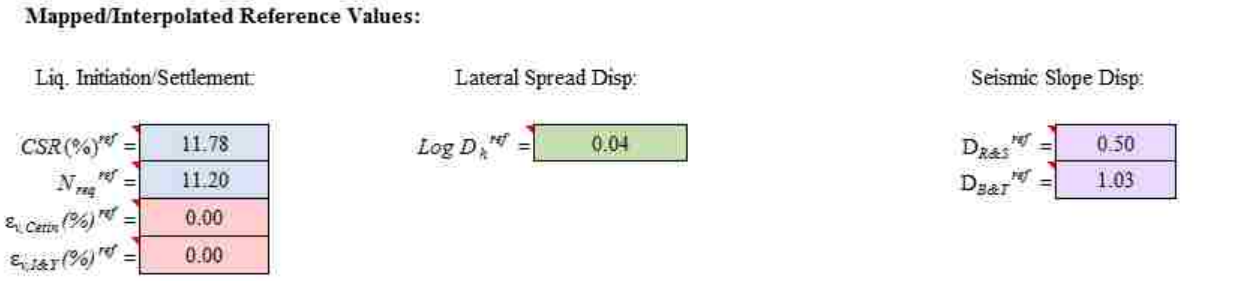

Figure 8-8: Mapped/interpolated slope displacement values.

5) If the user wishes to use a deterministic analysis as an upper-bound to the performance-based results, the user should enter the deterministic values of *PGA*, M_w, and percentile of the seismic slope displacement to be considered.
   a. Deterministic values of *PGA* and M_w should be developed by an experienced engineer with proper training in DSHA.
   b. It is suggested that a deterministic analysis should be considered when the engineer suspects that the project could benefit from a deterministic cap. In areas of low seismicity, this is likely unnecessary.

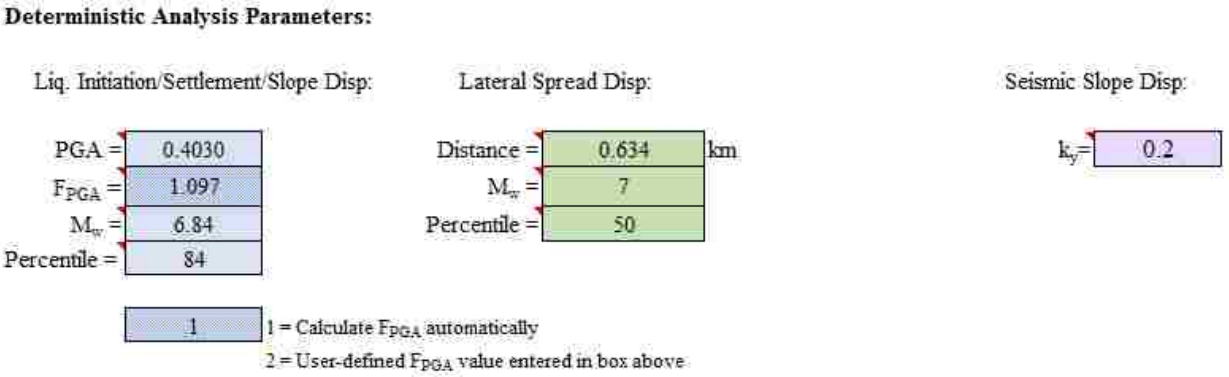

Figure 8-9: Deterministic analysis parameters for slope displacement computation.

6) Several dropdown menus are displayed near the top of the *inputs* worksheet that allow the user to select what analyses (i.e., liquefaction initiation, settlement, lateral spread, or seismic slope stability) and models (e.g., Rathje and Saygili 2009, Bray

and Travasarou 2007) the user would like to consider. Select the desired analyses, models, and options before proceeding to the next step.

7) Once everything is correctly entered into the *inputs* worksheet, press the "analyze" button. The calculation results are displayed on the *final summary* tab.

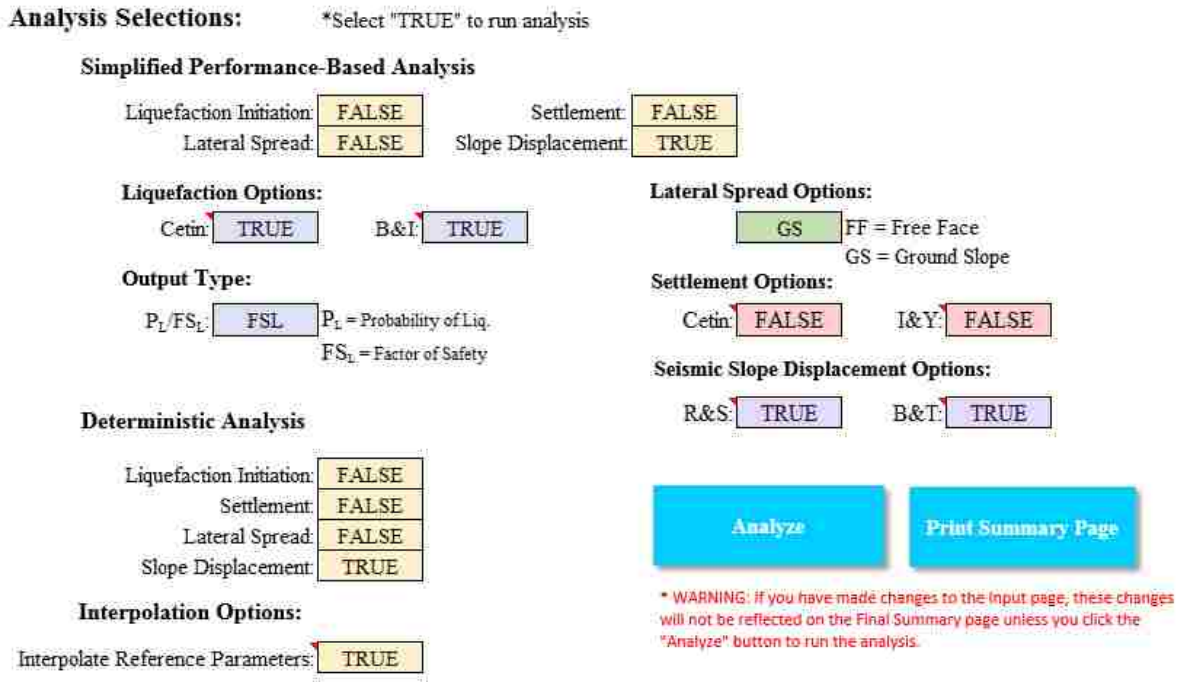

Figure 8-10: Final check of all inputs and "analyze".

8) The *final summary* worksheet displays plots, tables and a summary of inputs in a printable format. The headers of these pages reflect information such as company name, project name/number, date, etc. entered at the top of the *inputs* worksheet. Figure 8-11 is an example of the *final summary* section of the seismic slope displacement analysis.

Summary of Inputs for Seismic Slope Displacement Analysis:

Input Parameters	
PGA =	0.6
F_{PGA} =	1
M_w =	6.85
k_y =	0.17
Site Class =	D

Refence Value	
$D_{R\&S}^{ref}$ =	0.5
$D_{B\&T}^{ref}$ =	1.0

Inputs for Deterministic Analysis	
PGA =	0.403
k_y =	0.2
M_w =	6.84
Percentile =	84

Seismic Slope Displacement Results:

Simplified PB Results:

$D_{R\&S}^{site}$ = **0.040** cm

$D_{B\&T}^{site}$ = **0.552** cm

Deterministic Results:

$D_{R\&S}$ = **0.000** cm

$D_{B\&T}$ = **3.637** cm

Figure 8-11: Example of final summary of slope displacement analysis.

8.3 Summary

This chapter introduces *SPLiq*. Various components and aspects of the tool are described, and step-by-step instructions are provided for the user to perform a simplified performance-based seismic slope displacement analysis. With this tool and description, an engineer will be able to use the simplified performance-based seismic slope displacement procedure presented in this thesis.

9 CONCLUSIONS

Millions of lives have been lost over the years as a result of the effects of earthquakes. One of these devastating effects is slope failure. Over the years, seismologists and engineers have collaborated to better record ground motions during an earthquake and better understand the resulting effects. As technology advances, the data obtained has become more refined, allowing engineers to use the data to predict earthquake effects in areas where earthquakes have not yet occurred. As part of these efforts, Newmark (1965) proposed what is now called the Newmark sliding block method. This method models a mass, in this case a rigid block, sliding down an inclined plane. Permanent deformations of the rigid block accrue when the acceleration of the block surpasses the frictional and cohesive resistance created between the bottom of the block and the surface of the inclined plane. A few of the assumptions from this method have been criticized as over-simplifications through time, and modified or more sophisticated Newmark sliding block models have been developed as a result.

As Newmark sliding block methods have continued to progress and evolve, the need to account for the uncertainties in the methods has increased. Deterministic methods have been used to incorporate parameters that would account for some of the uncertainty in the analysis as well as probabilistic approaches applied deterministically (pseudo-probabilistic method). Fully probabilistic methods, like the performance-based earthquake engineering framework developed by the PEER Center, allows engineers to account for all of the uncertainties related to ground

motions and its resultant effects. Although this relatively new approach is generally well regarded and widely accepted, a fully probabilistic approach requires significant computational effort and is rarely applied on engineering projects today.

The work presented in this thesis provides a solution to this problem by introducing a simplified performance-based approach that closely approximates the results produced by a fully probabilistic seismic slope displacement analysis at targeted return periods. The development of the simplified performance-based approach involved the following:

1) Development of the simplified procedure using a probabilistic approach as described in Chapters 3 and 4.
2) Validation of the simplified procedure using seismic information from 10 different cities to quantify how well the simplified procedure approximates the results from a fully probabilistic seismic slope displacement analysis. The results of this validation suggest that the proposed procedure approximates the fully probabilistic results very well when the predicted displacements are 50 cm (20 in) or less.
3) Evaluation and quantification of interpolation errors due to grid spacing effects in the use of seismic slope displacement reference parameter maps. A grid spacing study was conducted including 35 cities in areas of varying seismicity. The optimum grid spacing was defined such that values interpolated from four grid points would be within a margin of 5% error and/or absolute difference of 5 cm or less.
4) Development of seismic slope displacement reference parameter maps for the states of Connecticut, Idaho, Montana, Utah, and South Carolina at return periods of 475, 1,033, and 2,475 years. These reference parameter maps are found in Appendix B. A full description of the mapping process applied in this study is found in Chapter 6.

5) A comparative study between the simplified performance-based, pseudo-probabilistic, and deterministic methods is performed in three cities of varying seismicity. The purpose of this comparison was not to prove that the simplified method is better than the others, but to understand how and under what circumstances the results of the evaluated approaches might govern in engineering design. In general, it is recommended that an engineer use the lower of the simplified performance-based approach and the deterministic approach for design. It is recommended that the pseudo-probabilistic approach no longer be used for engineering design where possible.

The following important observations are noted and highlighted from this study:

1) In the validation study, the simplified performance-based procedure with both the Rathje and Saygili (2009) and Bray and Travasarou (2007) models shows very good agreement with the fully probabilistic procedure up to predicted displacements of about 50 cm (20 in). At larger predicted displacements, the Rathje and Saygili model tends to show more scatter in its approximation of the fully probabilistic procedure. This scatter was mostly observed in areas of high seismicity and in areas of low seismicity when k_y was very close to 0.1 g, which is also the value for k_y^{ref}. For such cases, the simplified performance-based procedure with the Bray and Travasarou (2007) model demonstrated much more stability and a better approximation of the fully probabilistic procedure. To account for these limitations, *SPLiq* was modified to disable the Rathje and Saygili (2009) model when unreasonable displacement values are predicted.
2) When comparing the simplified method to the pseudo-probabilistic and deterministic methods, it was observed that in areas of low seismicity like Butte, MT, the deterministic method predicted significantly higher displacements when compared to

the simplified performance-based and pseudo-probabilistic methods. In areas of moderate seismicity like Salt Lake City, UT, there is no clear pattern as to which method predicts the larger displacements. This will depend largely on the local seismic environment. Lastly, in areas of high seismicity like San Francisco, CA, the simplified performance-based method tends to predict larger displacements than the deterministic method.

From the results and observations obtained from this study the following is recommended:

1) When developing seismic slope displacement reference parameter maps, areas of concern (e.g., sensitive or highly populated sites) may require a tighter grid spacing than proposed by the optimized grid spacing study presented in this thesis.
2) The validation study presented in this thesis analyzed sites that have been commonly been analyzed in past performance-based validation studies. To better understand how well the proposed simplified performance-based seismic slope stability procedure approximates the fully probabilistic procedure in a particular region of interest, a localized validation study that takes into account local site effects and any potential unique seismic sources (e.g., subduction zones, volcanoes, etc.) is recommended.
3) When performing a seismic slope stability analysis with simplified Newmark sliding block models, both a deterministic analysis and a simplified performance-based analysis should be performed to allow the engineer to apply sound engineering judgement in selecting which predicted displacement will govern design. Engineers should cease to apply the pseudo-probabilistic procedure when performing seismic slope displacement analysis due to the inconsistent and oft-misinterpreted results that it produces across different seismic environments.

4) Seismic slope displacement reference parameter maps should be updated from time to time as updated and more accurate seismic source models become available and/or the ability of engineers to predict more accurate seismic slope displacements increases.

REFERENCES

Abrahamson. (2007). Personal communication. (E. M. Rathje, & G. Saygili, Interviewers)

Abrahamson, N., & Silva, W. (1997). Empirical Response Spectral Attenuation Relations for Shallow Crustal Earthquakes. *Seismological Research Letters*, 94-127.

Abrahamson, N., & Silva, W. (2008). Summary of the Abrahamson & Silva NGA Ground-Motion Relations. *Earthquake Spectra*, 67-97.

Ambraseys, N. (1958). *The seismic stability of earth dams.* London: PhD Dissertation, University of London.

American Association of State Highway and Transportation Officials. (2012). AASHTO LRFD Bridge Design Specifications. Washington D.C.: 6th Edition, ISBN: 978-1-56051-523-4, AASHTO.

American Association of State Highway and Transportation Officials. (2014). AASHTO LRFD Bridge Design Specifications. Washington D.C.: 7th Ed., ISBN: 1-56051-592-0, AASHTO.

Ancheta, T., Darragh, R., Stewart, J., Seyhan, E., Silva, W., Chiou, B., . . . and Donahue, J. (2014). NGA-West2 Database. *Earthquake Spectra*, 989-1005.

Armstrong, R. J., Malvick, E. J., Hansra, H., & Eiermann, C. (2013). Evaluation of empirical predictive models used to predict earthquake-induced slope deformations. *Geo-Congress 2013* (pp. 1250-1259). San Diego, CA: ASCE.

Blume, J., Newmark, N., & Corning, L. (1961). *Design of Multi-story Reinforced Concrete Buildings for Earthquake Motions.* Chicago: Portland Cement Association.

Boore, D. M., & M., A. G. (2008). Ground-Motion Prediction Equations for the Average Horizontal Component of PGA, PGV, and 5% Damped PSA at Spectral Periods between 0.01 s and 10.0 s. *Earthquake Spectra*, 99-138.

Bray, J. D. (1990). *The Effects of Tectonic Movements on Stresses and Deformations in Earth Embankments.* Berkeley: PhD Dissertation, University of California.

Bray, J. D., & Rodriguez-Marek, A. (2004). Characterization of forward-directivity ground motions in the near-fault region. *Soil Dynamic and Earthquake Engineering*, 815-828.

Bray, J. D., ASCE, F., & Travasarou, T. (2007, April). Simplified Procedure for Estimating Earthquake-Induced Deviatoric Slope Displacements. *Journal of Geotechnical and Geoenvironmental Engineering*, 381-392.

Caltrans. (2013). *Guidelines on Foundation Loading and Deformation Due to Liquefaction Induced Lateral Spreading.* Sacramento, CA: Caltrans.

Campbell, K. W., & Bozorgnia, Y. (2008). NGA Ground Motion Model for the Geometric Mean Horizontal Component of PGA, PGV, PGD and 5% Damped Linear Elastic Response Spectra for Periods Ranging from 0.01 to 10 s. *Earthquake Spectra*, 139-171.

Casagrande, A. (1936). Characteristics of cohesionless soils affecting the stability of slopes and earth fills. *Journal of Boston Society of Civil Engineers*, 257-275.

Chiou, B. S.-J., & Youngs, R. R. (2008). An NGA Model for the Average Horizontal Component of Peak Ground Motion and Response Spectra. *Earthquake Spectra, 24*(1), 179-215.

Christian, J. T., Ladd, C. C., & Baecher, G. B. (1994). Reliability Applied To Slope Stability Analysis. *Journal of Geotechnical and Geoenvironmental Engineering*, 2180-2207.

Cornell, C., & Krawinkler, H. (2000, April). Progress and challenges in seismic performance assessment. *PEER News*, pp. 1-3.

Deierlein, G., Krawinkler, H., & Cornell, C. (2003). A framework for performance-based earthquake engineering. *2003 Pacific Conference on Earthquake Engineering* (pp. 1-3). Stanford, CA: PEER Center.

Dietrich, W., McKean, J., Bellugi, D., & Perron, T. (2007). The prediction of shallow landslide location and size using a multidimensional landslide analysis in a digital terrain model.

Ekstrom, L. T., & Franke, K. W. (2016). Simplified Procedure for the Performance-Based Prediction of Lateral Spread Displacements. *Journal of Geotechnical and Geoenvironmental Engineering*.

Elgamal, A.-W., Scott, R., Succarieh, M., & Yan, L. (1990). La Villita dam response during five earthquakes including permanent deformations. *Journal of Geotechnical and Geoenvironmental Engineering*, 1443-1462.

ESRI. (2011). ArcGIS Desktop: Release 10. Redlands, CA: Environmental Systems Research Institute.

Fitzenz, D. D., & Nyst, M. (2015). Building Time-Dependent Earthquake Recurrence Models. *Bulletin of the Seismological Society of America*, 120-133.

Franke, K. (2005). *Development of a performance-based model for the prediction of lateral spreading displacements.* Seattle: M.S Thesis University of Washington.

Franke, K. W. (2011). *A Performance-Based Model for the Computation of Kinematic Pile Response Due to Lateral Spreading and Its Application on Select Bridges Damaged*

During the M7.6 Earthquake in the Limon Province, Costa Rica. Provo: PhD Dissertation, Brigham Young University.

Franke, K. W., & Kramer, S. L. (2014). Procedure for the Empirical Evaluation of Lateral Spread Displacement Hazard Curves. *Journal of Geotechnical and Geoenvironmental Engineering*, 110-120.

Franke, K. W., Mayfield, R. T., & Wright, A. D. (2014b). Simplified Uniform Hazard Liquefaction Analysis for Bridges. *Journal of the Transportation Research Board*, 47-55.

Franke, K. W., Wright, A. D., & Hatch, C. K. (2014d). PBliquefY: A New Analysis Tool For The Performance-Based Evaluation Of Liquefaction Triggering. *Tenth U.S. National Conference on Earthquake Engineering.* Anchorage, AK: Earthquake Engineering Research Institute.

Franke, K., Mayfield, R., & and Wright, A. (2014d). Simplified uniform hazard analysis for bridges. *Transportation Research Record.* Washington D.C.

Franke, K., Wright, A., & Hatch, C. (2014c). PBLiquefY: A new analysis tool for the performance-based evaluation of liquefaction triggering. *Proceedings, 10th National Conference on Earthquake Engineering.* Oakland, CA: EERI.

Gazetas, G., & Uddin, N. (1994). Permanent Deformation of Preexisting Sliding Surfaces in Dams. *Journal of Geotechnical Engineering*, 2041-2061.

Hamada, M., Towhata, I., Yasuda, S., & Isoyama, R. (1987). Study of permanent ground displacement induced by seismic liquefaction. *Computers and Geotechnics*, 197-220.

Harmsen, S., Perkins, D., & Franke, A. (1999). Deaggreation of Probabilistic Ground Motions in the Central and Eastern United States. *Bulletin of the Seismological Society of America*, 1-13.

Huang, Y.-M. (2008). *Performance-based design and evaluation for liquefaction-related seimic hazards.* Seattle, Washington: University of Washington.

International Building Code. (2014). *2015 International Building Code.* Country Club Hills, IL: International Code Council.

Jibson, R. W. (1993). Predicting Earthquake-Induced Landslide Displacements Using Newmark's Sliding Block Analysis. *Transportation Research Record*, 9-17.

Jibson, R., Harp, E., & Michael, J. (2000). A method for producing digital probabilistic seismic landslide hazard maps. *Engineering Geology*, 271-289.

Kayen, R., Moss, R., Thomson, E., Seed, R., Cetin, K., Kiureghian, A., . . . Tokimatsu, K. (2013). Shear-Wave Velocity–Based Probabilistic and Deterministic Assessment of Seismic Soil Liquefaction Potential. *Journal of Geotechnical and Geoenvironmental Engineering*, 407-419.

Keefer, D. K. (1984). Landslides Caused By Earthquakes. *Geological Society of America Bulletin*, 406-421.

Kieffer, D. S., Jibson, R., Rathje, E. M., & Kelson, K. (2006). Landslides Triggered by the 2004 Niigata Ken Chuetsu, Japan, Earthquake. *Eartquake Spectra*, S47-S73.

Kim, J., & Sitar, N. (2003). Importance of Spatial and Temporal Variability in Analysis of Seismically-Induced Slope Deformation. *9th International Conference on Applications of Statistics and Probability in Civil Engineering.* San Francisco: Millpress Science.

Kramer, S. (1996). *Geotechnical Earthquake Engineering.* Upper Saddle River, NJ: Prentice Hall .

Kramer, S. L. (2008). *Evaluation of liquefaction hazards in Washington State.* Seattle: WSDOT Report.

Kramer, S. L. (2014). Performance-based design methodologies for geotechnical earthquake engineering. *Bull Earthquake Engineering*, 1049-1070.

Kramer, S. L., & Mayfield, R. T. (2007). Return period of soil liquefaction. *Journal of Geotechnical and Geoenvironmental Engineering*, 802-813.

Kramer, S. L., & Smith, M. W. (1997). Modified Newmark Model for Seismic Displacements of Compliant Slopes. *Journal of Geotechnical and Geoenvironmental Engineering*, 635-644.

Ledezma, C., & Bray, J. D. (2010). Probabilistic Performance-Based Procedure to Evaluate Pile Foundations at Sites with Liquefaction-Induced Lateral Displacement. *Journal of Geotechnical and Geoenvironmental Engineering*, 464-476.

Lemos, P. J., & Coelho, P. A. (1991). Displacements of Slopes Under Earthquake Loading. *Second International Conference of Recent Advances in Geotechnical Earthquake Engineering and Soil Dynamics* (pp. 1051-1056). St. Louis, Missouri: Scholarsmine.

Lin, J.-S., & Whitman, R. V. (1986). Earthquake Induced Displcements of Sliding Blocks. *Journal of Geotechnical Engineering*, 44-59.

Luco, N. (2002). *PROBABILISTIC SEISMIC DEMAND ANALYSIS, SMRF CONNECTION FRACTURES, AND NEAR-SOURCE EFFECTS.* Stanford: PhD Dissertation Stanford University.

Lumb, P. (1970). Safety factors and the probability distribution of soil strength. *Canadian Geotechnical Journal, 7*(3), 225-242.

Marrone, J., Ostadan, F., Youngs, R., & Litehiser, J. (2003). Probabilistic Liquefaction Hazard Evaluation: Method and Application. *Transactions of the 17th International Conference on Structural Mechanics in Reactor Technology (SMiRT 17).* Prague, Czech Republic.

Mayfield, R. T., Kramer, S. L., & Huang, Y.-M. (2010, January). Simplified Approximation Procedure for Perfomance-Based Evaluation on Liquefaction Potential. *Journal of Geotechnical and Geoenvironmental Engineering*, 140-150.

McCrink, T., & Real, C. (1996). *Evaluation of the Newmark method for mapping earthquake-induced landslide hazards in the Laurel 7-1/2 minute Quadrangle, Santa Cruz County, California.* Reston, VA: U.S. Geological Survey.

Newmark, N. (1965). Effects of Earthquake on Dams and Embankments. *Fifth Rankine Lecture*, (p. 22). London.

Phoon, K.-K., & Kulhawy, F. H. (1999). Characterization of Geotechnical Variability. *Canadian Geotechnical Journal*, 612-624.

Porter, K. (2003). An Overview of PEER's Performance-Based Earthquake Engineering Methodology. *Ninth International Conference of Applications of Statistics and Probability in Civil Engineering.* San Francisco (CA).

Rathje, E. M., & Saygili, G. (2008). Empirical Predictive Models for Earthquake-Induced Sliding. *Journal of Geotechnical and Geoenvironmental Engineering*, 790-803.

Rathje, E. M., & Saygili, G. (2009, March). Probabilistic Assesment of Earthquake-Induced Sliding Displacements of Natural Slopes. *Bulletin of the New Zeland Society of Earthquake Engineering, 42*(1), 18-27.

Reiter, L. (1990). Earthquake Hazard Analysis - Issues and Insights. *Columbia University Press*, p. 254.

Saygili, G. (2008). *A Probabilistic Approach for Evaluating Earthquake-Induced Landslides.* Austin: PhD Dissertation, University of Texas .

SEAOC, V. (1995). Performance based seismic engineering of buildings. Sacramento(CA): Structural Engineers Association of California, USA.

Seed, H., & Idriss, I. (1970). *Soil Moduli and Damping Factors for Dynamics Response Analyses.* Berkeley, CA: Earthquake Engineering Research Center.

Stewart, J. A. (2003). Amplification factors for spectral acceleration in tectonically active regions. *Bull.Seismol. Soc. Am.*, 93(7): 332-352.

Stewart, J. P., & Whang, D. (2003). Simplified procedure to estimate ground settlement from seismic compression in compacted soils. *2003 Pacific Conference on Earthquake Engineering.* Christchurch, New Zealand.

Stewart, J., Bray, J. D., McMahon, D. J., Smith, P. M., & Kropp, A. (2001). Seimic Performance of Hillside Fills. *Journal of Geotechnical and Geoenvironmental Engineering*, 905-919.

Tinti, S., & Manucci, A. (2006). Gravitational stability computed through the limit equilibrium method revisited. *Geophysical Journal International*, 1-14.

Travasarou, T., & Bray, J. (2003). Optimal ground motion intensity measures for assessment of seismic slope displacements. *2003 Pacific Conference on Earthquake Engineering.* Christchurch, New Zealand.

Travasarou, T., Bray, J. D., & Der Kiureghian, A. (2004). A Probabilistic Methodology for Assesing Seismic Slope Displacements. *13th World Conference on Earthquake Engineering.* Vancouver, B.C., Canada .

Ulmer, K., Ekstrom, L., & Franke, K. (2015). Optimum Grid Spacing for Simplified Performance-based Liquefaction and Lateral Spread Displacement Parameter Maps. *6th International Conference on Earthquake Geotechnical Engineering.* Christchurch, New Zealand.

USGS. (2008). *USGS 2008 Interactive Deaggregations*. Retrieved from United States Geological Survey: http://geohazards.usgs.gov/deaggint/2008/ (accessed June 15, 2015)

USGS. (2016, January 29). Retrieved from United States Geological Survey: http://earthquake.usgs.gov/earthquakes/eqarchives/year/eqstats.php

USGS, M. B. (2006). *"Quaternary Fault and Fold Database of the United States"*. Retrieved from http://earthquake.usgs.gov/hazards/qfaults/(date accessed: January 21,2015).

Vahedifard, F., & Meehan, C. L. (2011). Error Analysis of Predicted Seismic Displacement of Earth Dams Using Simplified Sliding Block Methods. *Geo-Frontiers 2011: Advances in Geotechnical Engineering* (pp. 3245-3254). Dallas, TX: ASCE.

Wartman, J., D., B. J., & Seed, R. B. (2003). Inclined Plane Studies of the Newmark Sliding Block Procedure. *Journal of Geotechnical and Geoenvironmental Engineering, 129*(8), 673-684.

Wells, D. L., & Coppersmith, K. J. (1994). New empirical relationships among magnitude, rupturelength, rupture width, rupture area, and surface displacement. *Bulletin of the Seismological Society of America*, 974-1002.

Yegian, M. K., & Ghahraman, V. G. (1991a). Earthquake-Induced Permanent Deformations: Probabilistic Approach. *Journal of Geotechnical Engineering*, 35-50.

Yegian, M., & Marciano, E. G. (1991b). Seismic Risk Analysis for Earth Dams. *Journal of Geotechnical and Geoenvironmental Engineering*, 18-34.

APPENDIX A: SUPPLEMENTARY VALIDATION DATA

The following tables are supplementary to the validation presented in Chapter 5. Table A-1 and Table A-2 show the results from the simplified seismic slope displacement procedure. The D^{ref} values were generated from *PBLiquefY* using a k_y^{ref} value of 0.1 g. To calculate D^{site}, equation 4-7 was used with a f_a^{ref} value of 1, k_y^{site} of 0.1, 0.2, 0.3, 0.4, and 0.5 g and f_a^{site} values from Table 5-2. Table A-3 shows the results of the full probabilistic seismic slope displacement procedure. These values were all generated from *PBLiquefY* with k_y^{site} of 0.1, 0.2, 0.3, 0.4, and 0.5 g and f_a^{site} values from Table 5-2.

Table A-1: Results from simplified seismic slope displacement procedure based on Rathje and Saygili (2009).

	Site	D^{ref} Rathje & Saygili (cm)			ΔlnD (Rathje & Saygili)			D^{site} Rathje & Saygili (cm)		
		475 Yrs.	1033 Yrs.	2475 Yrs.	475 Yrs.	1033 Yrs.	2475 Yrs.	475 Yrs.	1033 Yrs.	2475 Yrs.
	Butte	<0.5	<0.5	0.7	15.3	3.3	1.5	0.0	13.8	3.2
	Charleston	<0.5	12.5	81.8	2.0	0.4	0.0	3.6	18.1	81.8
	Eureka	96.0	280.1	670.9	0.0	0.0	0.0	96.0	280.1	670.9
k_y^{ref}=0.1	Memphis	0.5	17.5	92.6	1.8	0.5	0.0	3.0	28.2	92.6
k_y^{site}=0.1	Portland	2.9	18.5	72.9	1.3	0.6	0.2	11.1	34.3	86.0
	Salt Lake City	2.6	24.0	87.6	1.2	0.3	0.0	8.8	31.2	87.6
	San Francisco	47.6	105.5	205.0	0.2	0.0	0.0	55.8	105.5	205.0
	San Jose	36.7	73.7	137.8	0.1	0.0	0.0	41.1	73.7	137.8
	Santa Monica	22.2	57.2	126.6	0.3	0.0	0.0	30.4	57.2	126.6
	Seattle	12.5	42.7	117.8	0.6	0.1	0.0	21.9	49.4	117.8
	Butte	<0.5	<0.5	0.7	-33.7	-6.1	-1.7	0.0	0.0	0.1
	Charleston	<0.5	12.5	81.8	-2.6	-1.5	-1.2	0.0	2.7	25.6
	Eureka	96.0	280.1	670.9	-1.4	-0.9	-0.5	24.4	119.3	387.1
	Memphis	0.5	17.5	92.6	-2.2	-1.5	-1.5	0.1	3.9	21.3
k_y^{ref}=0.1	Portland	2.9	18.5	72.9	-1.5	-1.5	-1.6	0.7	4.1	15.0
k_y^{site}=0.2	Salt Lake City	2.6	24.0	87.6	-1.4	-1.5	-1.3	0.6	5.1	24.8
	San Francisco	47.6	105.5	205.0	-1.6	-1.5	-1.2	9.8	24.1	63.8
	San Jose	36.7	73.7	137.8	-1.6	-1.5	-1.2	7.4	16.7	40.5
	Santa Monica	22.2	57.2	126.6	-1.5	-1.5	-1.1	4.8	12.2	40.5
	Seattle	12.5	42.7	117.8	-1.5	-1.6	-1.3	2.8	8.7	31.6
	Butte	<0.5	<0.5	0.7	-347.7	-66.1	-14.1	0.0	0.0	0.0
	Charleston	<0.5	12.5	81.8	-26.2	-3.5	-2.3	0.0	0.4	8.5
	Eureka	96.0	280.1	670.9	-2.6	-1.7	-1.2	7.1	49.7	212.0
	Memphis	0.5	17.5	92.6	-20.9	-3.8	-2.8	0.0	0.4	5.8
k_y^{ref}=0.1	Portland	2.9	18.5	72.9	-9.8	-4.4	-3.2	0.0	0.2	3.0
k_y^{site}=0.3	Salt Lake City	2.6	24.0	87.6	-8.1	-3.3	-2.4	0.0	0.9	7.8
	San Francisco	47.6	105.5	205.0	-3.2	-2.8	-2.3	2.0	6.5	21.2
	San Jose	36.7	73.7	137.8	-3.1	-2.8	-2.4	1.6	4.5	12.9
	Santa Monica	22.2	57.2	126.6	-3.4	-2.9	-2.2	0.8	3.1	13.7
	Seattle	12.5	42.7	117.8	-4.1	-3.2	-2.5	0.2	1.8	9.6
	Butte	<0.5	<0.5	0.7	-1368.6	-277.9	-60.2	0.0	0.0	0.0
	Charleston	<0.5	12.5	81.8	-112.9	-7.7	-3.3	0.0	0.0	3.2
	Eureka	96.0	280.1	670.9	-3.8	-2.5	-1.8	2.1	22.0	115.5
	Memphis	0.5	17.5	92.6	-90.1	-9.5	-4.2	0.0	0.0	1.4
k_y^{ref}=0.1	Portland	2.9	18.5	72.9	-40.8	-13.1	-5.8	0.0	0.0	0.2
k_y^{site}=0.4	Salt Lake City	2.6	24.0	87.6	-32.6	-6.5	-3.5	0.0	0.0	2.6
	San Francisco	47.6	105.5	205.0	-5.8	-4.2	-3.3	0.1	1.6	7.8
	San Jose	36.7	73.7	137.8	-5.6	-4.3	-3.4	0.1	1.0	4.5
	Santa Monica	22.2	57.2	126.6	-7.0	-4.5	-3.2	0.0	0.6	5.1
	Seattle	12.5	42.7	117.8	-11.6	-5.7	-3.7	0.0	0.1	3.1
	Butte	<0.5	<0.5	0.7	-3757.7	-798.4	-180.7	0.0	0.0	0.0
	Charleston	<0.5	12.5	81.8	-333.6	-18.8	-4.4	0.0	0.0	1.1
	Eureka	96.0	280.1	670.9	-5.6	-3.3	-2.3	0.3	10.4	64.5
	Memphis	0.5	17.5	92.6	-267.9	-25.1	-6.6	0.0	0.0	0.1
k_y^{ref}=0.1	Portland	2.9	18.5	72.9	-122.8	-36.8	-12.3	0.0	0.0	0.0
k_y^{site}=0.5	Salt Lake City	2.6	24.0	87.6	-98.0	-14.7	-4.9	0.0	0.0	0.7
	San Francisco	47.6	105.5	205.0	-12.1	-6.7	-4.4	0.0	0.1	2.6
	San Jose	36.7	73.7	137.8	-11.2	-6.8	-4.7	0.0	0.1	1.3
	Santa Monica	22.2	57.2	126.6	-16.6	-7.7	-4.3	0.0	0.0	1.8
	Seattle	12.5	42.7	117.8	-31.9	-11.8	-5.2	0.0	0.0	0.6

Table A-2: Results from simplified seismic slope displacement procedure based on Bray and Travasarou (2007).

	Site	D^{ref} Bray & Travasarou (cm)			ΔlnD (Bray & Travasarou)			D^{site} Bray & Travasarou (cm)		
		475 Yrs.	1033 Yrs.	2475 Yrs.	475 Yrs.	1033 Yrs.	2475 Yrs.	475 Yrs.	1033 Yrs.	2475 Yrs.
	Butte	0.5	0.7	2.1	1.2	1.0	0.8	1.7	2.1	4.7
	Charleston	1.2	10.9	47.4	0.9	0.2	0.0	3.0	13.6	47.4
	Eureka	44.3	111.1	227.0	0.0	0.0	0.0	44.3	111.1	227.0
k_y^{ref}=0.1	Memphis	1.7	11.6	40.3	0.9	0.3	0.0	4.1	15.4	40.3
k_y^{site}=0.1	Portland	3.7	10.5	26.1	0.7	0.4	0.1	7.5	15.0	29.0
	Salt Lake City	3.8	16.6	49.5	0.7	0.2	0.0	7.4	19.6	49.5
	San Francisco	23.3	42.3	72.3	0.1	0.0	0.0	25.8	42.3	72.3
	San Jose	23.4	39.1	63.0	0.1	0.0	0.0	25.2	39.1	63.0
	Santa Monica	15.9	33.2	65.4	0.2	0.0	0.0	19.3	33.2	65.4
	Seattle	10.0	23.1	51.4	0.3	0.1	0.0	13.9	25.4	51.4
	Butte	0.5	0.7	2.1	-0.6	-0.6	-0.8	0.3	0.4	1.0
	Charleston	1.2	10.9	47.4	-0.7	-1.2	-1.2	0.6	3.4	14.5
	Eureka	44.3	111.1	227.0	-1.2	-1.1	-0.9	12.7	38.0	89.9
	Memphis	1.7	11.6	40.3	-0.7	-1.1	-1.3	0.8	3.7	11.2
k_y^{ref}=0.1	Portland	3.7	10.5	26.1	-0.8	-1.1	-1.2	1.6	3.5	7.5
k_y^{site}=0.2	Salt Lake City	3.8	16.6	49.5	-0.9	-1.2	-1.2	1.6	5.0	14.7
	San Francisco	23.3	42.3	72.3	-1.3	-1.3	-1.2	6.7	11.8	22.1
	San Jose	23.4	39.1	63.0	-1.3	-1.3	-1.2	6.6	10.8	18.9
	Santa Monica	15.9	33.2	65.4	-1.2	-1.3	-1.2	4.8	9.0	20.2
	Seattle	10.0	23.1	51.4	-1.1	-1.3	-1.2	3.3	6.6	15.0
	Butte	0.5	0.7	2.1	-1.8	-1.8	-1.8	0.1	0.1	0.3
	Charleston	1.2	10.9	47.4	-1.8	-2.1	-2.0	0.2	1.3	6.3
	Eureka	44.3	111.1	227.0	-2.1	-1.8	-1.6	5.3	17.5	45.1
	Memphis	1.7	11.6	40.3	-1.8	-2.1	-2.2	0.3	1.4	4.6
k_y^{ref}=0.1	Portland	3.7	10.5	26.1	-1.9	-2.1	-2.2	0.6	1.3	2.9
k_y^{site}=0.3	Salt Lake City	3.8	16.6	49.5	-1.9	-2.2	-2.1	0.6	1.9	6.2
	San Francisco	23.3	42.3	72.3	-2.2	-2.2	-2.0	2.6	4.8	9.5
	San Jose	23.4	39.1	63.0	-2.2	-2.2	-2.1	2.6	4.4	8.1
	Santa Monica	15.9	33.2	65.4	-2.1	-2.2	-2.0	1.9	3.6	8.7
	Seattle	10.0	23.1	51.4	-2.1	-2.2	-2.1	1.2	2.6	6.3
	Butte	0.5	0.7	2.1	-2.8	-2.6	-2.7	0.0	0.1	0.1
	Charleston	1.2	10.9	47.4	-2.6	-2.9	-2.7	0.1	0.6	3.2
	Eureka	44.3	111.1	227.0	-2.8	-2.5	-2.2	2.6	9.4	25.8
	Memphis	1.7	11.6	40.3	-2.6	-2.9	-2.9	0.1	0.7	2.3
k_y^{ref}=0.1	Portland	3.7	10.5	26.1	-2.7	-2.9	-2.9	0.3	0.6	1.4
k_y^{site}=0.4	Salt Lake City	3.8	16.6	49.5	-2.7	-2.9	-2.7	0.3	0.9	3.2
	San Francisco	23.3	42.3	72.3	-2.9	-2.9	-2.7	1.3	2.4	4.9
	San Jose	23.4	39.1	63.0	-2.9	-2.9	-2.7	1.2	2.2	4.1
	Santa Monica	15.9	33.2	65.4	-2.9	-2.9	-2.7	0.9	1.8	4.5
	Seattle	10.0	23.1	51.4	-2.9	-2.9	-2.8	0.6	1.2	3.2
	Butte	0.5	0.7	2.1	-3.5	-3.4	-3.3	0.0	0.0	0.1
	Charleston	1.2	10.9	47.4	-3.3	-3.5	-3.2	0.0	0.3	1.9
	Eureka	44.3	111.1	227.0	-3.4	-3.0	-2.6	1.5	5.6	16.2
	Memphis	1.7	11.6	40.3	-3.3	-3.5	-3.5	0.1	0.4	1.3
k_y^{ref}=0.1	Portland	3.7	10.5	26.1	-3.3	-3.5	-3.5	0.1	0.3	0.8
k_y^{site}=0.5	Salt Lake City	3.8	16.6	49.5	-3.4	-3.5	-3.3	0.1	0.5	1.8
	San Francisco	23.3	42.3	72.3	-3.5	-3.5	-3.2	0.7	1.3	2.8
	San Jose	23.4	39.1	63.0	-3.5	-3.5	-3.3	0.7	1.2	2.4
	Santa Monica	15.9	33.2	65.4	-3.5	-3.5	-3.2	0.5	1.0	2.6
	Seattle	10.0	23.1	51.4	-3.5	-3.5	-3.4	0.3	0.7	1.8

Table A-3: Results from full probabilisitic seismic slope displacement procedure.

	Site	Latitude	Longitude	Full PB Method Rathje & Saygili			Full PB Method Bray & Travasarou		
				D^{site} (cm)			D^{site} (cm)		
				475 Yrs	1033 Yrs	2475 Yrs	475 Yrs	1033 Yrs	2475 Yrs
k_y^{ref}=0.1 k_y^{site}=0.1	Butte	46.003	-112.533	<0.5	0.8	3.3	1.0	2.4	5.3
	Charleston	32.726	-79.931	1.4	19.8	90.9	3.1	15.3	50.5
	Eureka	40.802	-124.162	112.4	313.9	759.3	48.2	112.5	227.4
	Memphis	35.149	-90.048	2.6	28.8	109.4	4.2	16.5	44.4
	Portland	45.523	-122.675	11.0	41.5	121.3	8.1	17.3	34.0
	Salt Lake City	40.755	-111.898	7.7	33.6	99.3	7.8	21.7	52.9
	San Francisco	37.775	-122.418	66.0	132.3	246.2	29.3	48.1	76.8
	San Jose	37.339	-121.893	48.9	94.3	172.1	28.4	44.4	67.8
	Santa Monica	34.015	-118.492	35.0	74.5	150.2	21.8	38.5	68.5
	Seattle	47.53	-122.3	24.7	65.9	158.7	15.9	29.8	56.6
k_y^{ref}=0.1 k_y^{site}=0.2	Butte	46.003	-112.533	<0.5	<0.5	<0.5	<0.5	<0.5	1.1
	Charleston	32.726	-79.931	<0.5	2.7	25.1	0.6	3.7	14.9
	Eureka	40.802	-124.162	27.7	112.1	330.0	13.7	37.8	86.5
	Memphis	35.149	-90.048	<0.5	3.7	24.1	0.8	3.9	12.3
	Portland	45.523	-122.675	<0.5	3.9	16.8	1.7	3.9	8.4
	Salt Lake City	40.755	-111.898	<0.5	5.4	26.3	1.7	5.4	15.5
	San Francisco	37.775	-122.418	10.6	25.5	57.0	7.4	12.7	21.7
	San Jose	37.339	-121.893	8.3	17.8	36.9	7.2	11.7	18.9
	Santa Monica	34.015	-118.492	4.9	14.0	38.2	5.3	10.2	20.1
	Seattle	47.53	-122.3	2.6	9.9	33.2	3.7	7.4	15.8
k_y^{ref}=0.1 k_y^{site}=0.3	Butte	46.003	-112.533	<0.5	<0.5	<0.5	<0.5	<0.5	<0.5
	Charleston	32.726	-79.931	<0.5	<0.5	7.9	<0.5	1.4	6.3
	Eureka	40.802	-124.162	7.7	44.9	159.8	5.7	17.3	42.7
	Memphis	35.149	-90.048	<0.5	<0.5	6.3	<0.5	1.5	5.0
	Portland	45.523	-122.675	<0.5	<0.5	2.3	0.6	1.4	3.2
	Salt Lake City	40.755	-111.898	<0.5	0.9	8.1	0.6	2.1	6.5
	San Francisco	37.775	-122.418	1.7	5.8	16.2	2.8	5.1	9.0
	San Jose	37.339	-121.893	1.4	3.9	9.8	2.8	4.7	7.7
	Santa Monica	34.015	-118.492	0.7	3.1	11.8	2.0	4.0	8.5
	Seattle	47.53	-122.3	<0.5	1.5	8.5	1.3	2.9	6.5
k_y^{ref}=0.1 k_y^{site}=0.4	Butte	46.003	-112.533	<0.5	<0.5	<0.5	<0.5	<0.5	<0.5
	Charleston	32.726	-79.931	<0.5	<0.5	2.5	<0.5	0.7	3.2
	Eureka	40.802	-124.162	2.1	19.1	82.4	2.9	9.3	24.2
	Memphis	35.149	-90.048	<0.5	<0.5	1.4	<0.5	0.7	2.5
	Portland	45.523	-122.675	<0.5	<0.5	<0.5	<0.5	0.6	1.5
	Salt Lake City	40.755	-111.898	<0.5	<0.5	2.6	<0.5	1.0	3.3
	San Francisco	37.775	-122.418	<0.5	1.1	4.7	1.3	2.5	4.5
	San Jose	37.339	-121.893	<0.5	0.7	2.6	1.3	2.3	3.9
	Santa Monica	34.015	-118.492	<0.5	0.5	4.0	0.9	2.0	4.3
	Seattle	47.53	-122.3	<0.5	<0.5	2.2	0.6	1.4	3.2
k_y^{ref}=0.1 k_y^{site}=0.5	Butte	46.003	-112.533	<0.5	<0.5	<0.5	<0.5	<0.5	<0.5
	Charleston	32.726	-79.931	<0.5	<0.5	0.6	<0.5	<0.5	1.8
	Eureka	40.802	-124.162	<0.5	8.4	44.4	1.6	5.5	15.1
	Memphis	35.149	-90.048	<0.5	<0.5	<0.5	<0.5	<0.5	1.4
	Portland	45.523	-122.675	<0.5	<0.5	<0.5	<0.5	<0.5	0.8
	Salt Lake City	40.755	-111.898	<0.5	<0.5	0.6	<0.5	0.5	1.9
	San Francisco	37.775	-122.418	<0.5	<0.5	1.1	0.7	1.4	2.5
	San Jose	37.339	-121.893	<0.5	<0.5	0.6	0.7	1.2	2.2
	Santa Monica	34.015	-118.492	<0.5	<0.5	1.2	0.5	1.1	2.5
	Seattle	47.53	-122.3	<0.5	<0.5	<0.5	<0.5	0.7	1.8

APPENDIX B: SAMPLE SEISMIC SLOPE DISPLACEMENT REFERENCE PARAMETER MAPS

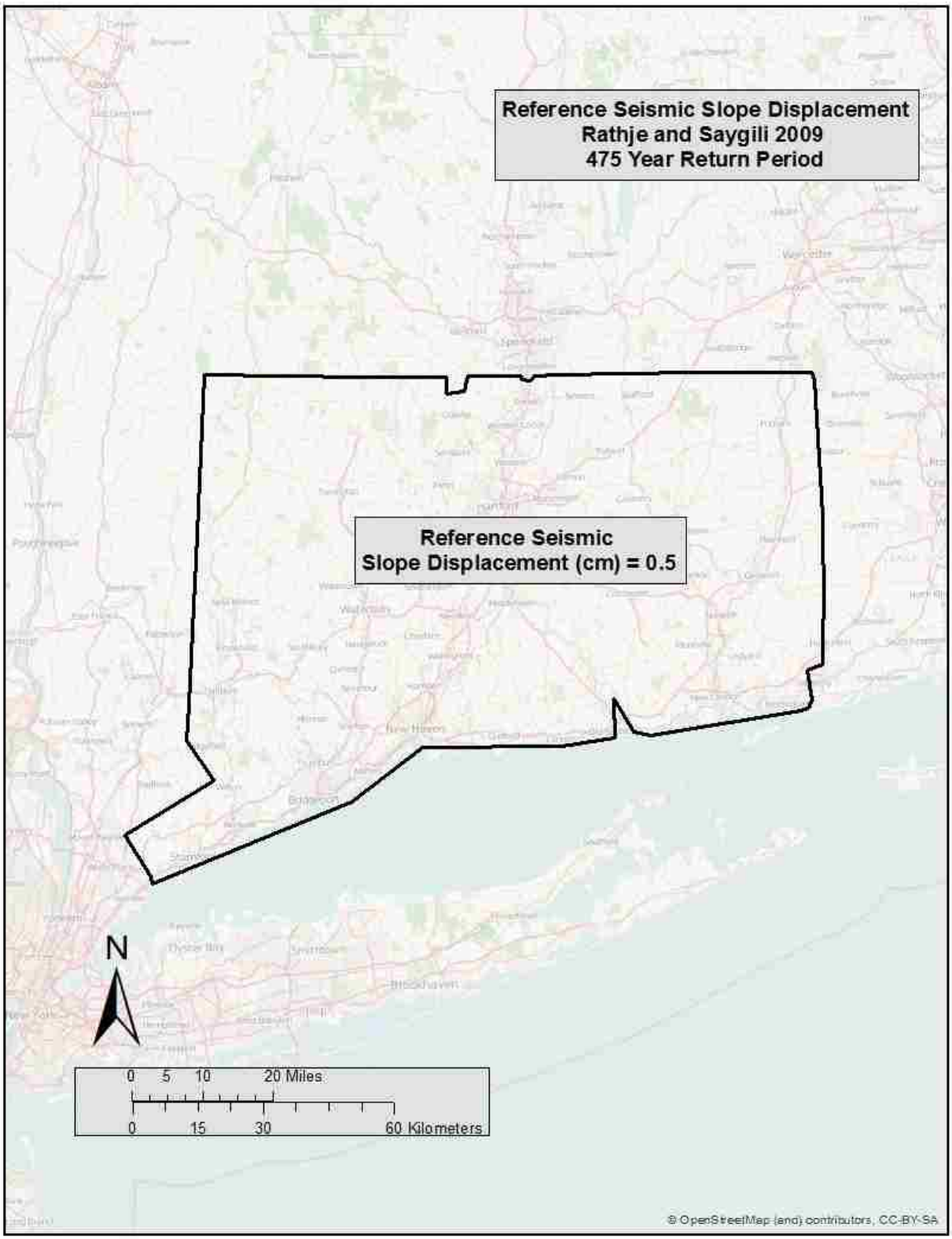

Figure B-1: Rathje and Saygili (2009) seismic slope displacement (D^{ref}) map for Connecticut (Tr = 475).

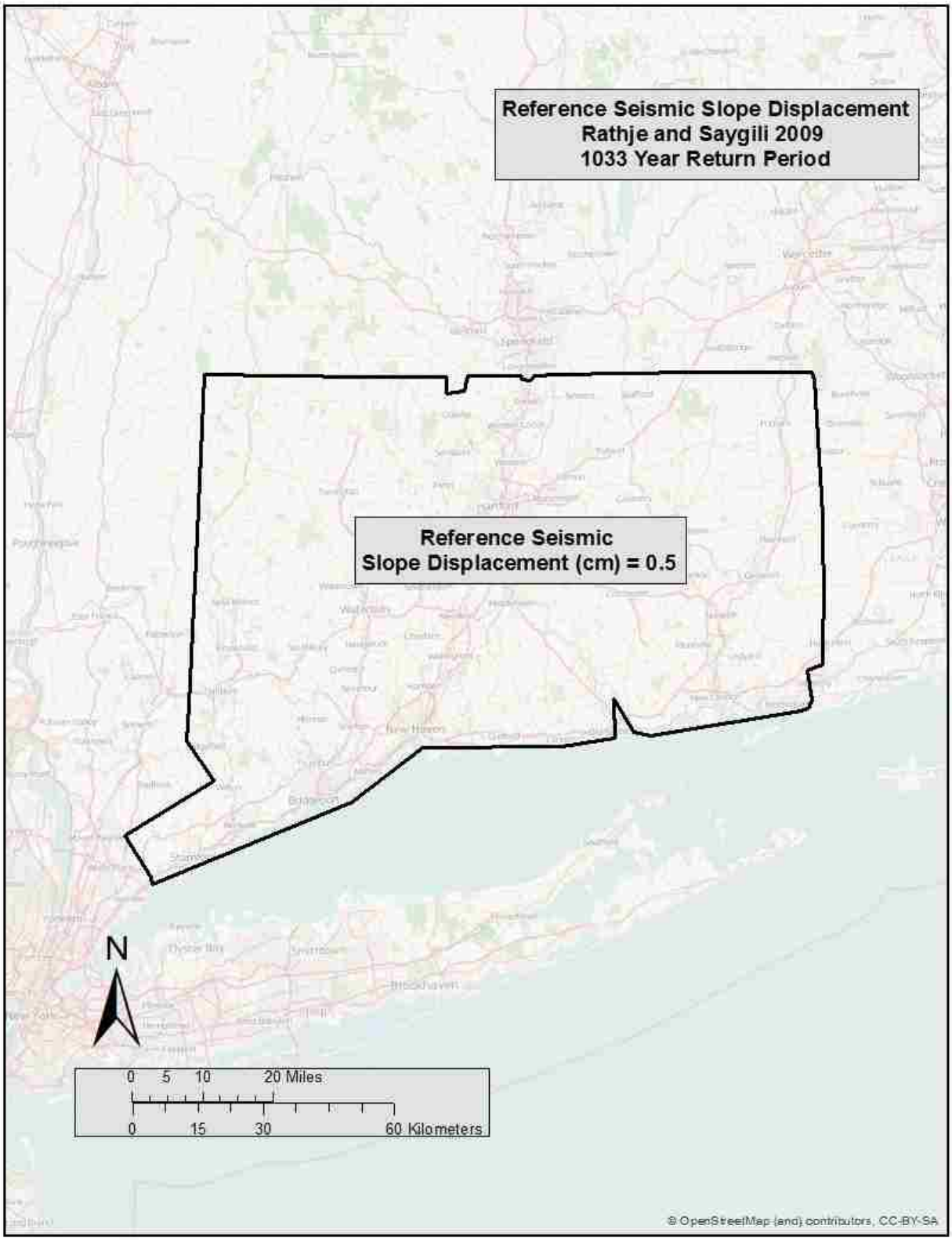

Figure B-2: Rathje and Saygili (2009) seismic slope displacement (D^{ref}) map for Connecticut (Tr = 1,033).

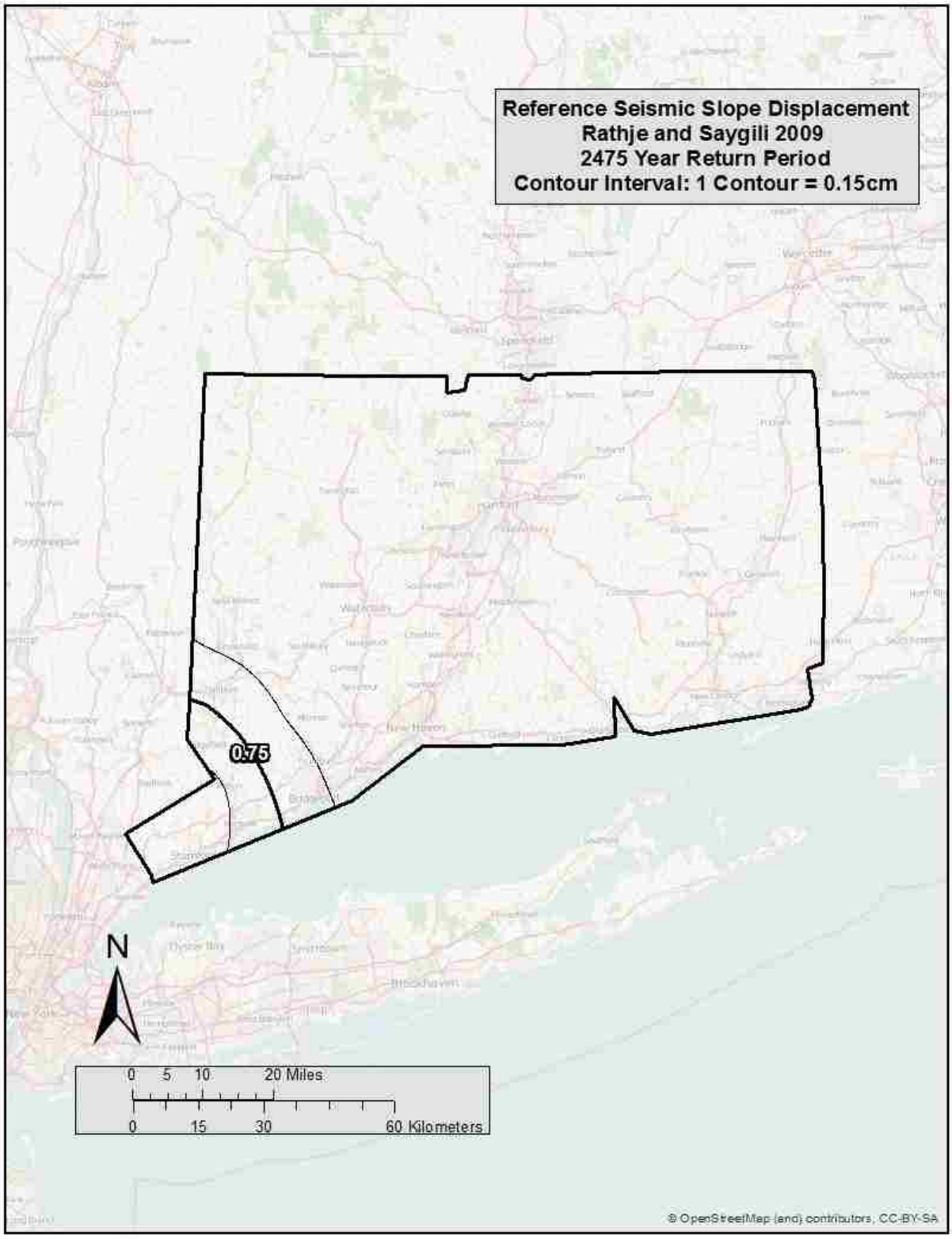

Figure B-3: Rathje and Saygili (2009) seismic slope displacement (D^{ref}) map for Connecticut (Tr = 2,475).

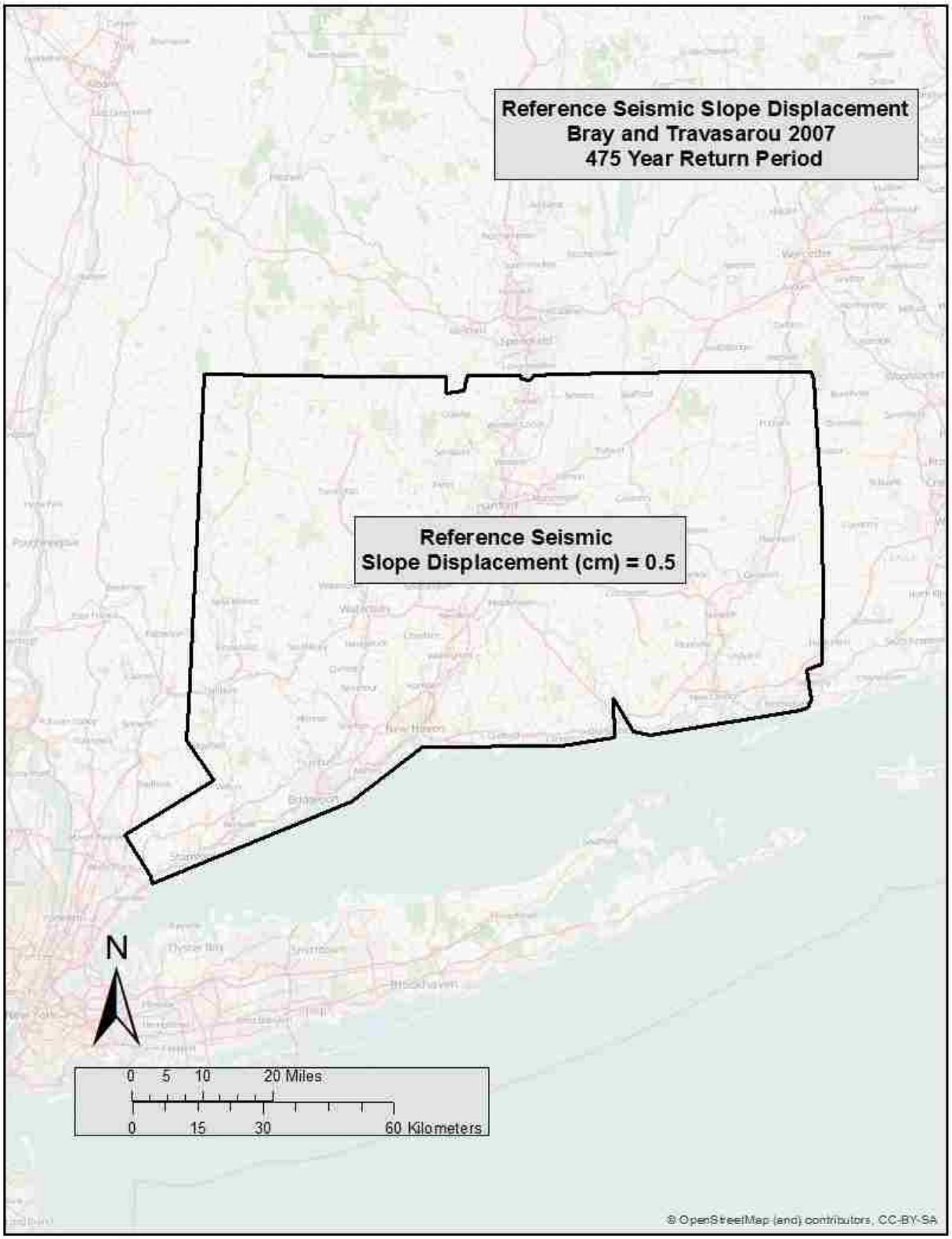

Figure B-4: Bray and Travasarou (2007) seismic slope displacement (D^{ref}) map for Connecticut (Tr = 475).

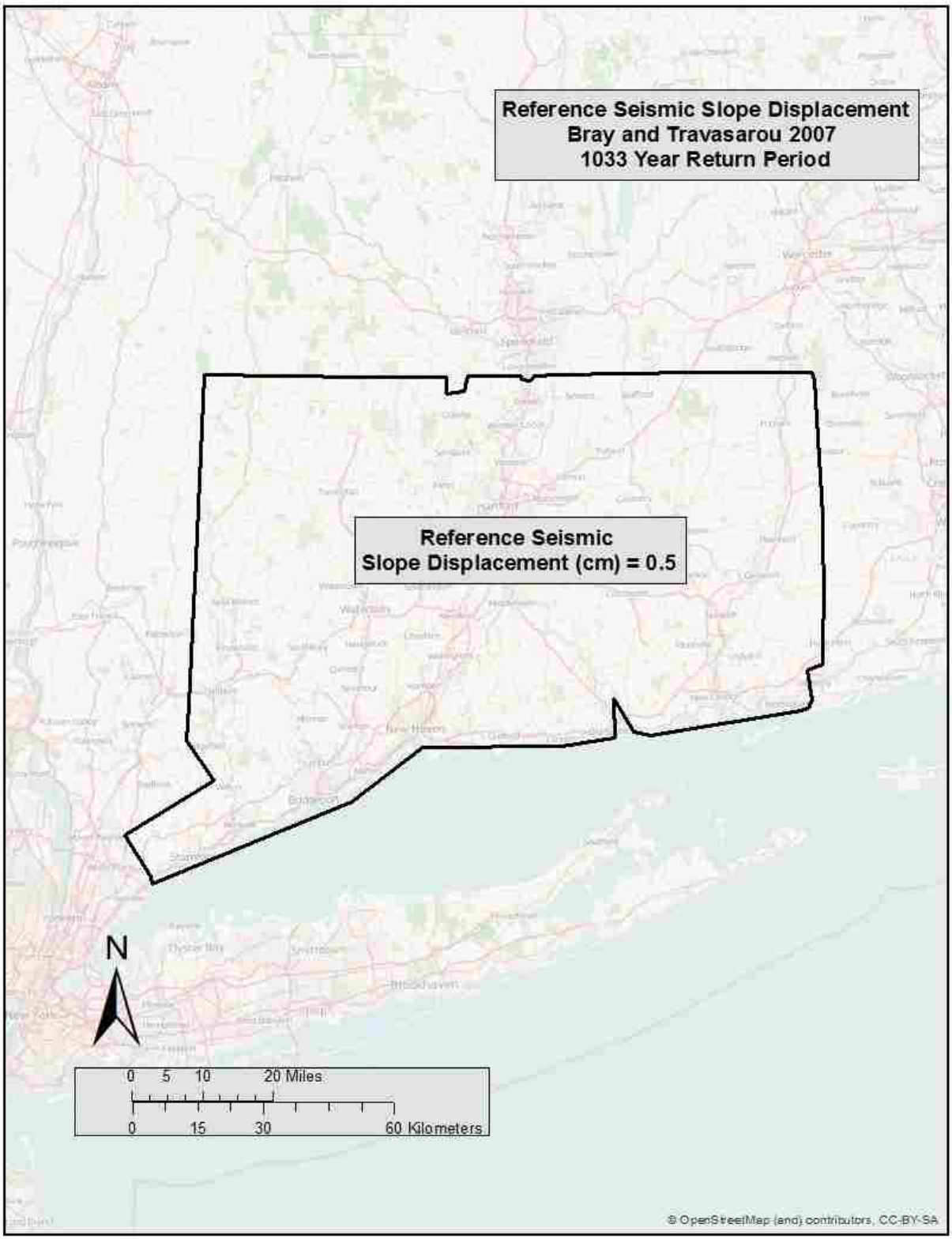

Figure B-5: Bray and Travasarou (2007) seismic slope displacement (D^{ref}) map for Connecticut (Tr = 1,033).

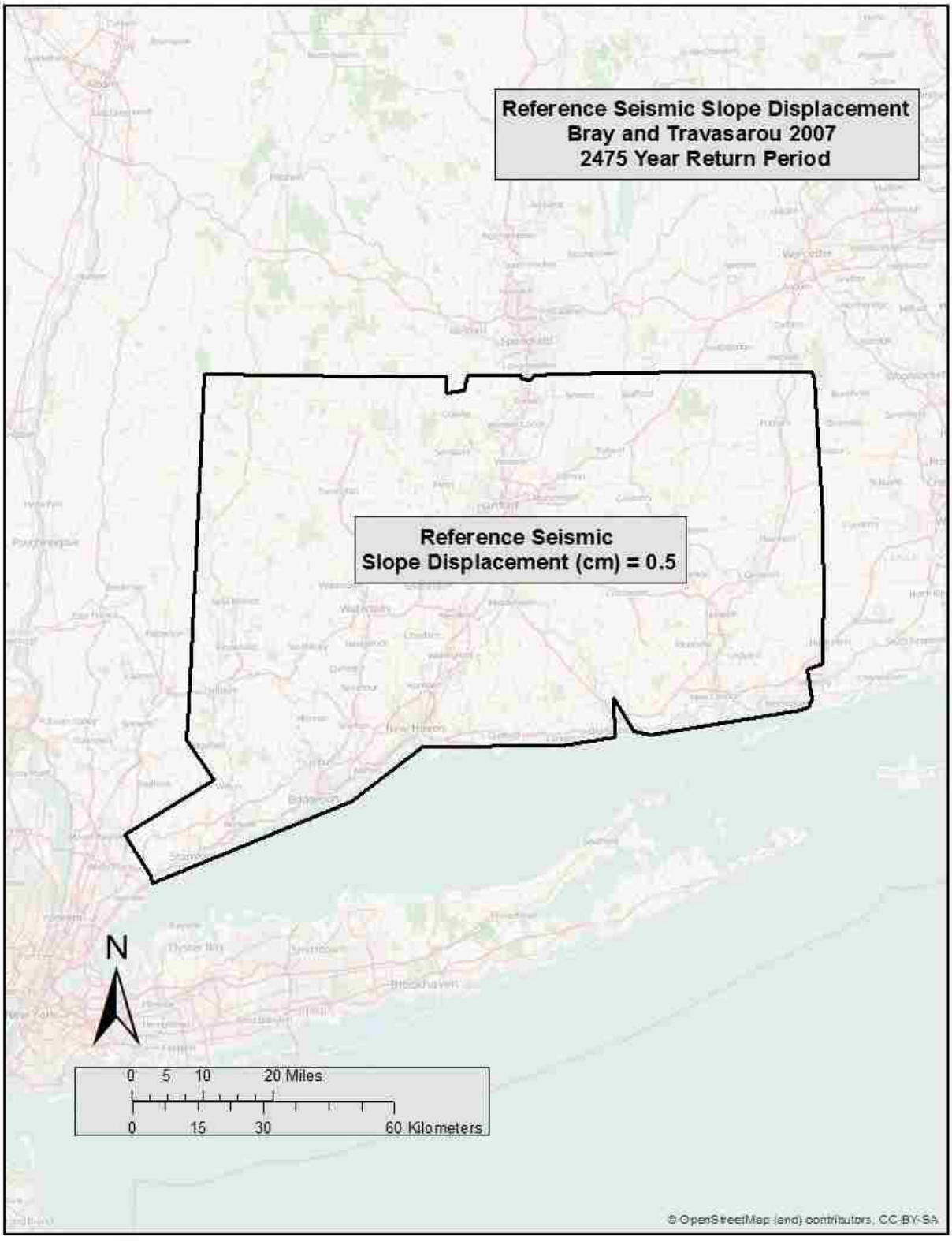

Figure B-6: Bray and Travasarou (2007) seismic slope displacement (D^{ref}) map for Connecticut (Tr = 2,475).

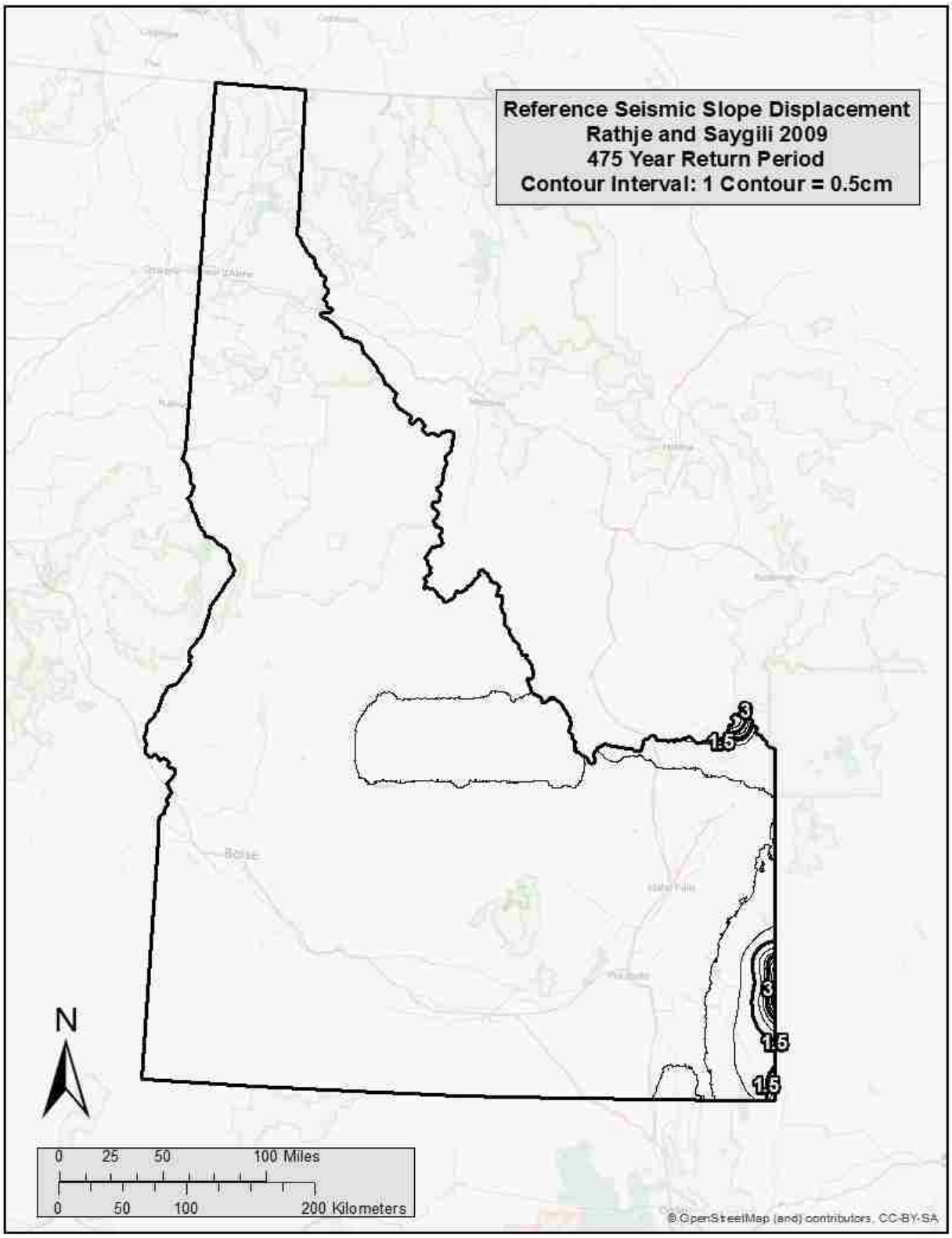

Figure B-7: Rathje and Saygili (2009) seismic slope displacement (D^{ref}) map for Idaho (Tr= 475).

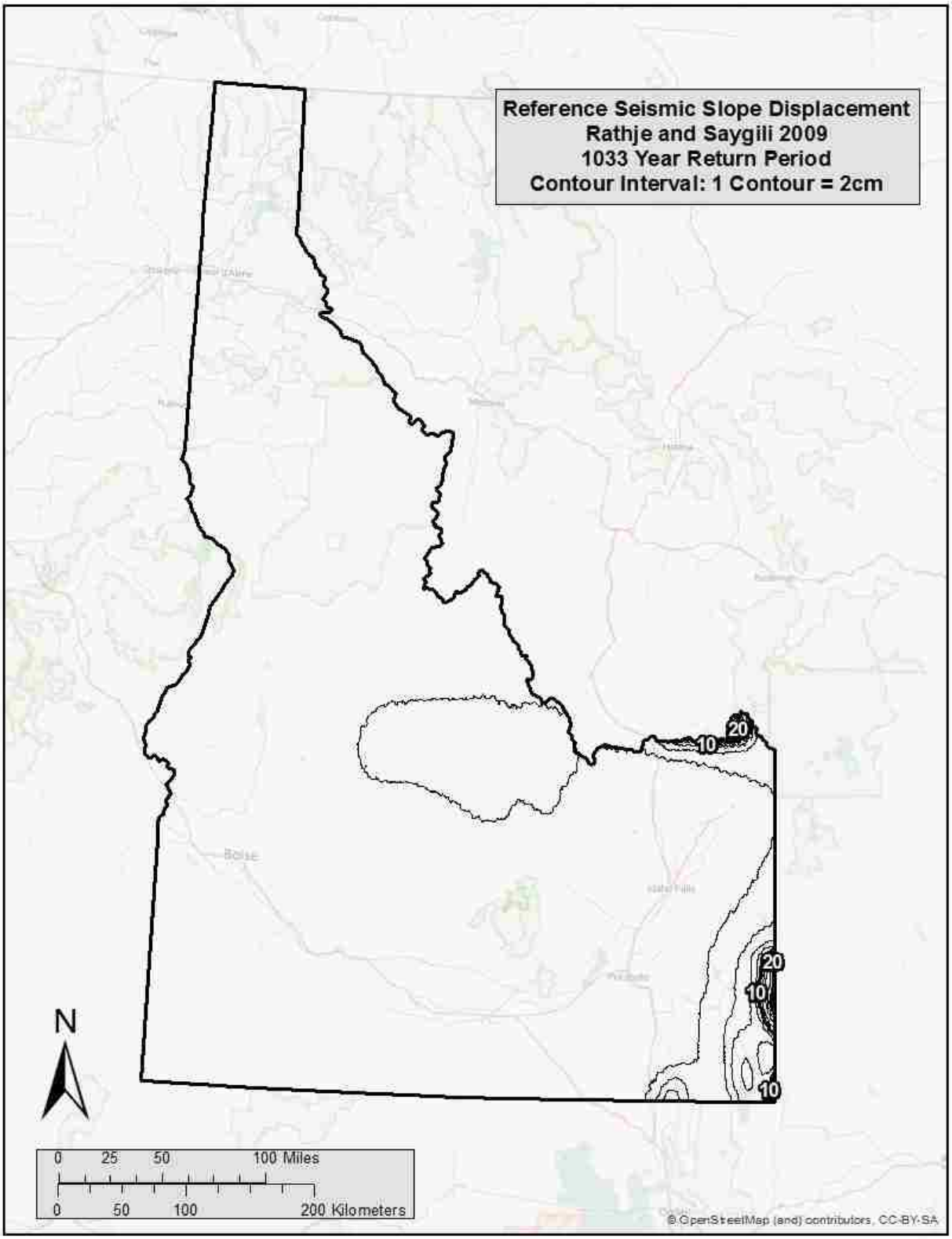

Figure B-8: Rathje and Saygili (2009) seismic slope displacement (D^{ref}) map for Idaho (Tr= 1,033).

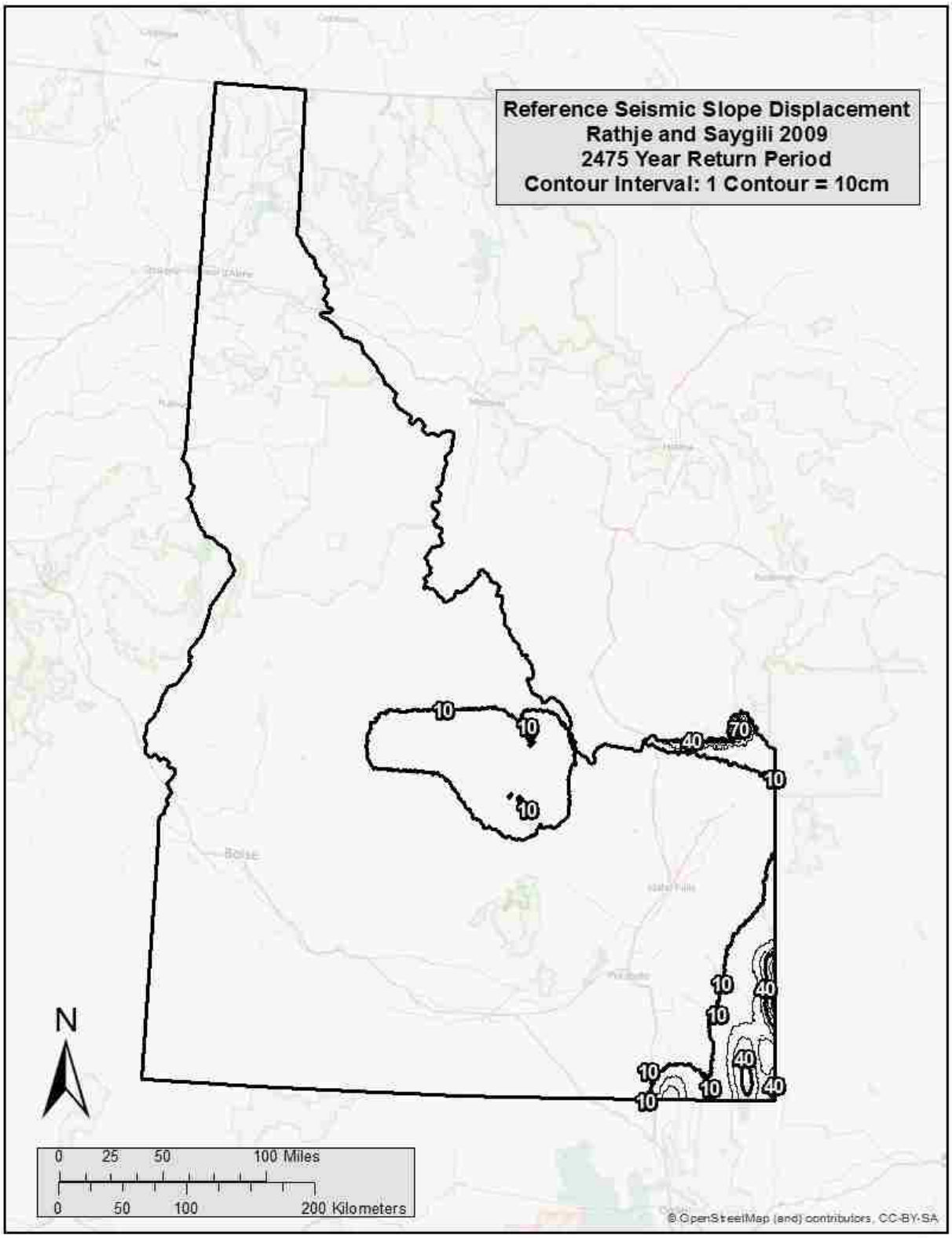

Figure B-9: Rathje and Saygili (2009) seismic slope displacement (D^{ref}) map for Idaho (Tr= 2,475).

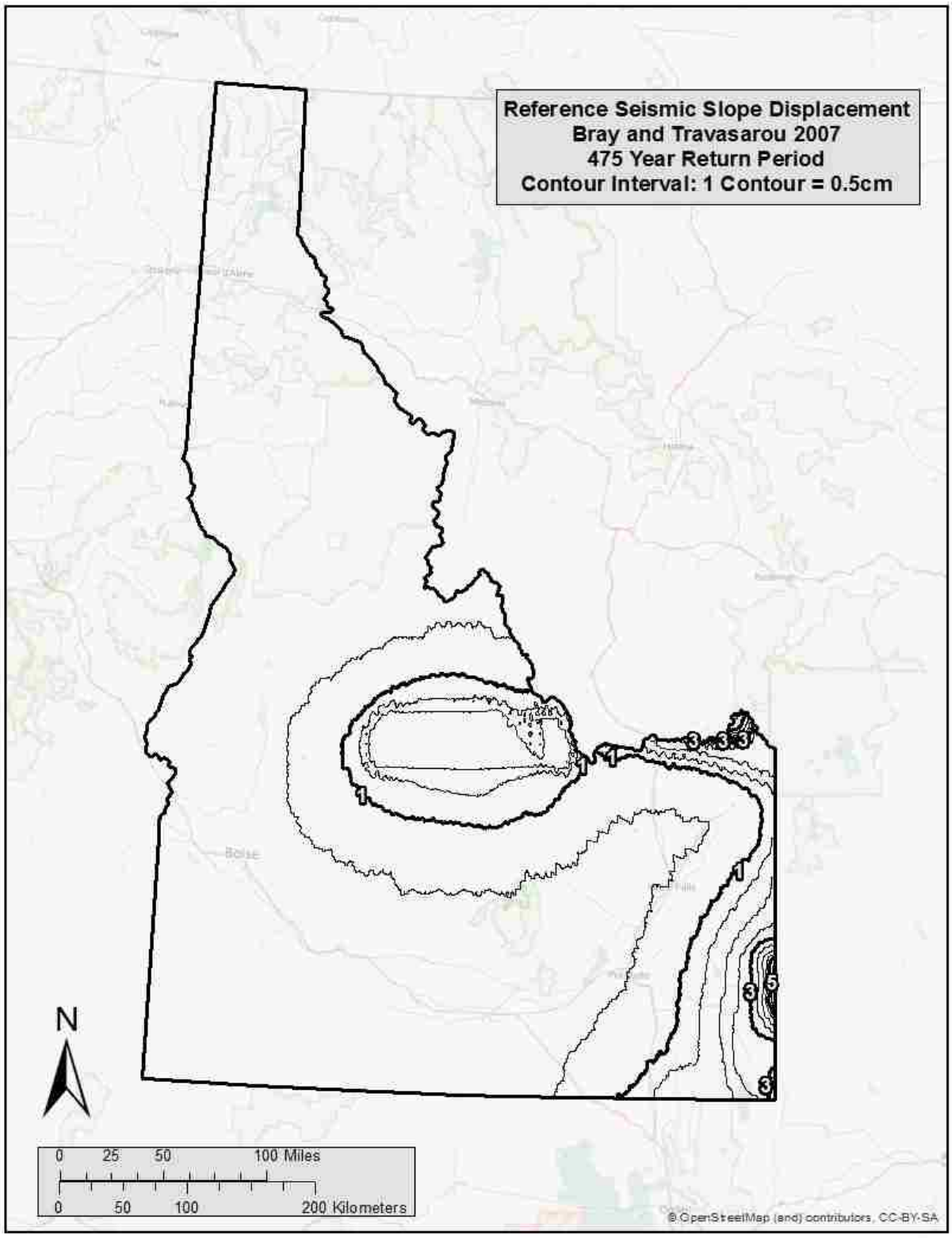

Figure B-10: Bray and Travasarou (2007) seismic slope displacement (D^{ref}) map for Idaho (Tr = 475).

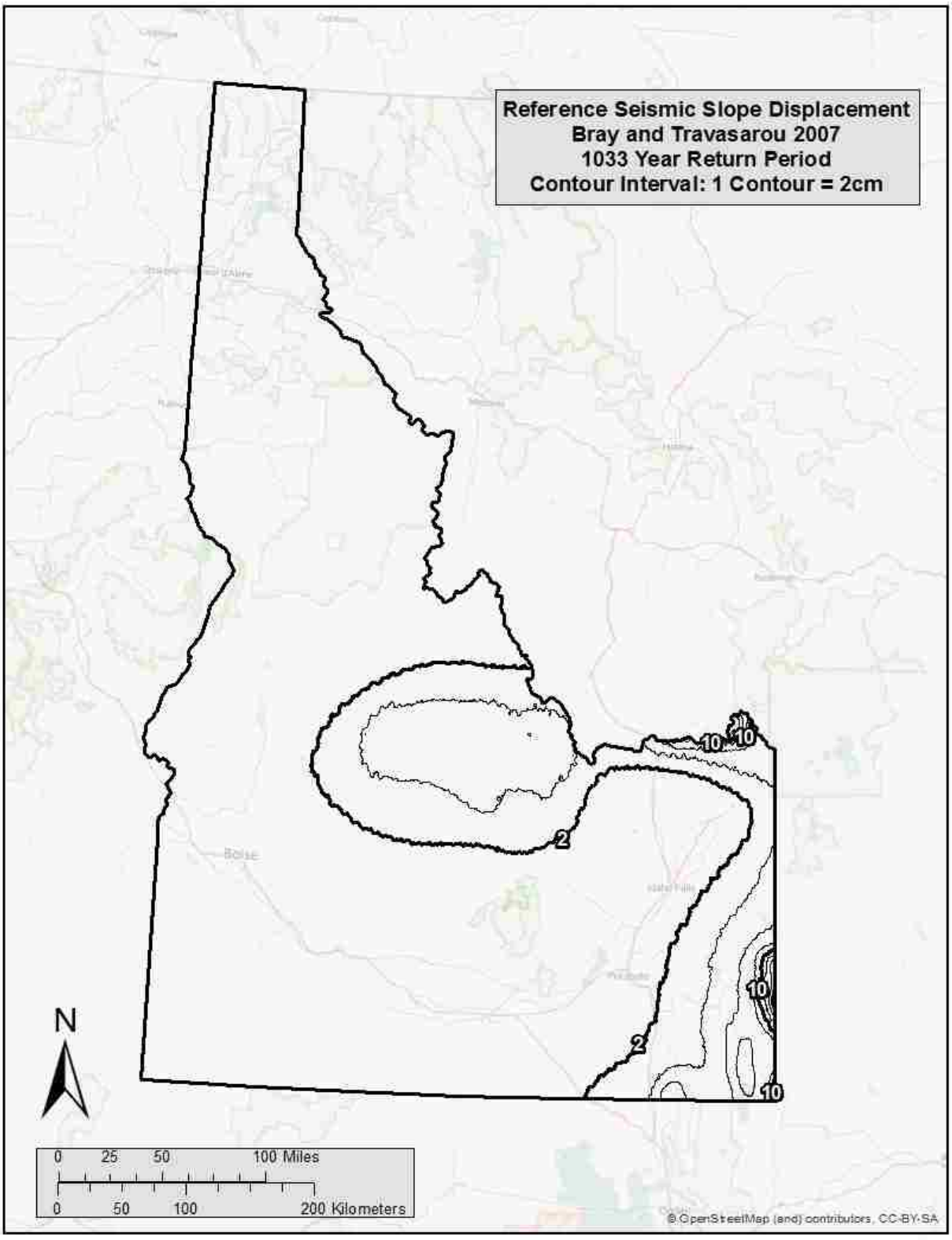

Figure B-11: Bray and Travasarou (2007) seismic slope displacement (D^{ref}) map for Idaho (Tr = 1,033).

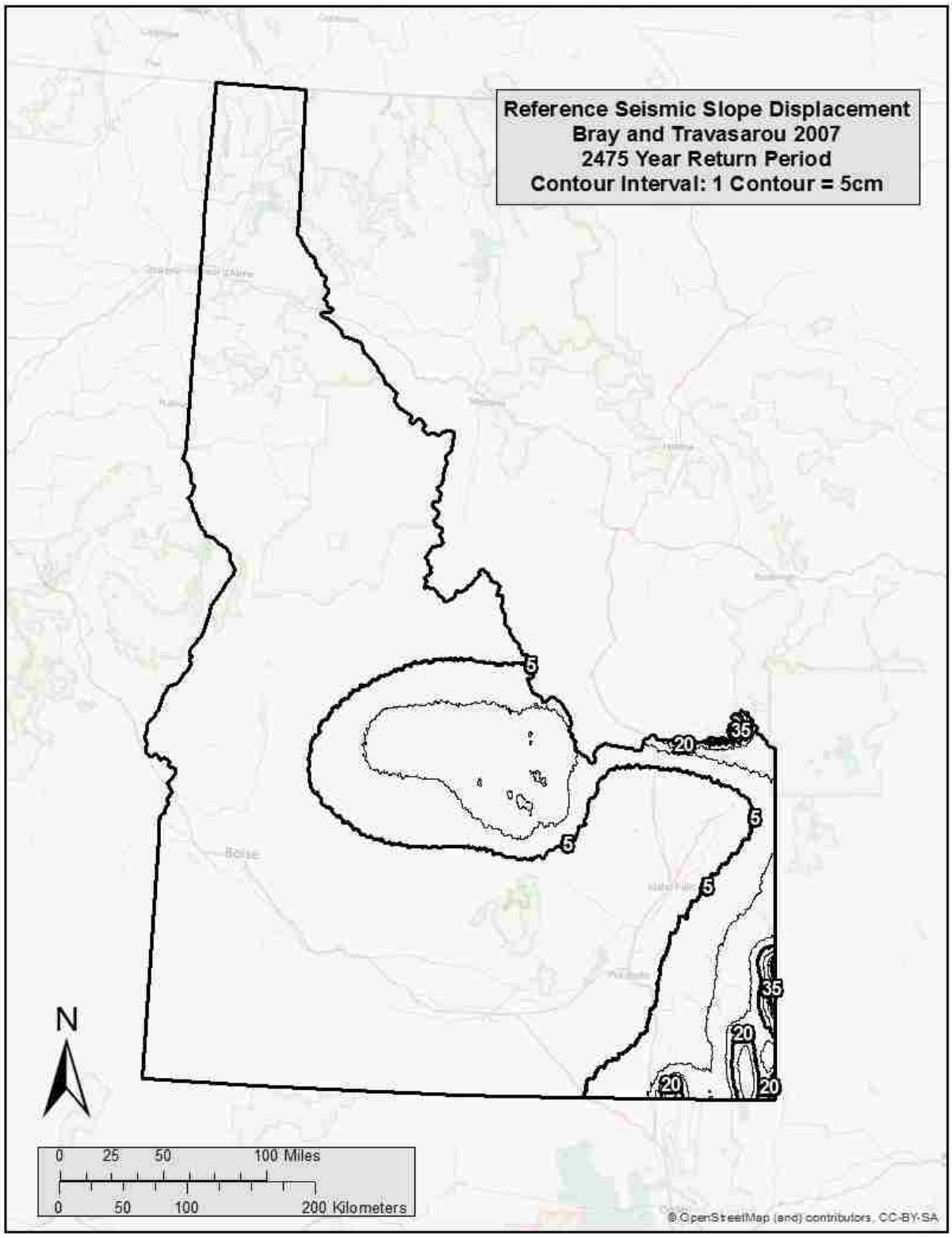

Figure B-12: Bray and Travasarou (2007) seismic slope displacement (D^{ref}) map for Idaho (Tr = 2,475).

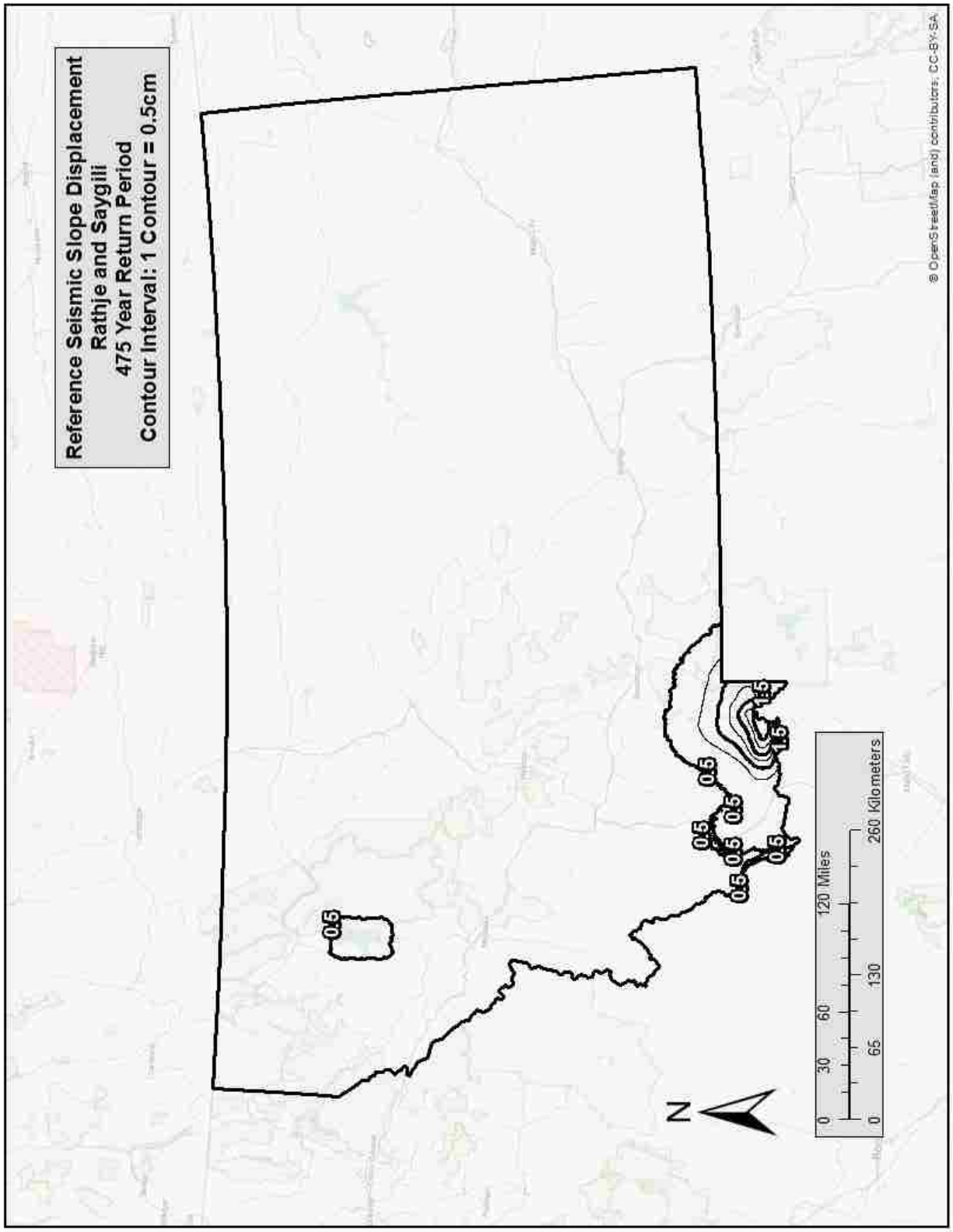

Figure B-13: Rathje and Saygili (2009) seismic slope displacement (D^{ref}) map for Montana (Tr = 475).

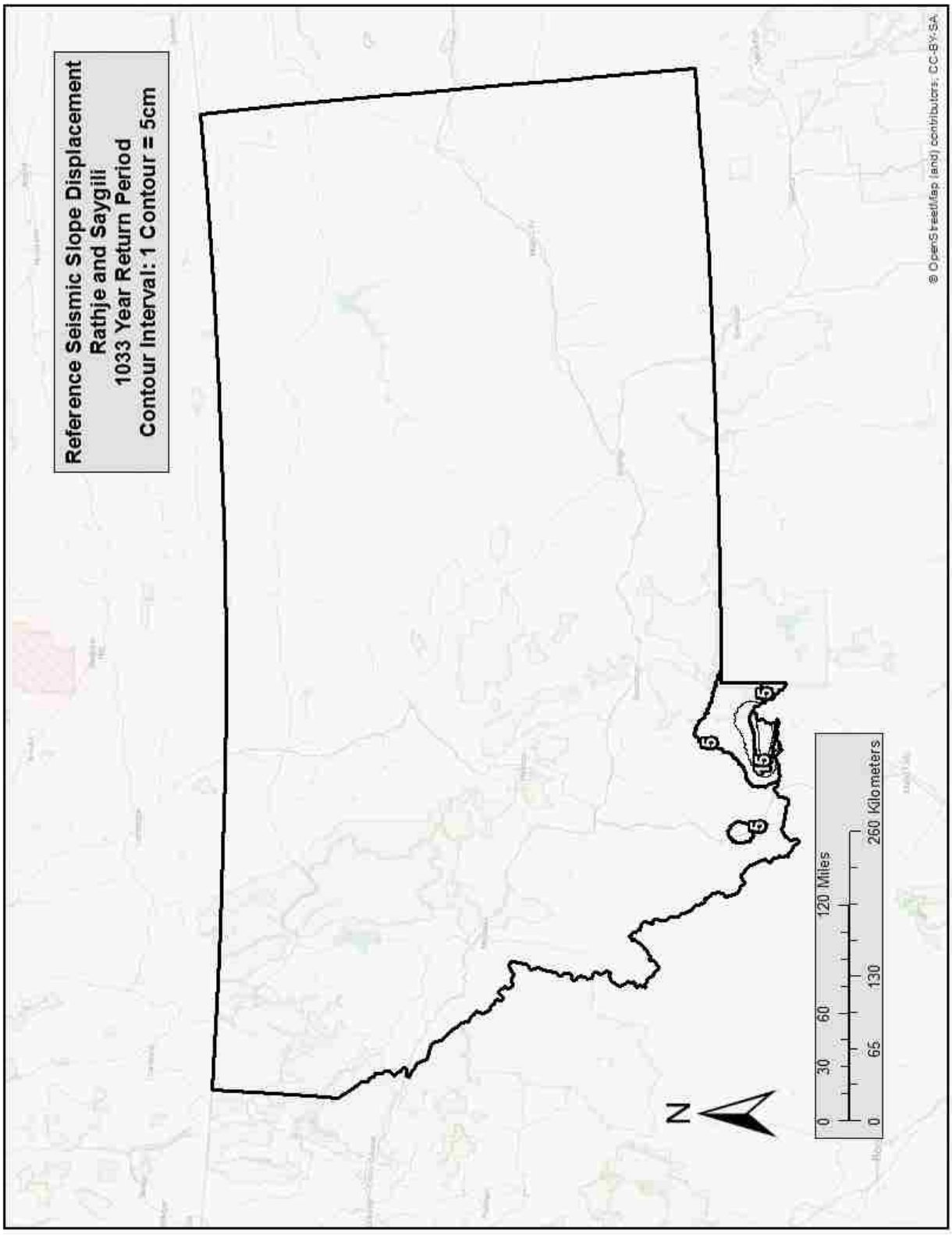

Figure B-14: Rathje and Saygili (2009) seismic slope displacement (D^{ref}) map for Montana (Tr = 1,033).

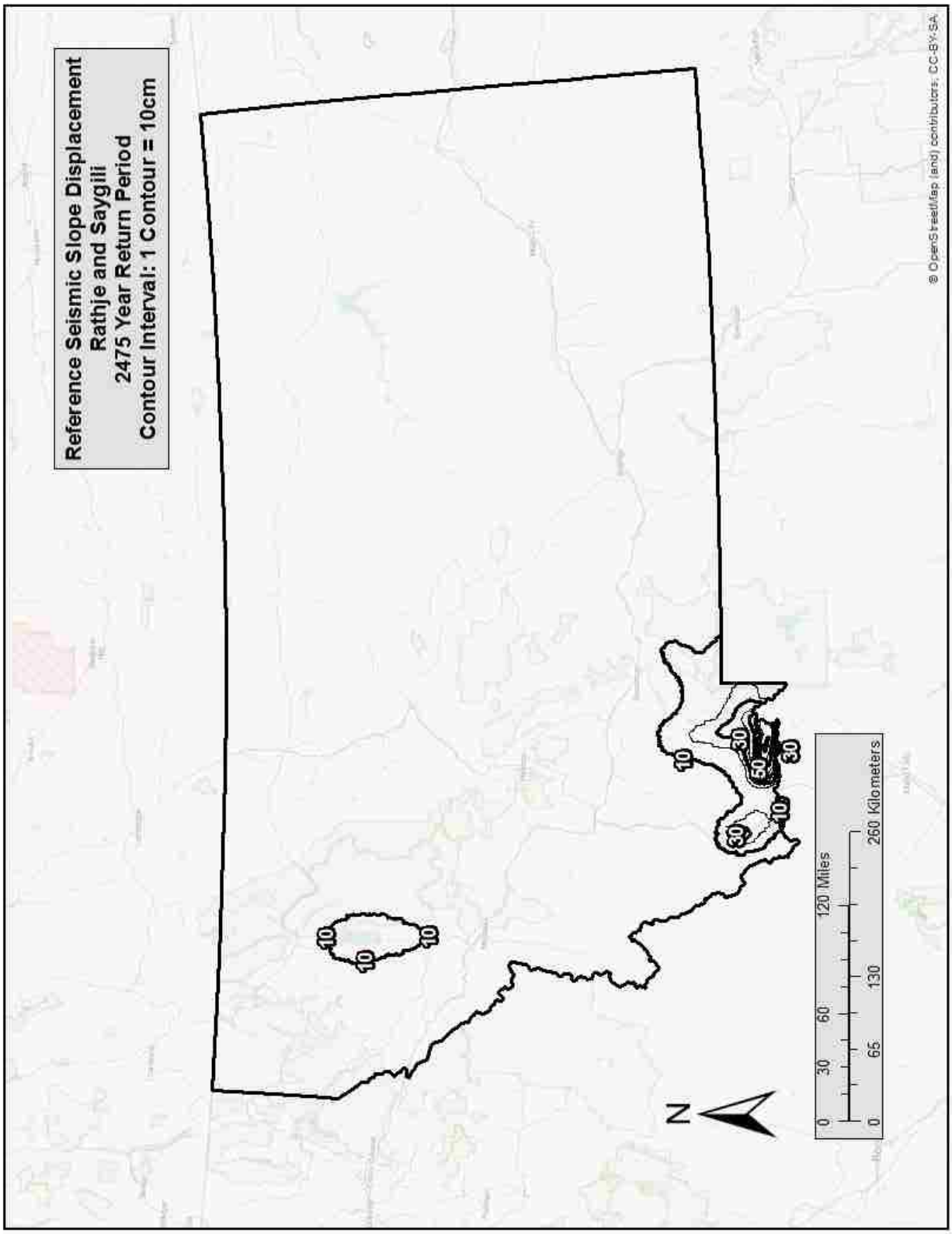

Figure B-15: Rathje and Saygili (2009) seismic slope displacement (D^{ref}) map for Montana (Tr = 2,475).

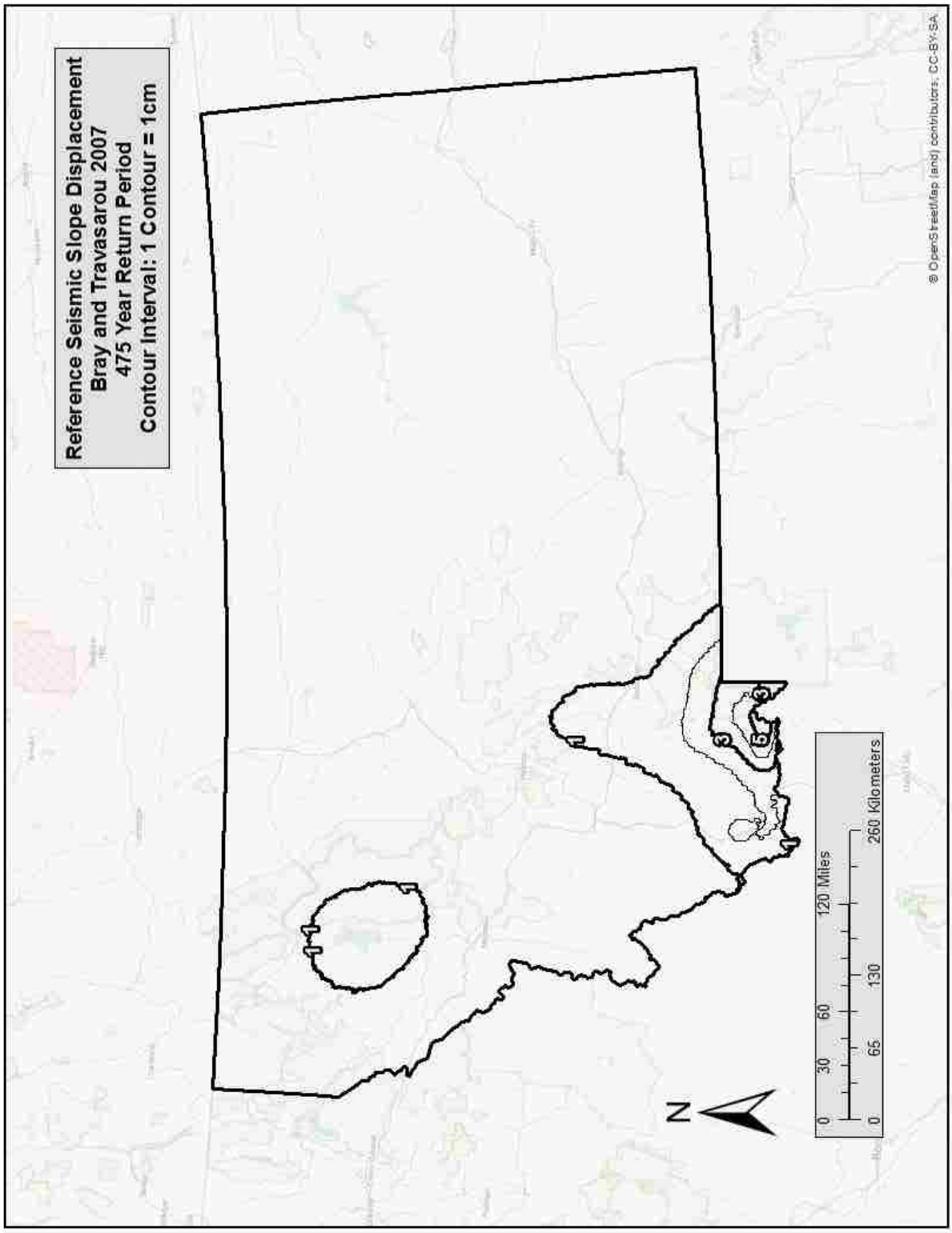

Figure B-16: Bray and Travasarou (2007) seismic slope displacement (D^{ref}) map for Montana (Tr = 475).

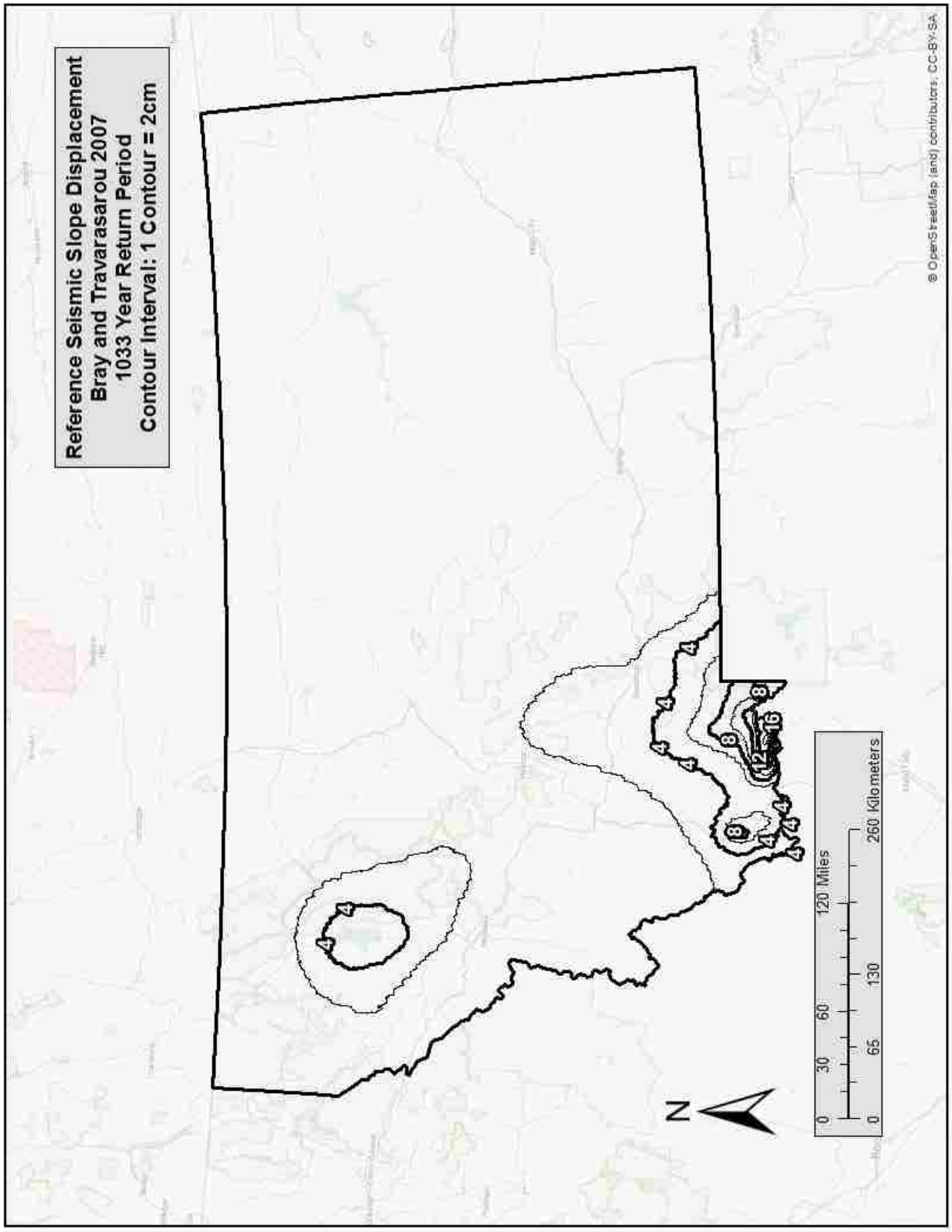

Figure B-17: Bray and Travasarou (2007) seismic slope displacement (D^{ref}) map for Montana (Tr = 1,033).

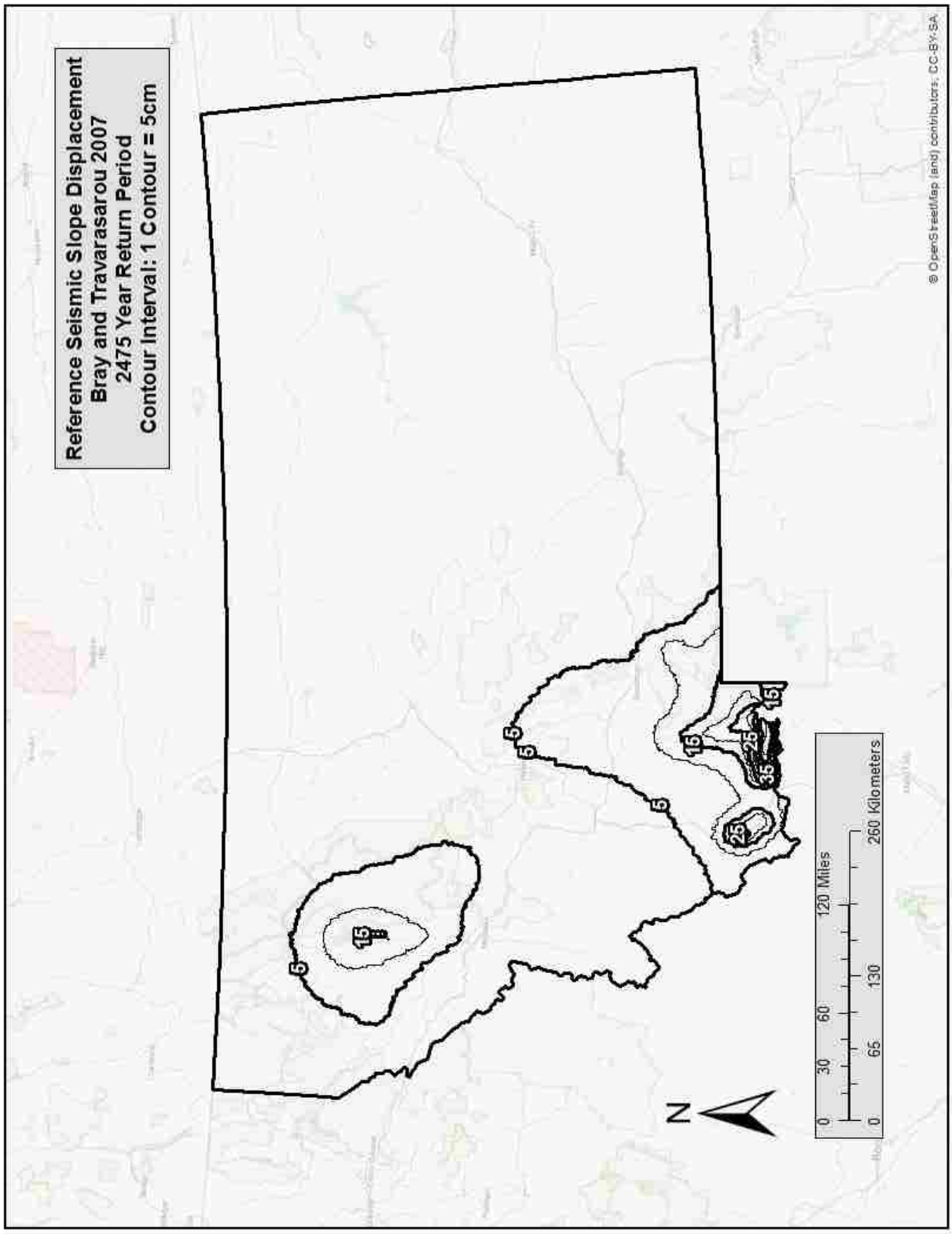

Figure B-18: Bray and Travasarou (2007) seismic slope displacement (D^{ref}) map for Montana (Tr = 2,475).

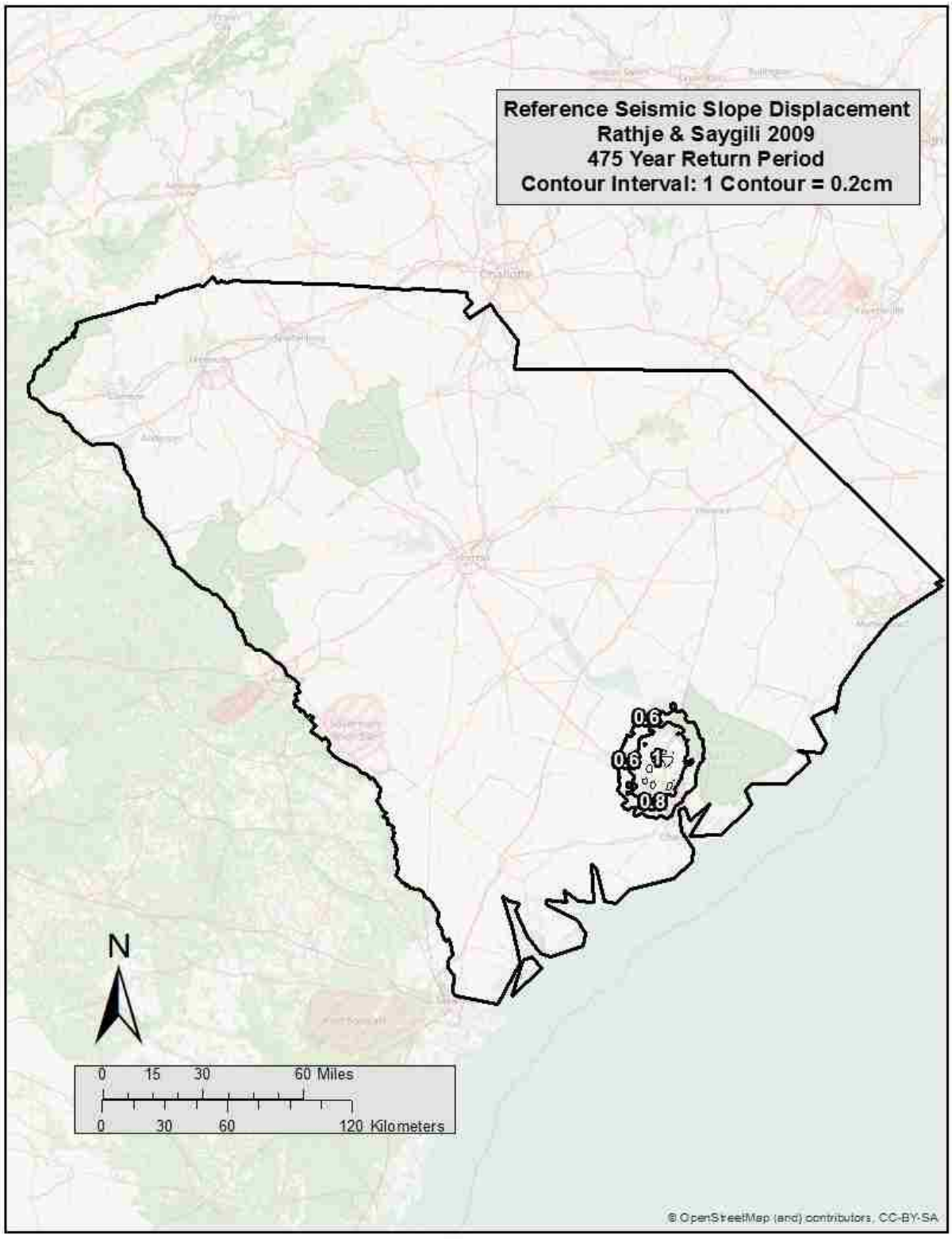

Figure B-19: Rathje and Saygili (2009) seismic slope displacement (D^{ref}) map for South Carolina (Tr = 475).

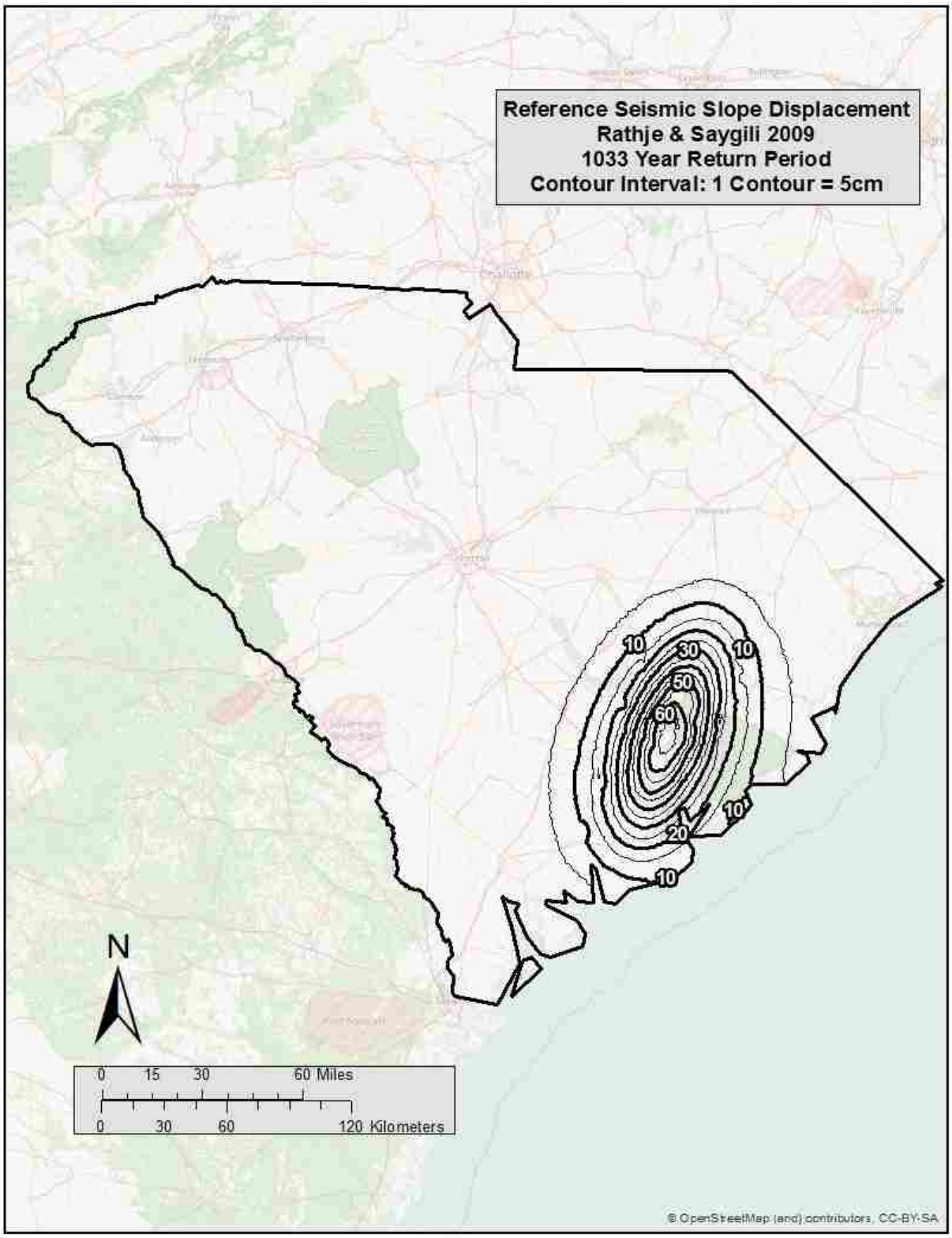

Figure B-20: Rathje and Saygili (2009) seismic slope displacement (D^{ref}) map for South Carolina (Tr = 1,033).

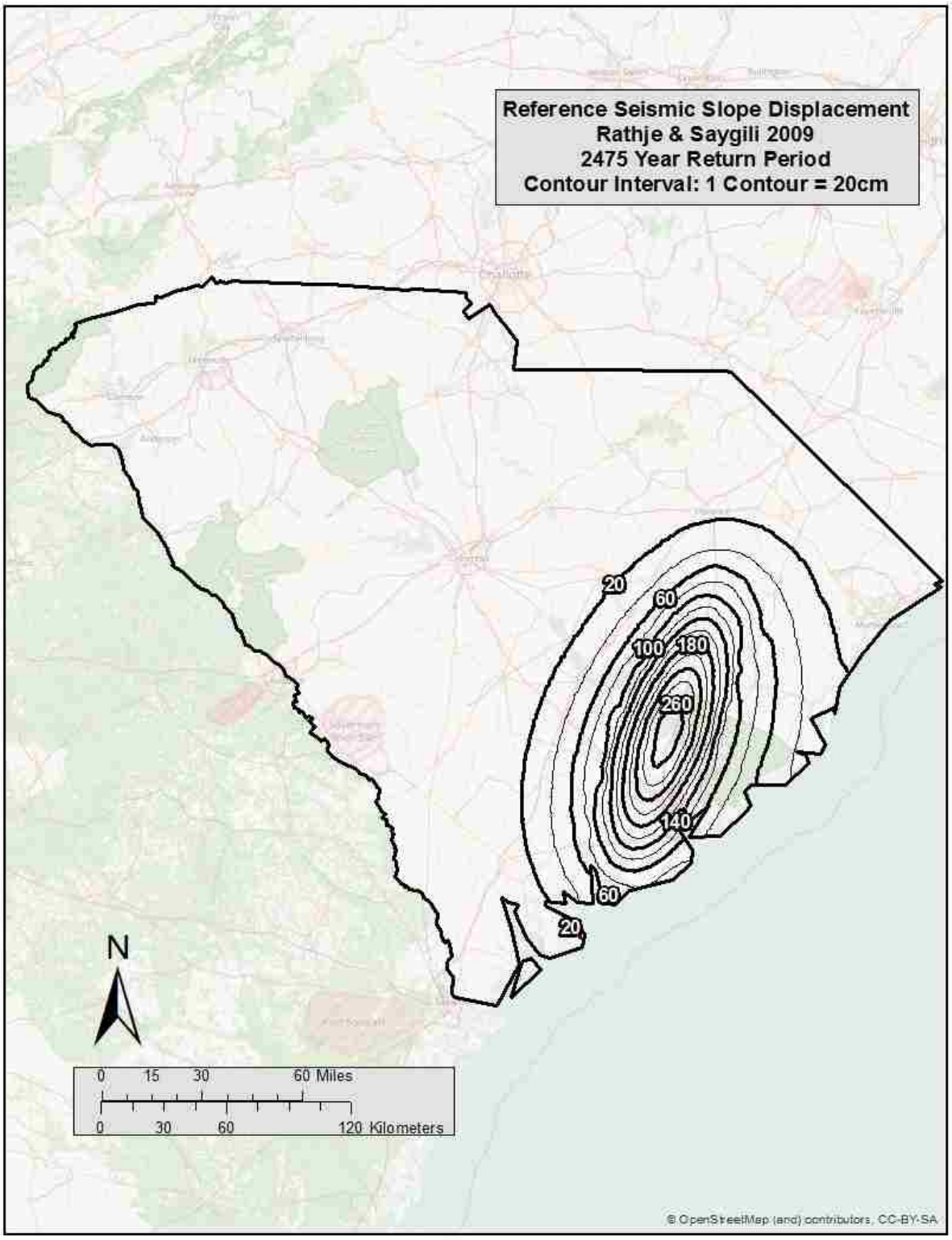

Figure B-21: Rathje and Saygili (2009) seismic slope displacement (D^{ref}) map for South Carolina (Tr = 2,475).

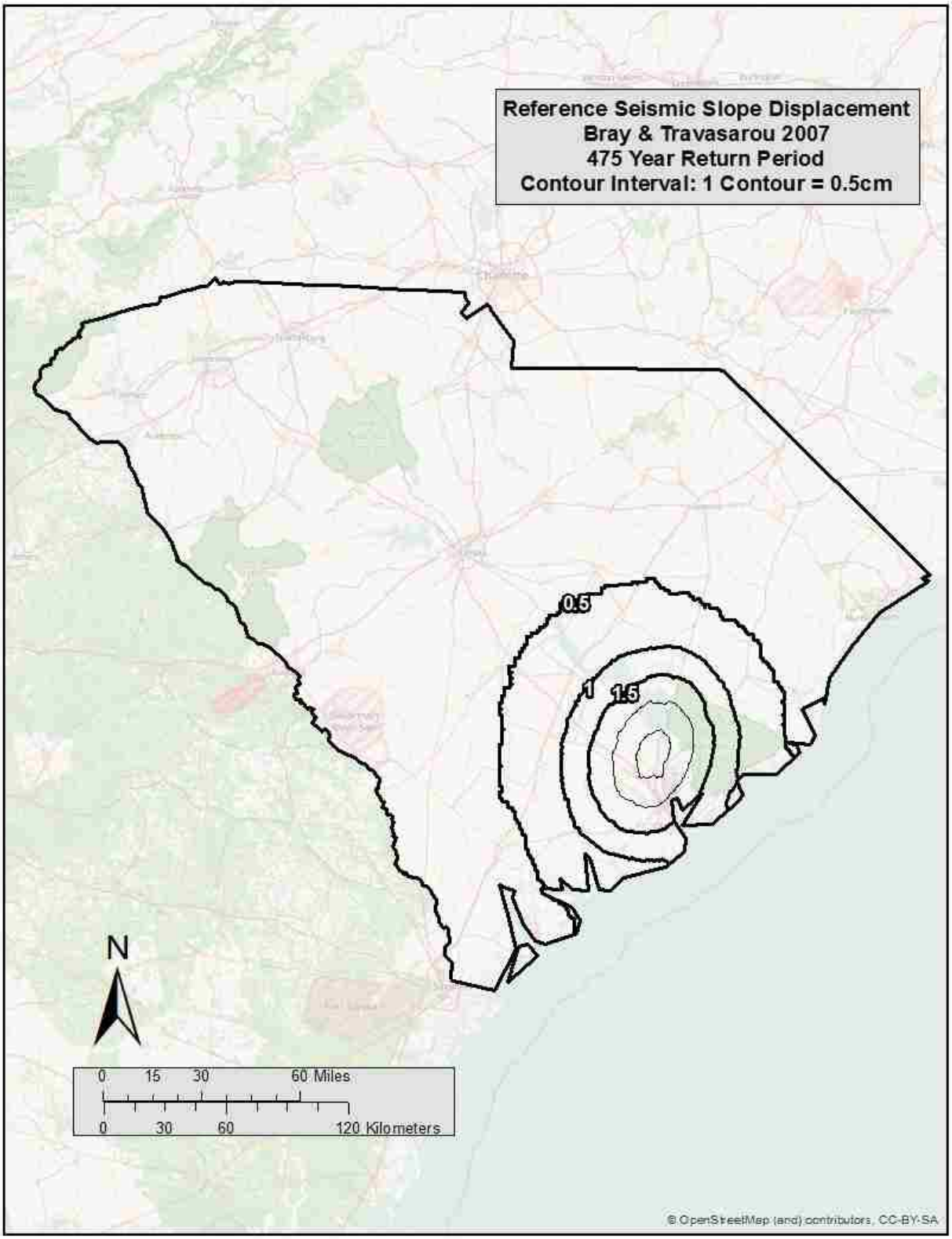

Figure B-22: Bray and Travasarou (2007) seismic slope displacement (D^{ref}) map for South Carolina (Tr = 475).

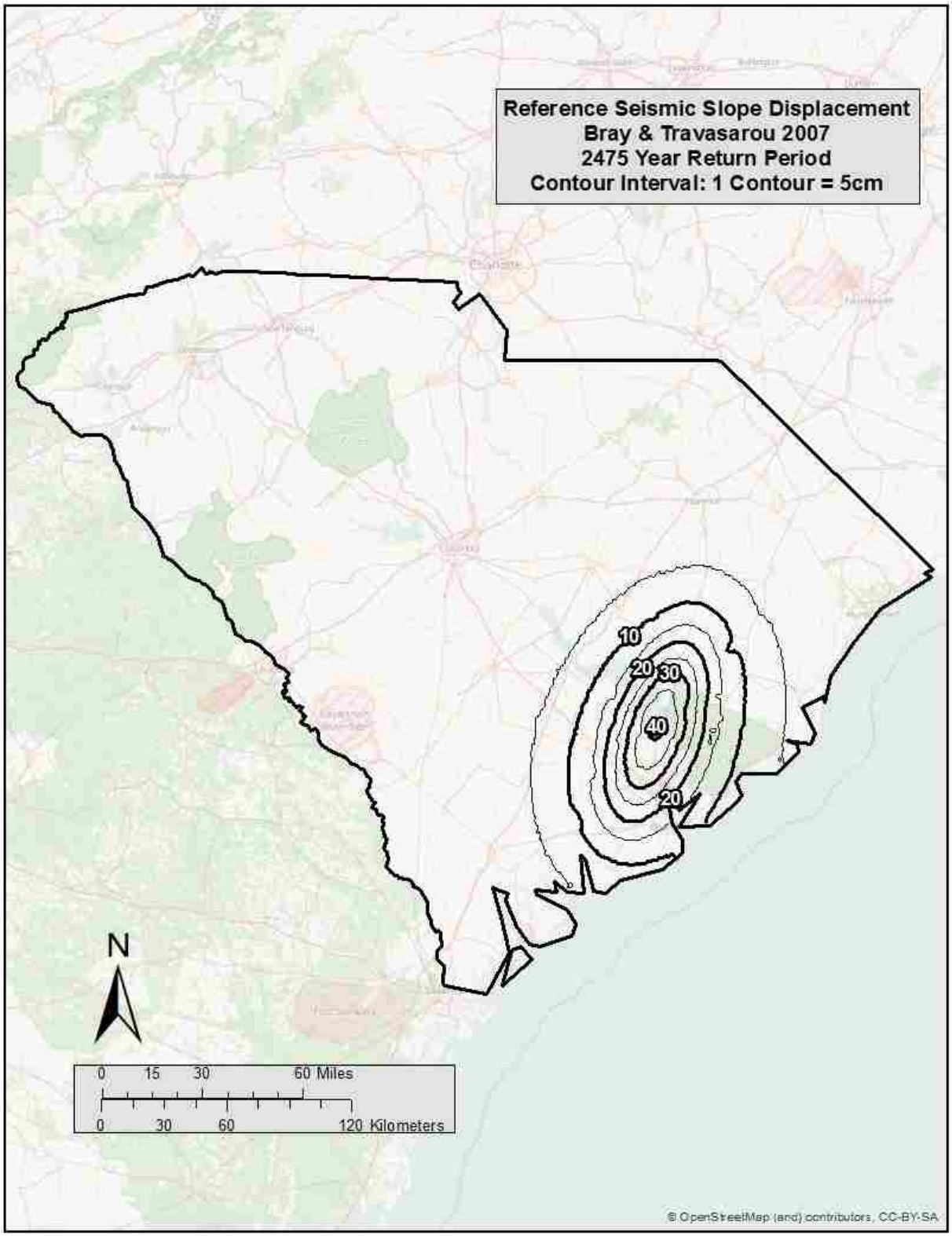

Figure B-23 Bray and Travasarou (2007) seismic slope displacement (D^{ref}) map for South Carolina (Tr = 1,033).

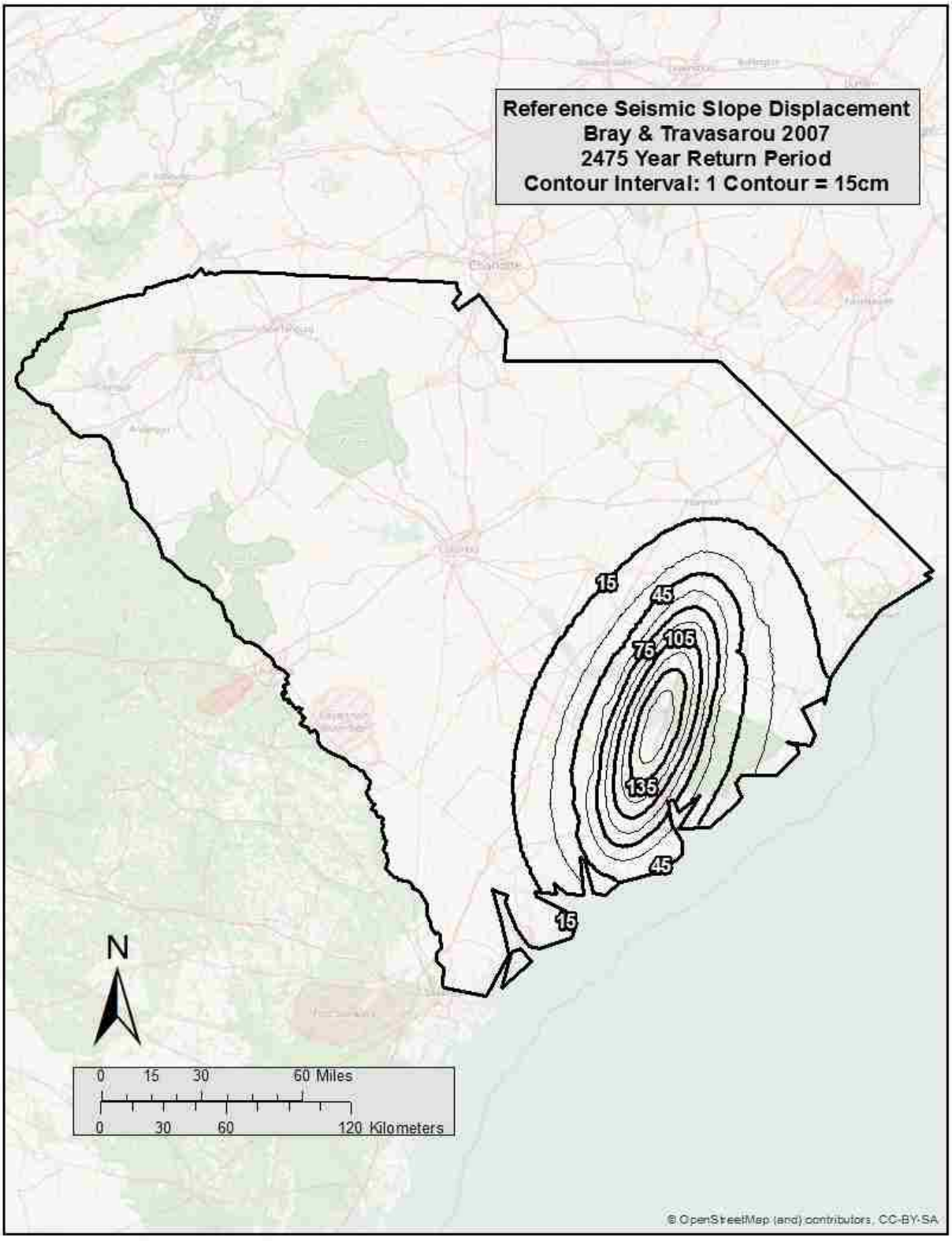

Figure B-24: Bray and Travasarou (2007) seismic slope displacement (D^{ref}) map for South Carolina (Tr = 2,475).

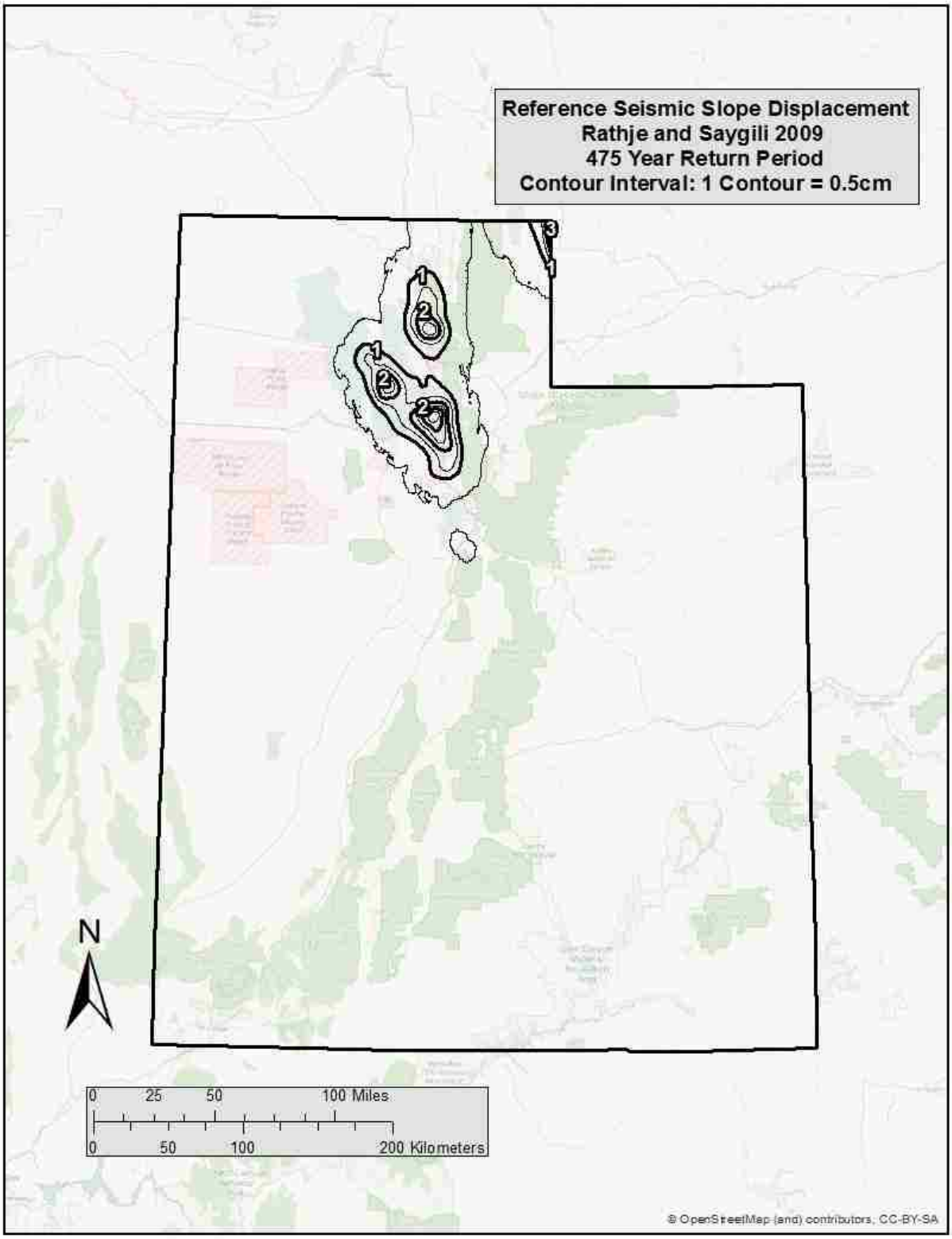

Figure B-25: Rathje and Saygili (2009) seismic slope displacement (D^{ref}) map for Utah (Tr= 475).

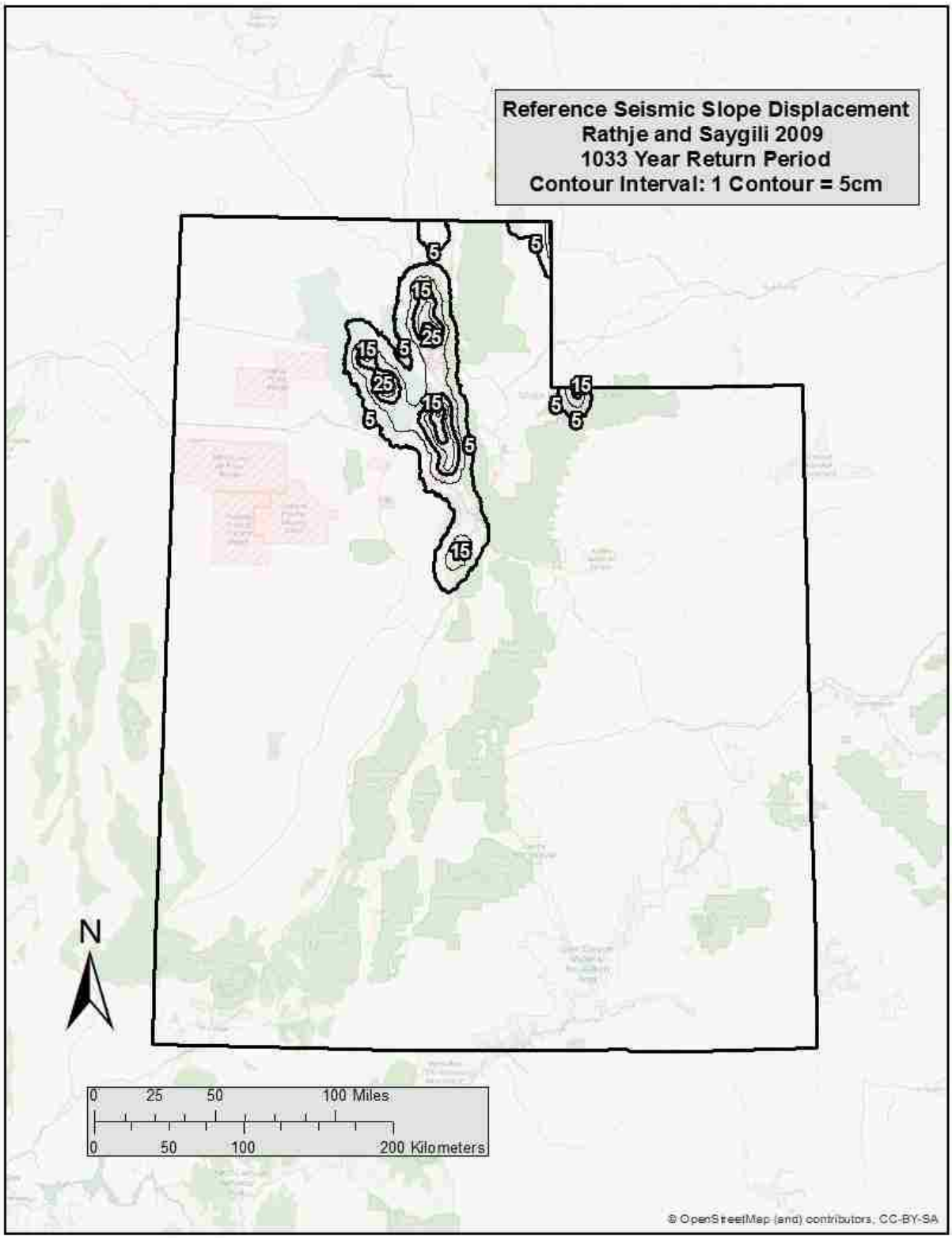

Figure B-26: Rathje and Saygili (2009) seismic slope displacement (D^{ref}) Map for Utah (Tr= 1,033).

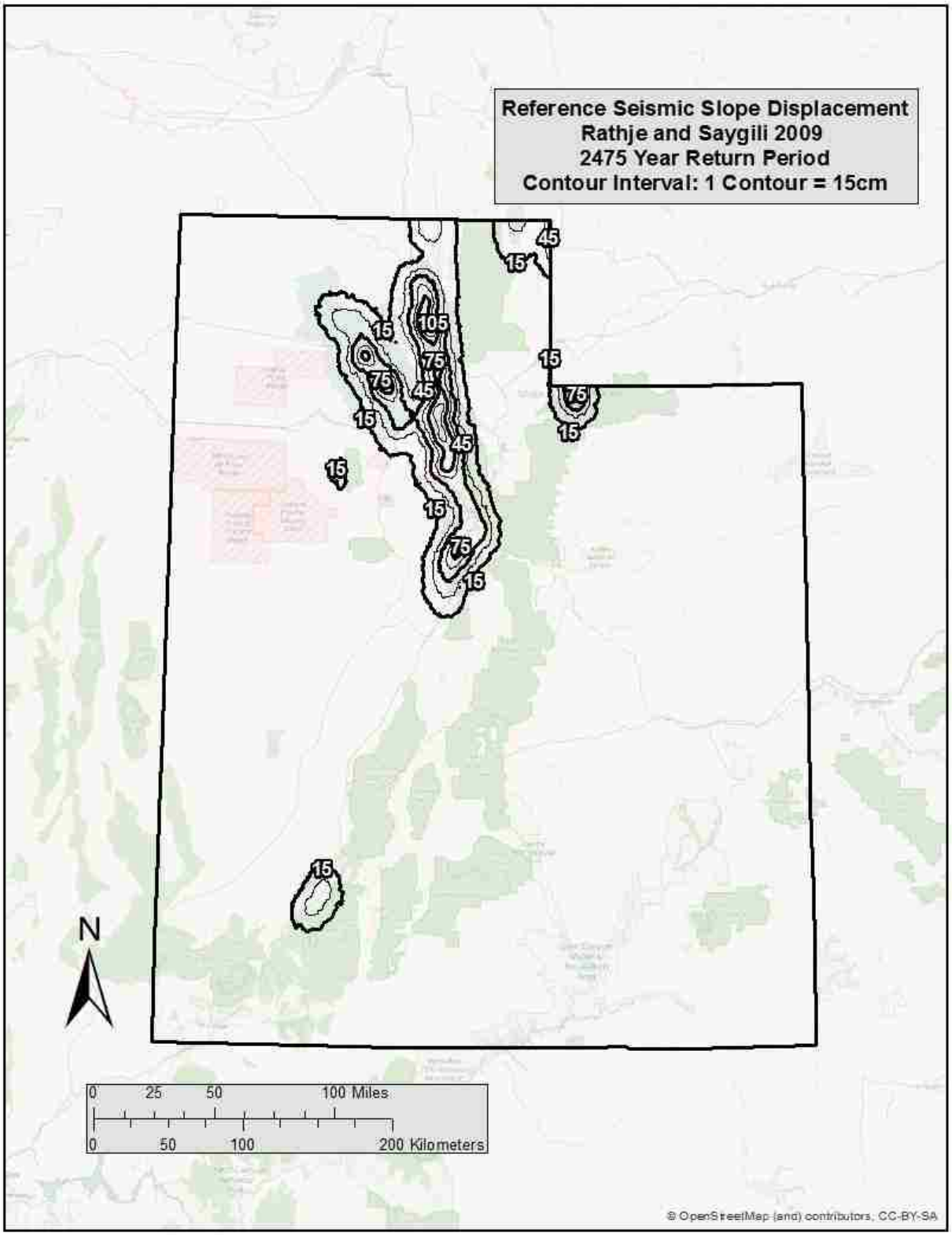

Figure B-27: Rathje and Saygili (2009) seismic slope displacement (D^{ref}) map for Utah (Tr= 2,475).

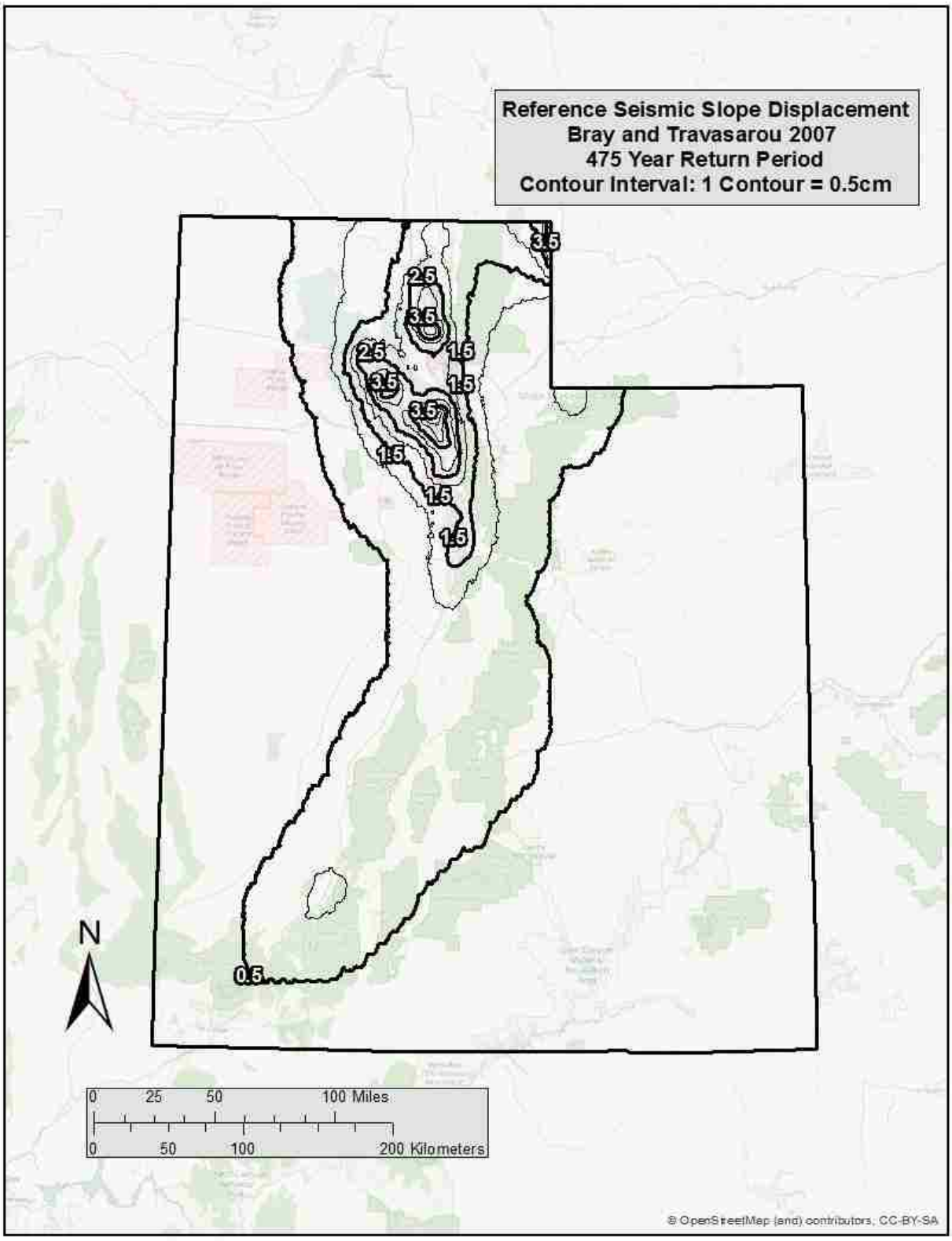

Figure B-28: Bray and Travasarou (2007) seismic slope displacement (D^{ref}) map for Utah (Tr = 475).

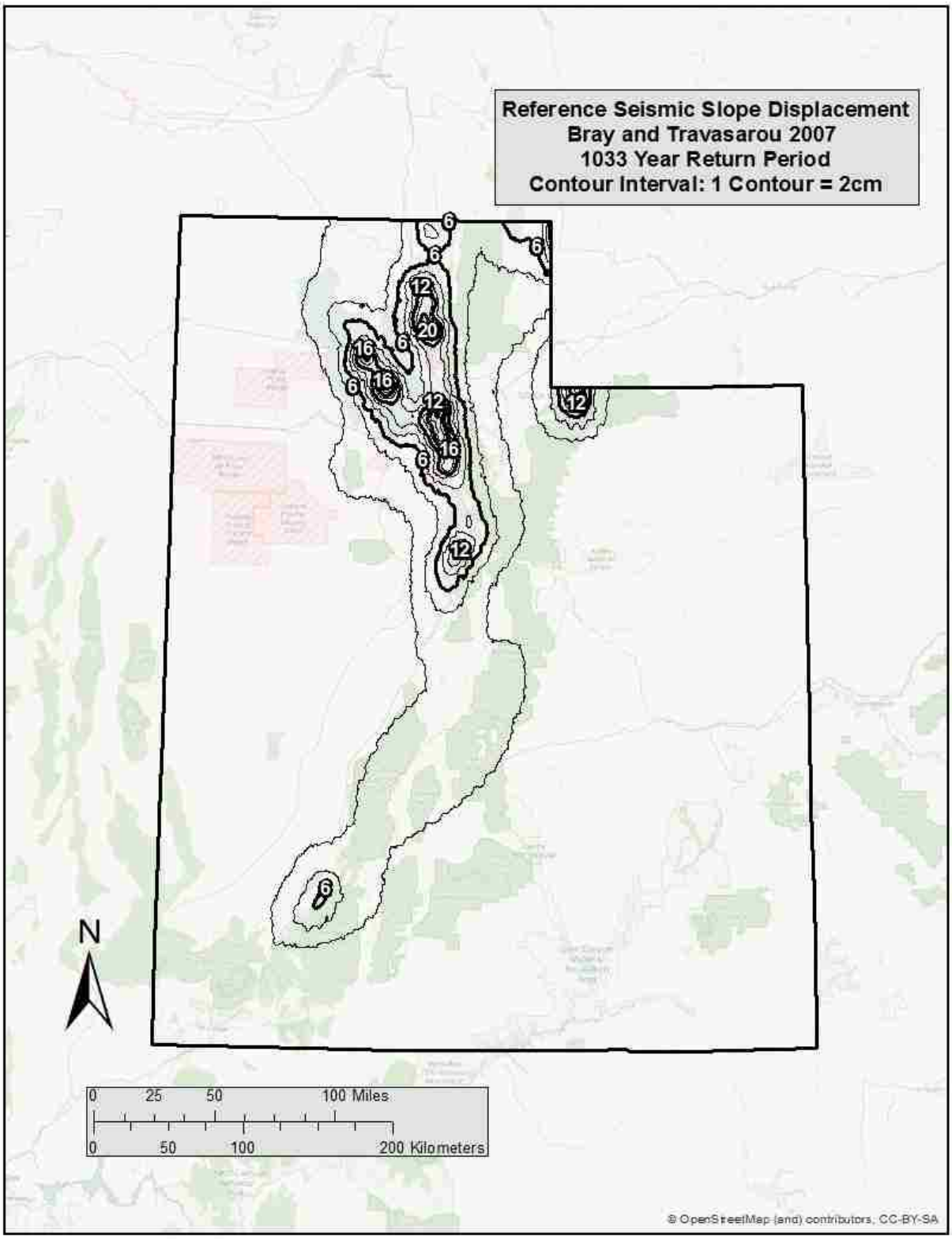

Figure B-29: Bray and Travasarou (2007) seismic slope displacement (D^{ref}) map for Utah (Tr = 1,033).

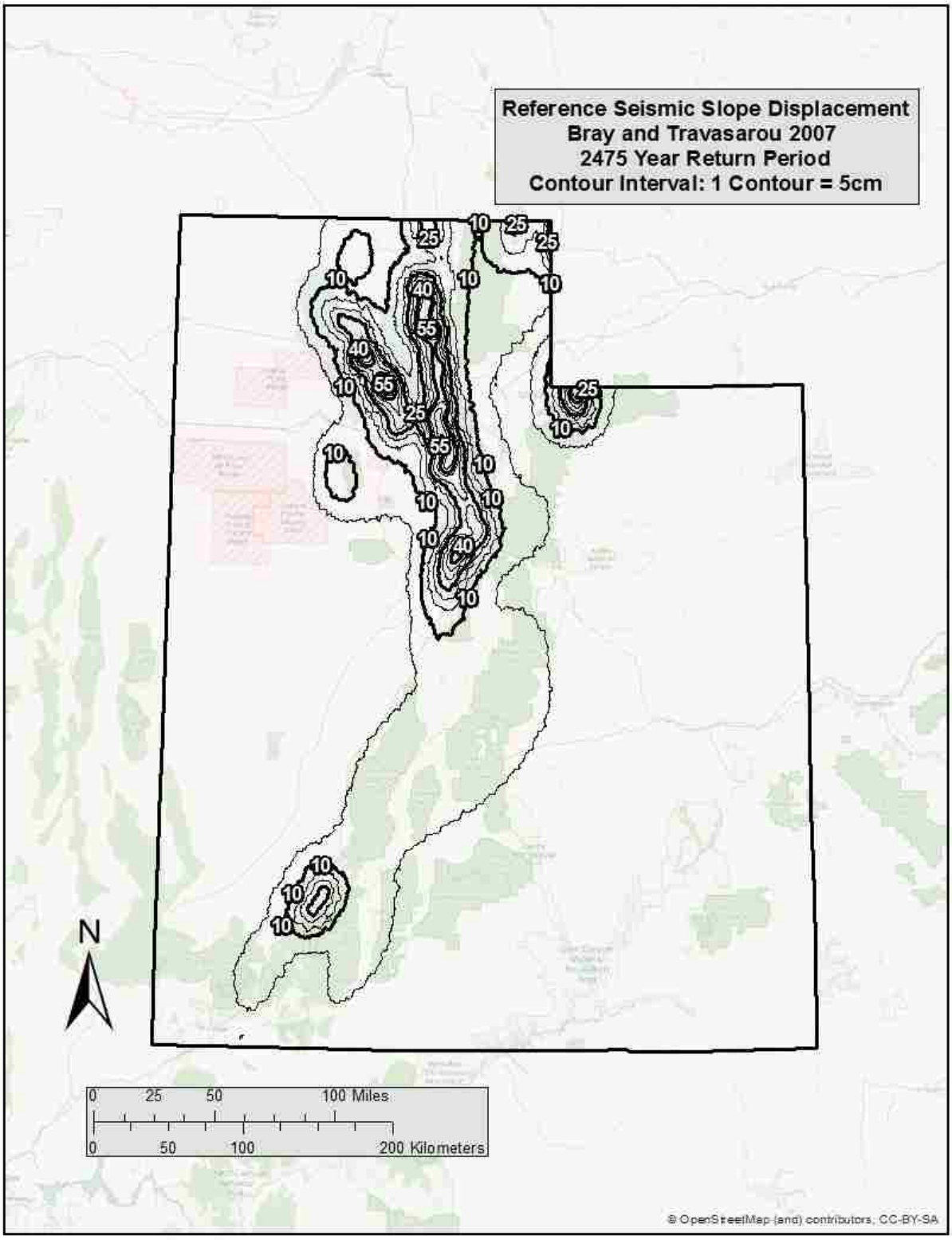

Figure B-30: Bray and Travasarou (2007) seismic slope displacement (D^{ref}) map for Utah (Tr = 2,475).

APPENDIX C: TABLES OF PARAMETERS USED IN DETERMINISTIC ANALYSIS

Table C-1: Faults considered in deterministic analysis.

					Median Acceleration			(Median + 1 St. Dev) Acceleration		
					T_R = 1,033 year			T_R = 1,033 year		
San Francisco		**Seismic Source**	**Dist (km)**	**Mw**	***PGA***	F_a	a_{max}	***PGA***	F_a	a_{max}
	1	Northern San Andreas	10.77	8.05	0.3175	1.183	0.3754	0.5426	1.0	0.5426
	2	San Gregorio Connected	16.64	7.5	0.2139	1.372	0.2935	0.3660	1.134	0.4150
	3	Hayward-Rodgers Creek	18.23	7.33	0.1918	1.416	0.2717	0.3282	1.172	0.3846
	4	Mount Diablo Thrust	36.08	6.7	0.1050	1.590	0.1670	0.1811	1.438	0.2604
	5	Calaveras	34.28	7.03	0.0981	1.6	0.1570	0.1682	1.464	0.2462
Salt Lake City										
	1	Wasatch Fault, SLC Section	1.02	7	0.5911	1.0	0.5911	1.0050	1.0	1.0050
	2	West Valley Fault Zone	2.19	6.48	0.5694	1.0	0.5694	0.9842	1.0	0.9842
	3	Morgan Fault	25.04	6.52	0.0989	1.6	0.1583	0.1713	1.457	0.2497
	4	Great Salt Lake Fault zone, Antelope Section	25.08	6.93	0.1016	1.597	0.1622	0.1742	1.452	0.2529
	5	Oquirrh-Southern, Oquirrh Mountain Fault	30.36	7.17	0.0958	1.6	0.1532	0.1641	1.472	0.2415
Butte										
	1	Rocker Fault	4.92	6.97	0.5390	1.0	0.5390	0.9202	1.0	0.9202
	2	Georgia Gulch Fault	45.91	6.42	0.0435	1.6	0.0696	0.0754	1.6	0.1206
	3	Helena Valley Fault	75.56	6.6	0.0294	1.6	0.0470	0.0507	1.6	0.0812
	4	Canyon Ferry Fault	81.32	6.92	0.0327	1.6	0.0523	0.0561	1.6	0.0898
	5	Blacktail Fault	84.27	6.94	0.0317	1.6	0.0508	0.0545	1.6	0.0872
	6	Madison Fault	86.51	7.45	0.0420	1.6	0.0671	0.0719	1.6	0.1150

Table C-2: Characteristics of rocker fault (near Butte) and calculations to determine PGA and M_w.

Rocker Fault

***M_w calculated based on Wells and Coppersmith (1994):**

Length = 43 km

(Use "all" slip type, because it's a normal fault and the # of normal events is small)

***PGA calculated based on NGA equations (PEER 2009)**

BA08, CB08, and CY08 used with equal weighting

M_w =	6.97		
Dip =	70	degrees	(Another fault near Butte, has a dip of 70-75 degrees)
Depth to bottom of rupture =	16	km	(Assumed)
R_x =	4.92	km	(measured using Google Earth)
Z_TOR =	0	km	(Assumed)
Width =	17.03	km	
R_jb =	0	km	(Assuming the site is on the hanging wall side)
R_rup =	1.68	km	
V_s30 =	760	m/s	
U=	0		
F_RV=	0		
F_NM =	1		
F_HW =	1		
F_measured =	0		
Z_1 =	DEFAULT		
Z_2.5=	DEFAULT		
F_AS=	0		
HW Taper =	1		
--> PGA (50%) =	0.5390	g	(From NGA spreadsheet)
--> PGA (84%) =	0.9202	g	(From NGA spreadsheet)